DYNAMICS OF SLENDER CYLINDRICAL ELEMENTS CONVEYING FLUID AND SUBJECTED TO STEADY AXIAL FLOW

By
S. R. BHATE

DEPARTMENT OF MECHANICAL ENGINEERING
INDIAN INSTITUTE OF TECHNOLOGY KANPUR
AUGUST, 1976

DYNAMICS OF SLENDER CYLINDRICAL ELEMENTS CONVEYING FLUID AND SUBJECTED TO STEADY AXIAL FLOW

A Thesis Submitted
in Partial Fulfilment of the Requirements
for the Degree of

MASTER OF TECHNOLOGY

By
S. R. BHATE

to the

DEPARTMENT OF MECHANICAL ENGINEERING
INDIAN INSTITUTE OF TECHNOLOGY KANPUR

JANUARY, 1977

CERTIFICATE

This is to certify that the work entitled "Dynamics of Slender Circular Cylinderical Elements Conveying Fluid and Subjected to Steady Axial Flow" has been carried out under our supervision and has not been submitted elsewhere for the award of a degree.

K. Sri Ram

K. Sri Ram
Associate Professor
Department of Mech. Engg.
I.I.T. Kanpur

B. Sahay

B. Sahay
Assistant Professor
Department of Mech. Engg.
I.I.T. Kanpur

ACKNOWLEDGEMENT

I am extremely thankful to Dr. V. Sundararajan for suggesting this topic and the inspiration I received from him during early part of this work. I express deep gratitude towards Dr. B. Sahay and Dr. K. Sri Ram for useful discussions, encouragement and timely guidance.

I acknowledge with thanks the invaluable cooperation and technical assistance received from Messrs. M.M. Singh, S.S. Pathak, R.S. Tripathi, G.K. Tiwari, B.L. Sharma, Ram Jiyawan and C.P. Singh during the design, fabrication and assembly of the experimental set-up planned for future work. I am thankful to all the staff of Central Workshop where most of the experimental set-up was fabricated.

I must express my appreciation to Messrs S.P. Kapoor, N.P. Roberts and W. Singh of the Computer Centre, I.I.T. Kanpur for their invaluable help during the computational work.

To Mr. J.D. Verma go my thanks for his accurate typing.

Thanks are also due to Mr. Lalta Prasad and Ajodhya Prasad of the Department of Mech. Engg. for neatly duplicating the stencils.

I am thankful to Mr. B.L. Arora and S.S. Kushwaha for their timely help in tracing the figures.

Finally, the financial assistance received from Bhabha Atomic Research Centre (Grant No. DAE/ME/VS-13) is being gratefully acknowledged.

S.R. Bhate

TABLE OF CONTENTS

LIST OF FIGURES

NOMENCLATURE

(Note: The subscripts 1 and 2 refer to the quantities related to internal and external flow respectively.)

A	:	Cross sectional area of the cylinder.
A_f	:	Flow area.
C_b	:	Base drag coefficient.
$C_D - C_f$	:	Friction drag coefficients.
c	:	Equal to $(4/\pi)\ C_D\ L\ (\rho_2 A/EI)^{\frac{1}{2}}$
$c_b\ c_f$	:	Equal to $(4/\pi)\ C_b$ and $(4/\pi)\ C_f$, respectively.
$C_o\ C_L$	:	Rotational spring constants.
D	:	Diameter of cylinder.
D_h	:	Hydraulic Diameter = $4\ A_f$/wetted perimeter.
EI	:	Flexural rigidity of the cylinder.
F_{IN}	:	Inviscid hydrodynamic force on the cylinder, per unit length.
F_{VN}	:	Normal viscous force on cylinder, per unit length.
F_{p_x}, F_{p_y}	:	Steady state pressure forces on cylinder, per unit length.
h	:	Geometry factor, equal to D/D_h
i	:	Referred to as the angle of incidence.
k_o, k_L	:	Linear spring constants.
L	:	Unsupported length of cylinders.
m	:	Mass of cylinder, per unit length.
M	:	Virtual mass of fluid, per unit length.
$\mathcal{M}$	:	Moment on a cross section of the cylinder.

T : Axial tension.

$\bar{T}$: Externally applied uniform tension.

t : Time

U_b : Mean flow velocity, cross sectional average.

u : Dimensionless flow velocity, equal to $\left\{\frac{\rho A}{EI}\right\}^{1/2} U_b L$

x : Axial coordinate.

y : Lateral displacement of cylinder.

α : Dimensionless internal damping coefficient $= \left\{I / [E(m + \rho_1 A + \rho_2 A)]\right\}^{1/2} \mu / L^2$

β : Dimensionless mass ratio equal to $\rho_2 A / (m + \rho_1 A + \rho_2 A)$

Γ : Dimensionless uniform tension $= \bar{T} L^2 / EI$

γ : Dimensionless gravity parameter $= (m - \rho_2 A + \rho_1 A) g L^3 / (EI)$

θ : Angle, the gravitational direction makes with x axis, radians

δ : Equal to 0 or 1 accordingly as the cylinder is free or not to slide axially at $x = L$

δ_b : Equal to +1 or -1 accordingly as the direction of the flow is along positive or negative x axis.

ϵ : Slenderness ratio, equal to L/D

η : Dimensionless displacement, equal to y/L

K_o, K_1 : Dimensionless spring constants equal to $k_o L^3 / EI$ and $k_L L^3 / EI$, respectively

K'_o, K'_1 : Dimensionless spring constants equal to $C_o L^2 / EI$ and $C_L L^2 / EI$, respectively.

μ : Dimensionless internal damping coefficient.

ν : Poisson's ratio

ξ : Dimensionless coordinate equal to x/L

Π : Dimensionless pressure parameter

$= \overline{(p_1 - p_2) A}\ L^2/EI$

ρ : Fluid density

ρ_{12} : Dimensionless density ratio

τ : Dimensionless time equal to

$\{ EI/[m + \rho_1 A + \rho_2 A] \}^{1/2} t/L^2$

χ : Coefficient of virtual mass

Ω : Circular natural frequency

ω : Dimensionless natural frequency, equal to

$\{ (\rho_1 A + \rho_2 A + m)/EI \}^{\frac{1}{2}} \Omega L^2$

Other quantities are defined in the text.

SYNOPSIS

A generalized mathematical model has been set up to describe small transverse vibrations of slender, straight and uniform circular cylinders conveying an incompressible fluid at steady velocity simultaneously subjected to a steady external axial flow of another incompressible fluid. The cylinders may be either isolated or be part of a cluster of identical cylinders, an arrangement commonly found in parallel flow heat exchangers, nuclear reactor fuel rod assemblies etc. Gravity, pressurization, surface roughness, material damping and directions of the flows has been taken into account. Equation of motion derived in the present study corrects an error in earlier formulations, related to the solid-fluid viscous interaction. The hydrodynamic and viscous interaction appears in the form of various coefficients related to the virtual mass, skin friction, overall friction for the flow channel, and normal viscous drag, which are functions of Reynolds number, geometry, compressibility. These have been systematically determined from the analytical and experimental results available so far.

The mathematical model has been applied to study the dynamic stability of cylinders and pipes with supported ends and clamped-free ends. The fluid interaction,

specifically Coriolis forces introduce mode coupling and make the problem non-self adjoint. Galerkin Method has been used to approximate the continuous system by a discrete one and dimensionless frequencies of the lowest three modes have been obtained with increasing flows. It has been shown that small flow velocities tend to damp the free motions in general but at sufficiently high velocities hydroelastic instabilities are possible. Both cylinders and pipes with supported ends are subject to buckling (divergence) in their first mode. The second mode instability, which sets in at higher flow velocities, is oscillatory (flutter) for cylinders (in general) and buckling for pipes if the mass ratio β is small. At slightly higher flow velocities coupled-mode flutter has been obtained for supported systems in general, the modes involved being first and second if the mass ratio is small and only the fundamental mode if mass ratio is high. For cylinders and pipes in cluster, the close spacing severely destabilizes the system. Virtual mass of the fluid decides the nature of the higher mode instabilities. Cantilever cylinders with blunt free end are subject to flutter in all the three modes, in addition to buckling in the first mode if the direction of flow is towards the fixed end. In general the external flow in case of pipes and internal flow in case of cylinders is shown to have destabilizing

effect on the systems, the effectiveness of the destabilization being dependent on the directions of the flows. Various instabilities have been analytically explained in terms of fluid-solid interaction.

Mechanism of energy transfer between the solid and fluid has been analytically shown to be responsible for the existence of various instabilities. Role of solid fluid interaction, both hydrodynamic and viscous, in causing various instabilities has been analytically examined using energy method.

Finally a method for obtaining the subcritical response when the system is subjected to an arbitrary force field has been presented. In particular when the excitation originates from turbulence induced random pressure fluctuations, the response problem is considered in detail. An experimental investigation is in progress to look into the type of excitation for a general cluster and to generate the data needed to study the response.

CHAPTER I

INTRODUCTION

I.1 Introduction to Flow Induced Vibration Problem

The term "flow induced vibration" includes a wide range of vibration problems associated with flexible solid structures activated by the energy derived from the fluid flowing around or through the structural members. High velocity coolant flowing through a reactor core is a source of energy that can induce and sustain vibration in reactor core components. Various components of nuclear reactor, such as fuel pins, control rods and heat exchanger tubes, are long and slender which may be set to vibration by the forces arising from the fluid flow. Structural vibrations often cause damage to such components through wear, fatigue and fretting. In fact, there have been numerous flow induced vibration problems, notably in EBR-II [75], GETR [76-77], Big Rock Point [78-81], Yankee [82-84], SPERT - III [77,85], and MSRE [86,87] reactors. These problems included i) sustained oscillations, which resulted in excessive wear, fretting and fatigue, ii) incorrect flow distribution, iii) broken specimen holders, iv) excessive vibration in heat exchangers and v) fluctuations in the power level of the reactor. The

examples of flow induced vibrations in other fields are numerous. Critical loads are imposed on structures by gusts and large turbulent motions in the atmosphere where the length scale of the turbulence is comparable to the size of the structures. The high frequency pressure fluctuations of small scale turbulence can cause a fatigue failure in a surface exposed to flow by providing excitation near a resonant frequency of the structure. A somewhat similar mechanism plays a role in the generation of water waves; resonant waves are excited by the pressure pattern convected over the surface in turbulent wind. Flow induced fluctuations can excite aircraft fuselage pannels causing noise transmission.

Vibration of elastic structures due to fluctuating lift forces set up as a result of vortex shedding process in the cross flow of a fluid have been observed since a long time due to common occurence of this phenomenon in nature. The vibrations due to parallel flow were observed much later, only after fluid carrying conduits, especially flexible ones, came into use. Indeed, the peculiar spontaneous motion of the free end of a flexible pipe by a sufficiently high flow rate was recognized as a self excited oscillation by Marcel Brillouin in 1885, but his work on the subject remained unpublished.

Analysis of the vibration problems may be divided into the considerations of the stability and response problems. In stability analysis investigation is made to determine whether conditions exist that can cause the structural response to diverge and, if so, to find these conditions (stability limits) in terms of the system parameters. In response analysis the problem is to predict the actual motion of the structure. The solution of the stability problem often supplies sufficient information to consider the vibration problem as solved. If the actual motion of the structure is desired, or if one wishes to know what happens to the structure under unstable conditions, the response problem must be studied in detail. This requires the knowledge of the damping mechanism and flow originated excitation which may be due to unsteady pressure field or pulsations in the flow rate. The response studies of flow induced vibration often necessitate solving a nonlinear differential equation coupled with the flow dynamics, the analysis might then be termed as "fluid-elastic analysis".

I.2 Previous Work on the Dynamics of Pipes Conveying Fluid

As stated earlier, the parallel flow induced motion was first observed in 1885 by Brillouin.

Bourrières [1], one of his students, was first to undertake the study of the dynamics of flexible pipes conveying fluid. He examined the oscillatory instabilities of cantilever pipes conveying fluid both theoretically and experimentally. He derived the correct equation of motion and, although unable to obtain analytically the critical velocity for the onset of oscillations, he determined most of the salient characteristics of the phenomenon.

Interest in the subject was reactivated in 1950, in connection with the study of vibrations of Trans-Arabian pipe line, by Ashley and Haviland [2]. They studied the flow induced damping in simply supported pipe and found it to increase rapidly with the flow rate. They further studied the wave type solutions and found that the effect of the flow is to expedite the waves travelling in the flow direction and retard the waves travelling in opposite direction. The same problem was studied independently by Housner [3] using a different approach. He found that for sufficiently high flow velocities the pipe may buckle, essentially like a column subjected to axial loading. A subsequent elegant and more general study by Niordson [6] led to the same equation of motion and to essentially the same conclusions regarding stability of pipe with simply supported ends.

Long [8] was the first, after Bourrières, to be concerned with cantilever pipes conveying fluid, although he considered other boundary conditions. His method of solution, using a power series for the mode shape, was applicable to relatively small flow velocities, considerably below the threshold of oscillatory instability, of the existence of which he seemed to be unaware. Nevertheless he did include the centrifugal force term in the equation of motion and confirmed experimentally that in contrast with those of simply supported pipes, forced motions of cantilever pipes are damped by internal flow in the range of flow velocities. The conclusion of Ashley and Haviland [2] that the flow of fluid damps the motion of the simply supported pipes was due to improper selection of lesser number of terms of the power series. The damping associated with cantilever pipe originates from Coriolis force and asymmetric modes about the centre of the span.

Handelman [7] presented an analytical method in which the character of the eigenvalues of the problem is determined from the structure of the differential equation of motion without determining specific solutions. Using a perturbation series in terms of flow velocity for the mode shape and eigenvalues he derived the same conclusion as Long [8] in case of pipes with

supported ends that no damping takes place when perturbation terms upto second and higher order are retained. For fixed-free ends Coriolis force promotes damping for small flow velocities. For near critical velocities the frequency of vibration is real for subcritical velocities and purely imaginary for velocities above critical; for fixed-free ends, however, there is no critical velocity for which frequency of vibration vanishes.

In all the above studies, excepting Bourrières, the only form of instability discovered was buckling. It was not until 1963 that Gregory and Paidoussis [26, 27] showed theoretically and experimentally that at sufficiently high flow velocities, cantilever pipes are subject to oscillatory instabilities (flutter) rather than buckling (divergence). The effect of flow for small values of flow velocity is to damp all the modes. For higher values of flow velocity, however, the second mode becomes less damped and subsequently the pipe becomes unstable. The buckling type of instability does not occur. Internal damping of the material was found to destabilize the pipe. The existence of oscillatory instabilities was fully anticipated by Benjamin [11, 12] in a study concerning the dynamics of articulated pipes which is a discrete representation of the continuous flexible system. Benjamin was the first to perceive the dynamical

problem independent of the fluid friction and he analytically predicted the existence of oscillatory instability of cantilever pipes conveying fluid. Both these effects later were confirmed by Gregory and Paidoussis [26, 27] . The dynamic behaviour of articulated and continuously flexible pipes conveying fluid is not strictly analogous. Benjamin [11, 12] found that the buckling instability is possible in the case of a vertical cantilever articulated system, where gravity is operative, if the fluid has sufficiently high density; on the other hand, Paidoussis [37] found that vertical continuous flexible pipes are never subject to buckling. This paradox was clarified by Paidoussis and Deksnis [38] . The stability of cantilever pipes was further discussed by Nemat-Nasser, Prasad and Hermann [25] with emphasis on the effect on stability of velocity dependent forces, such as dissipative and Coriolis forces; they showed that such forces may destabilize the system, an effect also reported previously by Gregory and Paidoussis [26, 27].

Subsequent work by Hermann [28] and Hermann and Nemat-Nasser [33] stressed the connection between the problem of instability of a cantilever conveying fluid and the more general problem of instability of a cantilever subjected to a "follower" type of force at the free end, i.e., a force retaining the same angular

disposition relative to the free end during small motions of the cantilever.

A recent study by Stein and Torbiner [39] mainly concerned with infinitely long pipes conveying fluid, brought a correction to the equation of motion as derived in some of the earlier papers. This correction arises from the effect of internal pressure and may become significant for sufficiently high pressure. Naguleswaran and Williams [35] studied this aspect of the problem both theoretically and experimentally. In case of pipes supported at both ends the effect of internal pressure was found similar to that of flow velocity; the pipe may buckle even at very small flow velocity by the action of sufficiently high internal pressure.

Thurman and Mote [36] presented a nonlinear analysis for a pipe with simply supported ends conveying fluid, using a perturbation technique. They found that in determining the natural frequencies of the system, the importance of the nonlinear terms increases with the flow velocity, so that the range of applicability of the linear theory becomes more restricted as the flow velocity increases.

More recently Chen [40] studied the stability of a pipe conveying fluid, with upstream end clamped

and downstream end constrained by a linear spring, so that the boundary conditions are intermediate between clamped-free and clamped-pinned; accordingly both buckling and oscillatory instabilities are possible, in general, depending on the spring constant. Both the types of instabilities with multiple stable and unstable ranges of flow velocity may occur for a range of spring constant values. For the value of dimensionless spring constant below a certain critical value (34.8145) the pipe does not loose the stability by buckling.

Paidoussis and Denise [43, 46] studied the dynamics of very thin elastic pipes conveying fluid, by utilizing thin shell theory to describe the motions of the pipe and potential flow theory to obtain the fluid forces. They analyzed both cantilever pipes and pipes with clamped ends. They found that in addition to instabilities in the beam modes of the system (corresponding to those found previously by beam theory for thicker pipes), instabilities in the shell modes are also possible, as verified by their experiments. Of particular interest was the finding that thin pipes with clamped ends are not only subject to buckling but also to coupled-mode flutter. For supported pipe as well as cantilever pipe the system loses stability by flutter in circumferential modes, in addition to usual

beam modes. Similar theoretical results were obtained later by Weaver and Unny [49] in the case of simply supported shells. The pipe was found to buckle in the beam mode at first but, at higher flow rate, instability by coupled mode flutter was predicted. The critical velocity for the coupled mode flutter depends on the circumferential mode number and the mode number for minimum critical velocity considerably depends on the length and thickness ratios. The critical flow velocities for short, thin shells are associated with a large number of circumferential modes; further, the longer and/or thicker the shell lower the critical circumferential mode number until the instability mode is the same as in a simple beam. Weaver and Unny also studied the divergence boundaries and critical mode shape, both theoretically and experimentally.

In all the studies discussed above the flow velocity was taken to be steady. Recently Chen [41] examined the stability of simply supported pipes conveying fluid with a flow velocity, U, which has a time dependent harmonic component superposed on the steady velocity, U_o, such that $U = U_o (1 + \mu \cos \omega t)$. His equation of motion incorporated the initial curvature, damping and axial tension in addition to unsteady flow. Using Galerkin method the governing equation was reduced to a system of coupled Mathieu-Hill type equations with multiharmonic coefficients.

He investigated the onset of parametric resonance using Hsu's [66] and Bolotin's [65] method and obtained the boundaries of the first two instability regions; moreover, he found that the combination of resonances is also possible. He studied the significance and effects of Coriolis force on free vibration, forced vibration and parametric resonance. The influence of Coriolis force on free vibration and parametric resonance was found small for a flow rate much less relative to the critical velocity. Initial curvature, which introduces nonhomogeneity in the differential equation of motion, may induce large deflections if the flow velocity is large. This particular aspect of the problem was studied by him in detail [42, 44] for a uniformly curved tube conveying fluid. He included the effect of fluid pressure in the equation of motion. Of particular interest was the finding that the curved tube with supported end loses stability at first by buckling in the first mode, then at higher flow velocity again by buckling in the second mode and so on. The flutter type of instability was not found to occur in case of tubes with supported ends. The effect of the fluid pressure on natural frequencies of the tube was found quite similar to that of flow velocity. This was already found for the straight pipes by Stein and Torbiner [39] and Naguleswaran and Williams [35] . Coriolis force

and internal friction did not affect the stability of curved tube with supported ends, as found in the case of straight tube [11, 12]. Further work of Chen [45] dealt with out of plane motion of a uniformly curved pipe. He derived essentially same conclusions as those for the in-plane motion; thus the pipe experiences buckling type of instability for conservative cases (supported ends) and flutter type of instability for nonconservative (cantilever pipe) cases as the flow velocity is gradually increased. No coupling between in-plane and out of plane motion was found and as such these can be studied independently.

Chen's work on parametric instabilities of simply supported pipe was followed by the work of Bohn and Hermann [47] wherein they examined the transverse motion of vertical articulated pipes when the flow rate harmonically varies about a nonzero mean. Both parametric and combination resonances were found to be possible. The amplitude of the pulsations in the flow rate required to cause the instability was found to decrease as the mean flow velocity approached the one required to cause the onset of instability either by flutter or divergence when the flow is steady. For the values of mean flow velocity greater than the one which causes the onset of instability by flutter or divergence when the flow is steady, there exists a range of

pulsation frequency and amplitude which can stabilize the system, where in the absence of pulsations the system would be unstable. Some of the regions on Strutt diagrams (curves of pulsation frequency versus amplitude showing stable and unstable zones) which constitute stable regions when mean flow velocity is less than critical become the regions of combination resonance when mean flow velocity exceeds the critical value.

In a recent paper, Paidoussis and Issid[55] considered the dynamic stability of pipes conveying fluid, where the flow velocity is either entirely steady or with a small harmonic component superimposed on it. He rederived the pertinent equation of motion correcting an error in Chen's formulation. This correction arises from the streamwise local acceleration ($\frac{\partial U}{\partial t}$) of the fluid in unsteady flow and had not been considered by Chen. Of particular interest was the finding that conservative systems were subject not only to buckling at sufficiently high velocities but also to flutter at higher flow velocities. The existence of these oscillatory instabilities in case of pinned-pinned and clamped-clamped pipes was explained as the consequence of Coriolis forces, the system being gyroscopic conservative. Accordingly the method of equilibrium fails to give correct higher critical velocities.

After the onset of buckling the Coriolis forces stabilize the system prior to the onset of coupled mode flutter. He also considered the case of cantilever pipe with viscoelastic and hysteretic damping. The viscoelastic damping was found to destabilize the pipe whereas the effect of hysteretic dissipation was not as severe. For the case of pulsatile flow velocity, primary and secondary principal instabilities were investigated using Bolotin's method and stability maps were presented for pipes with clamped or pinned ends as well as cantilever pipes. The extent of the instability region was found to increase with flow velocity for pipes with supported ends, while a more complex behaviour was found in the case of cantilever pipes. In all cases, dissipation reduced (or entirely eliminated) the extent of parametric instability zones.

I.3 Previous Work on the Dynamics of Rods Subjected to Axial Flow:

That the vibration caused by the energy derived from the parallel flow of a fluid along a cylindrical body could be significant was not evidenced until 1958 when Burgreen et. al. [9] demonstrated the phenomenon of rod vibration due to parallel flow, while studying the heat transfer of water flowing across a bundle of rods simulating a nuclear reactor core. This

was perhaps the earliest study motivated by the general concern that parallel flow induced vibration of cylindrical fuel elements may cause a mechanical design problem in reactor. Oscillations were observed to occur at all flow velocities. The fact that the frequency of oscillations remained relatively constant led them to believe that the vibration was of self-excited type. They developed an empirical expression for maximum amplitude of vibration by dimensional analysis of differential equation of motion in which excitation was assumed proportional to the dynamic pressure ($\frac{1}{2} \rho U^2$) of the fluid. This was followed by several experimental studies [18, 19, 20, 22, 23, 24, 32, 34] wherein the principal aim was to study the character of the vibrations and obtain an empirical expression for maximum amplitude of vibration which can be used for design purposes. The first analytical and experimental investigation of the dynamics of flexible slender cylinders subjected to axial flow was attempted in 1966, about eight years after the work of Burgreen et. al. [9] by Paidoussis [29, 30] . The analytical model devised for this purpose was based on Bernoulli-Euler beam theory to describe the flexural motions of the cylinder, slender body theory for the coupled inviscid hydrodynamic forces, and fairly simple linearized relationships for the corresponding viscous forces. The

cylinders were either supported at both ends or were like a cantilever with a suitably streamlined, free downstream end. The theoretically determined main characteristics of the dynamical behaviour of the system were found to be the following: i) small flow velocities have a damping effect on free motion of the system, ii) for sufficiently high flow velocities the system is subject to hydroelastic instabilities; both divergence and flutter are generally possible, the former representing a static loss of stability and the latter being an oscillatory instability. Paidoussis showed that the cylinder supported at both ends represents a conservative gyroscopic system. Accordingly, damping effect at low flow velocities occurs entirely due to dissipative forces. Divergence was dominant in case of cylinders with supported ends though flutter also occurs at higher flow velocities in higher flexural modes. These oscillatory instabilities are specifically caused by lateral friction forces and in the absence of the drag forces only buckling is possible. Externally applied tension was found to stabilize the system and compression destabilize it. A cantilever cylinder in axial flow is inherently a non-conservative system, so that work done by the inviscid hydrodynamic forces in the course of free oscillations of the system need not be zero. Indeed, at small flow velocities this work is negative resulting in an added damping effect

over and above that due to dissipation. At higher flow velocities the work done by the inviscid hydrodynamic forces may become positive, so that the energy then may be gained by the cylinder from the fluid; indeed this is the dominant mechanism of energy transfer underlying the onset of flutter of cantilever cylinders.

Recently Paidoussis [48] extended the theory and applied it to the cylinders in confined flows. He took into account the gravity and pressurization effects which were not considered in his previous work on cylinders; in addition he corrected the relationship for normal friction drag, adding a term to account for the flow induced damping at zero flow velocity. The cylinders could be either isolated or be part of a cluster of identical cylinders. Small flow velocities were found to damp free vibration but at sufficiently high flow velocities possibilities of hydroelastic instabilities were found. Typically, simply supported cylinders were subject to buckling in their first mode, and then at higher flow velocities in their second mode; at slightly higher flow velocities coupled-mode flutter was shown to occur. Critical velocities for the cylinder in a closely spaced cluster were much lower than those for an isolated cylinder. Cantilever cylinders, on the other hand, were subject to buckling in their first mode and to flutter

in higher modes. The difference in the dynamic behaviour of the cylinder as compared to the one in his previous study [29, 30] was attributed to the correction in the representation of fluid frictional forces incorporated in his later study. This demonstrated the definite importance of fluid frictional forces in the dynamic behaviour of cylinders. Coupled-mode flutter was shown to occur for confined cylinders also; for cantilever cylinders however only ordinary flutter instability was found to occur. Moreover, for the case of cantilever cylinder with streamlined free end the loss of stability in the second mode preceeded by regaining of stability in the first, and in analogous manner, the regaining of stability in the second mode occured at a slightly higher value of flow velocity than was necessary for the onset of third-mode flutter. Apart from the study of dynamics he presented a method by which response of the cylinder subjected to an arbitrary force field may be obtained.

Further work of Paidoussis [61] deals with the stability of slender cylinders subjected to axial flow, the velocity being harmonically perturbed in time. Cylinders with pinned-pinned ends and clamped-free ends were considered. Principal primary and secondary instabilities were found to be possible for certain ranges of frequencies and amplitudes of the perturbations.

For small flow velocities flow induced damping opposes the onset of parametric instabilities. The parameters which destabilize the system when flow velocity is steady render parametric instability regions wider. In case of simply supported cylinder parametric instabilities occur over specific ranges of flow velocities. In the case of cantilever cylinders the instabilities were found to be associated with only some of the modes of the system and resulting regions in strutt diagrams were quite complex; moreover, in certain cases the secondary instability regions became more important than the primary ones. In general, however, the extent of the instability regions in strutt diagrams became wider as the system approached the point of instability in steady flow.

I.4 Present Work, Objectives and Scope:

From the review of previous work on the dynamics of pipes conveying fluid and cylindrical rods subjected to axial flow, it appears that a remarkable development has occured since Trans-Arabian pipeline was observed to vibrate (presumably as a result of internal flow) and cylindrical rods were observed to oscillate by Burgreen et. al. However the impetus for these studies, especially those related to pipes, did not come from desire to solve a practical problem, but rather from one or

more of the following considerations: i) the physical problem was inherently intriguing; ii) the problem offered scope for interesting mathematical manipulations; iii) the pipe problem represents one of the few cases where a (non-conservative) follower load is physically realizable, hence, it offers a rare opportunity for combined theoretical-experimental studies in the general area of dynamics of elastic systems subjected to non-conservative forces, and explains, to some extent, the large volume of research activity on this topic. It further appears that the development in the subject of dynamics of pipe transporting fluid and in the subject of slender rods subjected to fluid flow occured more or less independently. These two problems have a unique feature in common viz. the energy transfer between the flowing fluid and body by inviscid hydrodynamic forces. The centrifugal force set-up by the fluid flowing through a curved tube or along a curved rod, acts much like a compressive force at the end. The problem of rod differs from that of pipe only due to added frictional forces which can also be considered for a pipe submerged in a fluid, e.g. underwater pipeline. As regards vibrations due to pressure fluctuations in the flow either due to turbulence in the flow or due to its pulsatile nature, both pipes and rods vibrate or loose stability in a more or less similar manner. The first aim of the

present work is to synthesize these two problems into a single general parallel flow problem, so that in applications where a rod subjected to parallel flow also acts as a tube conveying fluid, the effect of both the flows on the dynamics of the rod can be assessed.

The present work was initiated with an aim to obtain an estimate of the response of structures comprising slender cylindrical tubes or rods subjected to fluid flow with prospective application to parallel flow heat exchangers, liquid fuel rocket piping, nuclear reactor coolant channels, fuel rod bundles, underwater pipelines etc. Accordingly, the equation of motion was set up taking into account every possible realistic effect. Model for viscous interaction between the tube and external fluid was chosen and various fluid parameters were systematically determined to obtain the correct estimate of damping. However, since the mechanical structure was regarded as the system excited by pressure fluctuations in the flow (internal and external), either due to turbulence or pulsatile nature of the flow, the quantitative knowledge of excitation was a must before response could be obtained. Except for the case of a flat plate [13] and circular pipe [14, 16, 17] no reliable measurements on pressure fluctuations due to turbulence are available so far. Analytically these can be obtained

by numerical simulation of the flow field only for some simple geometries such as annular geometry [62] but the method is both difficult and computationally uneconomical due to large computer memory core and time requirements. Therefore an experimental investigation has been planned. In the meanwhile with the available information at hand a major portion of the solution of the problem could be sought.

For any dynamical system, for a given excitation, the response depends on the natural frequencies and associated damping. The vibration problem in most cases, is considered solved if the natural frequencies and damping is known. In addition, if the conditions at which the system will loose the stability are known in advance, these can be avoided at the design stage itself. Accordingly, an investigation of the effect of internal and external flow on the natural frequencies and damping taking into account the gravity, pressure, material damping and confinement in case of clusters was planned. Since fluid friction forces play an important role in the dynamics of rod subjected to axial flow, consideration of the surface roughness and viscosity of the fluid is important which has not received due attention so far, presumably because in all the previous formulations the fluid friction appears as skin friction coefficient and normal drag

coefficient which have to be specified. Further, the friction coefficients have been taken to be constants. In the present work they have been treated as functions of Reynolds number, surface roughness and geometry. Present work brings in a correction to the equation of motion formulated by Paidoussis [48, 61]. In view of the author, Paidoussis' representation of the normal drag forces on a cylinder subjected to axial flow, though accounts for fluid induced damping when fluid is stationary, fails to correctly represent the drag for small values of flow velocity, since the drag depends on relative velocity between the body and the fluid.

Since the present work deals with two flows, their relative direction for symmetrically supported cylinders and individual directions for cylinders with asymmetric end conditions become important. To the authors knowledge the importance of the direction of the flow has not been considered in published literature so far.

Briefly, then, the present work adds several more relevant parameters to the problems considered before and attempts to generalize the parallel flow induced vibration problem in addition to emphasizing some of the parameters in their true perspective.

CHAPTER II

THEORY

II.1 Introduction

In this chapter a generalized parallel flow induced vibration problem has been formulated. It is not being claimed as the most general one since it has been restricted to small transverse vibration of slender cylindrical elements subjected to steady incompressible turbulent flow, parallel to the common axis of the cluster. This formulation synthesizes the problems considered by Paidoussis [48] and Paidoussis and Issid [55] into a single problem of vibration of a cluster of tubular cylindrical elements carrying the fluid. When appropriately specialized it covers almost all situations involving parallel flow induced vibration investigated so far.

II.2 Formulation

For the problem under investigation consider a system of identical, straight and uniform slender cylindrical tubes (Fig. 2.1), which are assumed to be elastic. In practice, the tubes may be held in place by end plates or spacer plates at one or both of their ends. The entire assembly is surrounded by a rigid circular channel through which an incompressible fluid flows parallel to the channel axis. It is assumed that

the supports do not significantly disturb the flow except over a certain length which is small compared to the unsupported length of the tubes. Each tube is assumed to carry equal flow of another incompressible fluid, which may be exchanging heat with the fluid surrounding the tubes. This is an idealized model for Parallel flow heat exchangers.

For convenience, the flow in the tubes will be termed as inner flow while the flow in the channel will be referred to as outer flow, Subscripts 1 and 2 denoting the related quantities respectively. Flow in one or both the regions may be two phase flow, in which case the portion of one phase will be assumed small so that the flow may be taken as equivalent single phase flow with appropriate fluid properties. For the purpose of expressing fluid forces on cylindrical elements, both the flows will be assumed to be perfectly parallel, uniform and steady. Further, it is assumed apriori, that the vibration amplitude remains small compared to the significant length scales of both the flows, to the extent that the consequential perturbation in the flow can be ignored. In the present state of the formulation one has to idealize the flow field since full differential analysis of the coupled solid-fluid interaction problem is not being attempted, the general form of which can be stated formally as:

$$\partial u_i/\partial t + (u_k u_i)_{,k} + \frac{1}{\rho} p_{,i} = \nu u_{i,kk} \qquad (a)$$

together with

$$\mathcal{L}\left[\eta_{lk}(x_l, t), u_i\right] = 0 \qquad (b) \qquad (2.1)$$

and

$$u_i = D\eta_i/Dt \qquad (c)$$

at bounding surfaces

where

η_{lk} = kth component of the motion of the lth element

u_i = ith component of the flow velocity

p = fluid pressure

ν = kinematic viscosity of the fluid

D/Dt = Eulerian Derivative.

In the above set of equations, (2.1 a) are the Navier-Stokes equations for constant property fluid, written in tensor notation. Equations (2.1 b) is a set of differential equation which must be satisfied at all bounding surfaces, the vector operator $\mathcal{L}$ consisting of various derivatives to account for flexural restoring forces, tangential and normal forces due to surrounding fluid and inertia forces arising from the motion of the solid. Finally equations (2.1 c) is a set of no penetration and no slip conditions, taken for impermeable surface and viscous fluid.

The set of coupled equations (2.1) which are generally nonlinear partial differential equations, is difficult to solve. For rigid walls and parallel flow, the wall pressure fluctuations have been studied recently by Schumann [62] by simulating equations (2.1 a and c) on a digital computer.but the method is computationally uneconomical. Studying the motion of the solid coupled with the fluid flow by simulation would prove to be much more difficult due to the appearance of differentially coupled boundary conditions (2.1 b, c).

Returning to our idealized situation, consider a small transverse motion y of one of the inner cylinders about its position of rest. It will be assumed that the motion is planar and independent of the other spans of the same cylinder so that the cylinder need not be treated as a multispan structure. Further, the flow field in two different cells (Fig. 2.1) and consequential excitation on cylinders surrounding the cells will be assumed uncorrelated so that an element can be analyzed independent of others and the entire system as such need not be considered. This amounts to assuming that the flow in any of the cells is uncorrelated to the motion of the cylinders. This assumption greatly simplifies the coupled problem

and enables one to consider a single cylinder in a cluster as the system excited by the flow around and within. As the spacing between cylinders and significant length scale of the flow increases compared to the vibration amplitude, the accuracy of the previous assymption can be expected to increase. Angle of incidence i and curvature $\partial i/\partial x$ are assumed to be small so that separation in the cross flow is not likely to occur and forces on a section of cylinder under consideration, exerted by the outer flow may be assumed to be the same as those acting on a corresponding section of a long cylinder having identical cross section and inclination to the flow direction. The forces and moments acting on a small section δx of the cylinder are shown in Figure (2.2 a). The assembly is assumed to be inclined at an angle θ to the gravitational direction. F_L and F_N are the resultant longitudinal and normal fluid forces per unit length, acting on the section, while T is the axial tensile force. The forces F_{px} and F_{py} which are the result of mean fluid pressure, will be discussed at length later.

Consistent with the small motion assumption, the spatial derivatives of y will be assumed small. For the section of the cylinder under consideration, the force balance in x direction gives,

$$\frac{\partial T}{\partial x} + m g_x + F_L + F_N \frac{\partial y}{\partial x} - F_{px} = 0 \qquad (2.2\ a)$$

where m is the mass of the cylinder per unit length and

$$F_L = F_{L1} + F_{L2}$$

$$F_N = F_{N1} + F_{N2}$$

Forces acting on the section of fluid, contained in the above section of cylinder, are shown in Figure (2.2 b). The force balance in x direction can be written as,

$$-\frac{\partial}{\partial x}(p_1 A) - F_{L1} + \rho_1 A g_x - F_{N1} \frac{\partial y}{\partial x} = 0 \qquad (2.2\ b)$$

where p is the fluid pressure, ρ denotes fluid density and A is the cross sectional area of inner flow.

Force balance in y direction, for the element of cylinder and fluid, respectively, may be written as

$$\frac{\partial Q}{\partial x} - F_N + F_{py} + F_L \frac{\partial y}{\partial x} + \frac{\partial}{\partial x}\left(T \frac{\partial y}{\partial x}\right) - m\left(\frac{\partial^2 y}{\partial t^2} - g_y\right) + f(x,t) = 0 \qquad (2.3\ a)$$

and

$$F_{N1} - \frac{\partial}{\partial x}\left(p_1 A \frac{\partial y}{\partial x}\right) - F_{L1} \frac{\partial y}{\partial x} - F_{IN1} = 0 \qquad (2.3\ b)$$

where $m \frac{\partial^2 y}{\partial t^2}$ and F_{IN1} are inertia forces, Q is the shear force on cross section of cylinder and f (x, t) is the flow originated excitation force, being considered separately from F_N and assumed independent

of y or its derivatives. Since the elements have been assumed slender, shear deformation and rotary inertia will be neglected. Further, if the material of the cylinder is assumed to follow Kelvin-Voigt type relation, the moment balance can be written as

$$Q = -\frac{\partial M}{\partial x} = -\frac{\partial}{\partial x}\left[EI\frac{\partial^2 y}{\partial x^2} + \mu I\frac{\partial}{\partial t}\left(\frac{\partial^2 y}{\partial x^2}\right)\right] \quad (2.4)$$

where μ is the material damping constant and EI the flexural rigidity.

The forces F_{px} and F_{py} arising from mean pressure of outer fluid can be obtained by integrating around the outer surface; however, following the suggestion of Paidoussis [48], they can be found conveniently as follows: consider the elementary section shown in Figure (2.2 a) momentarily frozen and immersed in the fluid on all sides as shown in Figure (2.3); then, there will be additional forces $P_2 A$ and $P_2 A + [\partial(P_2 A)/\partial x]\,\delta x$ on the cross sectional faces of the element, but the resultant of these forces and of the forces $F_{px}\,\delta x$ and $F_{py}\,\delta x$ is known and equal to the buoyancy force. Accordingly, $P_2 \triangleq P_2(x)$ will be taken at most linear function of x, which covers mean pressure distribution due to gravity and skin friction drop. The force balance then gives,

$$\left[-\frac{\partial}{\partial x}(p_2 A) - F_{px}\right]\delta x\,\hat{i} + \left[F_{py} - \frac{\partial}{\partial x}\left\{(p_2 A)\frac{\partial y}{\partial x}\right\}\right]\delta x\,\hat{j}$$

$$= -\iint_{(\text{Area})} p_2 \hat{n}\, d\,(\text{Area})$$

$$= -\iiint_{(\text{vol.})} \nabla p_2\, d(\text{vol.}) \quad \text{(using Gauss's Divergence Theorem)}$$

$$= -\frac{\partial p_2}{\partial x} A\,\delta x\,\hat{i}$$

Hence,

$$F_{px} = \frac{\partial p_2}{\partial x} A - \frac{\partial}{\partial x}(p_2 A) \qquad \text{(a)}$$

$$F_{py} = \frac{\partial}{\partial x}\left(p_2 A \frac{\partial y}{\partial x}\right) \qquad \text{(b)} \qquad (2.5)$$

It can be observed that the force F_{py} is equivalent to a tensile force of magnitude $(p_2 A)$ acting on the cross section of the cylinder, also $F_{px} = 0$ if $\frac{\partial A}{\partial x} = 0$; however, for convenience, this will be invoked later.

Substituting equations (2.5) into equations (2.2 a) and (2.3 a)

$$\frac{\partial}{\partial x}(T + p_2 A) + \left(m g_x - \frac{\partial p_2}{\partial x} A\right) + F_L + F_N \frac{\partial y}{\partial x} = 0 \qquad (2.6)$$

$$\frac{\partial Q}{\partial x} - F_N + F_L \frac{\partial y}{\partial x} + \frac{\partial}{\partial x}\left[(T + p_2 A)\frac{\partial y}{\partial x}\right] - m\left(\frac{\partial^2 y}{\partial t^2} - g_y\right) + f(x,t) = 0 \qquad (2.7)$$

Adding equations (2.6) and (2.2 b)

$$\frac{\partial}{\partial x}(T + pA) + \left(m g_x + \rho_1 A g_x - \frac{\partial p_2}{\partial x} A\right) + F_{L_2} + F_N \frac{\partial y}{\partial x} = 0 \qquad (2.6\text{ b})$$

where

$$p \triangleq p_2 - p_1$$

Similarly, adding equations (2.7) and (2.3 b)

$$\frac{\partial Q}{\partial x} - \left(F_{IN1} + F_{N2}\right) + F_{L2}\frac{\partial y}{\partial x} + \frac{\partial}{\partial x}\left[(T + pA)\frac{\partial y}{\partial x}\right] - m\left(\frac{\partial^2 y}{\partial t^2} - g_y\right) + f(x,t) = 0 \qquad (2.7b)$$

As will be seen later, if $y \sim O(\epsilon)$, $(\epsilon << 1)$, then $F_{N2}\frac{\partial y}{\partial x} \sim O(\epsilon^2)$ and rest of the terms in equation (2.6 b) are $\sim O(\epsilon)$; thus neglecting the last term in equation (2.6 b) and integrating between the limits x and L while invoking axial uniformity, $\frac{\partial A}{\partial x} \equiv 0$

$$(T + pA)\Big|_x = (T + pA)\Big|_L + \left[(m + \rho_1 A)g_x - \frac{\partial p_2}{\partial x}A\right](L - x) + \int_x^L F_{L_2}\,dx \qquad (2.8)$$

Combining equation (2.8) with equations (2.4), (2.6 b) and (2.7 b) one gets,

$$\mu I\frac{\partial^5 y}{\partial x^4 \partial t} + EI\frac{\partial^4 y}{\partial x^4} - \left\{(T + pA)\Big|_L + \left[(m + \rho_1 A)g_x - \frac{\partial p_2}{\partial x}A\right](L - x) + \int_x^L F_{L_2}\,dx\right\}\frac{\partial^2 y}{\partial x^2} + \left(F_{IN1} + F_{N2}\right) + \left[(m + \rho_1 A)g_x - \frac{\partial p_2}{\partial x}A\right]\frac{\partial y}{\partial x} \qquad (2.9)$$
$$+ m\left(\frac{\partial^2 y}{\partial t^2} - g_y\right) = f(x,t)$$

The terms $(T + pA)\Big|_L$, $\frac{\partial p_2}{\partial x}$, F_{IN1}, F_{N2} and F_{L2} are yet to be determined in explicit form.

The pressure drop due to gravity and wall friction drop can be written as

$$\frac{\partial p_2}{\partial x} = \rho_2 g_x - \frac{1}{2}\rho_2 U_{b_2}^2 \lambda_2 \delta_{b_2} / D_h \qquad (2.10)$$

where U_{b_2} is the bulk velocity of outer flow, λ_2 is the overall friction factor to be chosen according to the geometry and D_h, the hydraulic diameter. The discrete variable δ_b has been introduced to take into account the direction of the flow and hence of the resulting pressure drop. Thus

$\delta_b = +1$ if the flow direction is along the positive x axis

$= -1$ if the flow direction is along the negative x axis.

Henceforth, bulk velocity U_b will always be written as $U_b \delta_b$, the variable δ_b being dropped where unnecessary.

The forces F_N and F_L exerted by the fluid shall be expressed in terms of the gross momentum of the fluid. The force F_N can be thought of as consisting of two parts; one due to viscous drag, F_{VN}, and the other due to inertia of the fluid, F_{IN}. Thus,

$$F_N = F_{IN} + F_{VN}$$

As proposed by Lighthill [10], the force F_{IN} is taken as

$$F_{IN} = \left(\frac{\partial}{\partial t} + U_b \delta_b \frac{\partial}{\partial x}\right)\left[M\left(\frac{\partial}{\partial t} + U_b \delta_b \frac{\partial}{\partial x}\right) y\right] \qquad (2.11)$$

where M is the virtual Mass of the fluid.

For the problem under consideration

$$F_{IN} = F_{IN1} + F_{IN2}$$
$$= \rho_1 A\left(\frac{\partial}{\partial t} + U_{b_1}\delta_{b_1}\frac{\partial}{\partial x}\right)^2 y + \chi \rho_2 A\left(\frac{\partial}{\partial t} + U_{b_2}\delta_{b_2}\frac{\partial}{\partial x}\right)^2 y \qquad (2.12)$$

where χ is the added mass coefficient for the outer fluid; for inner fluid added mass coefficient has been taken equal to unity. This coefficient has been computed by Chen and Wambsganss [67] for annular flow and by Chen [68] for cluster of cylinders.

For the forces F_{VN} and F_L, following expressions were proposed by Taylor [5] and verified by Hoerner [21] for steady outer flow.

$$F_{VN2} = \frac{1}{2} \rho_2 D U_{b_2}^2 (C_f \sin i + C_{DP} \sin^2 i)$$
$$F_{L2} = \frac{1}{2} \rho_2 D U_{b_2}^2 C_f \cos i \qquad (2.13)$$

where C_f is the wall friction coefficient and C_{DP}, the form drag coefficient, D is the diameter of the cylinder. C_f can be written as

$$C_f = \pi \lim_{i \to 0} \left[\frac{(\text{Drag force}) x}{\frac{1}{2} \rho U_{b_2}^2 \pi D L} \right]$$

where L is the length of the cylinder.

The expressions (2.13) can be modified to take into account the direction of flow as,

$$F_{VN2} = \frac{1}{2} \rho_2 D U_{b_2}^2 (C_f \sin i + \delta_{b_2} C_{DP} \sin^2 i) \quad (a)$$
$$F_{L2} = \frac{1}{2} \rho_2 D U_{b_2}^2 \delta_{b_2} \cos i \quad (b) \qquad (2.13)$$

Equations (2.13) give only mean values in terms of the gross momentum of the fluid, since the coefficients vary from point to point with the developing flow, further, the forces F_{VN} and F_L are assumed to be instantaneous without memory. For periodic Laminar Boundary Layers the wall shear stress is known to lag behind the fluctuating velocity of the fluid. Exact nature of the viscous interaction in unsteady turbulent flows is not clearly known since these flows have not been studied in sufficient details

so far. Validity of the equations (2.13) for a surface excited by flowing fluid appears questionable; but if one is not interested in detailed motion history of the surface, it is a simple first approximation and offers an attractive alternative to the treatment of interaction problem. As will be seen later the force F_{VN2} plays an important role in the stability of cylindrical element and hence deserves more detailed investigation.

For the present problem, for small $\frac{\partial y}{\partial x}$ and $\frac{\partial y}{\partial t} / U_{b_2}$ the angle of incidence, $i = \tan^{-1}\left(\frac{\partial y}{\partial x}\right) + \tan^{-1}\left(\frac{\partial y}{\partial t} / U_{b_2}\delta_{b_2}\right)$, will be small and approximating sin i by $\left(\frac{\partial y}{\partial t} + U_{b_2}\delta_{b_2}\frac{\partial y}{\partial x}\right)/\left(U_{b_2}\delta_{b_2}\right)$ in equations (2.13), while dropping P from the coefficient C_{DP},

$$F_{VN2} = \tfrac{1}{2}\rho_2 D U_{b_2}\delta_{b_2}\left(f_1\left(\frac{\partial y}{\partial t} + U_{b_2}\delta_{b_2}\frac{\partial y}{\partial x}\right) + \tfrac{1}{2}\rho_2 D C_D\left(\frac{\partial y}{\partial t} + U_{b_2}\delta_{b_2}\frac{\partial y}{\partial x}\right)\right. \quad \text{(a)}$$

$$F_{L2} = \tfrac{1}{2}\rho_2 D U_{b_2}^2\delta_{b_2}(f_1 \quad \text{(b)} \qquad (2.14)$$

The second term in the equation (2.14 a) represents linearization for small U_b and in this form it correctly gives the direction of the normal drag force. It can be observed that all other terms in the equation (2.14 a) vanish for $U_{b_2} = 0$ and non-zero value of C_D accounts for viscous drag and consequential damping due to surrounding fluid. This

term slightly differs from the linearized term taken by Paidoussis [48] and in this form accounts for the viscous drag due to transverse velocity of cylinder relative to the fluid.

Finally consider the term $(T + pA)|_L$. For the case when the cylinder is free to slide axially or is completely free at $x = L$, recalling that the term pA arises from the pressure acting on the sides of the cylinder, at $x = L$ $T_L = - p_b A$ where p_b is the base pressure. If the cylinder carrying fluid is discharging to the atmosphere at high velocity, the reaction force may be taken care of by appropriately selecting p_b. Hence,

$$(T + pA)|_L = (p_L - p_b) A \tag{2.15}$$

which is somewhat like a form drag. In case of a cylinder free at down stream end the outer flow indeed causes a form drag of this type. All these cases may therefore be grouped into

$$(T + pA)|_L = \frac{1}{2} \rho D^2 U_b^2 \delta_b C_b \tag{2.16}$$

where C_b is the form drag coefficient to be chosen appropriately. On the other hand, if the total length of the cylinder remains constant between fixed supports, as may be the case when the cylinders are held between two rigid plates and axial tension is applied, then, at $x = L$ there will be an additional compressive

force $-\frac{1}{2}\left(F_L \cdot L + m g_x L\right)$, assuming that the weight and axial frictional drag are taken by both the supports equally. The existence of the second term depends on whether the length was fixed while the cylinder was horizontal or not. There will also exist a compressive force due to radial contraction arising from mean differential pressure p. For a thin tube this is $-2\nu\left(\overline{pA}\right)$ where $\overline{pA} = pA\big|_{x=\frac{L}{2}}$ and ν is the Poisson's ratio for the material. Finally considering externally imposed uniform tension $\overline{T}$,

$$\left(T + pA\right)\Big|_L = -\frac{L}{2}\left(F_L + m g_x - \frac{\partial p}{\partial x} A\right) + (1-2\nu)\,\overline{pA} + \overline{T} \qquad (2.17)$$

combining equations (2.16) and (2.17),

$$\left(T + pA\right)\Big|_L = \delta\left[(1-2\nu)\,\overline{pA} + \overline{T} - \frac{L}{2}\left(F_L + m g_x - \frac{\partial p}{\partial x} A\right)\right] + \frac{1}{2}(1-\delta)\,\rho D^2 U_b^2 C_b \delta_b \qquad (2.18)$$

where

$\delta = 0$ if the tube end at x = L is free to slide axially.

$= 1$ if the supports do not allow net axial extension.

For the problem under consideration equation (2.18) can be written

$$\left(T + pA\right)\Big|_L = \delta\left[(1-2\nu)\,\overline{pA} + \overline{T} - \frac{L}{2}\left(F_{L_2} + m g_x + \rho_1 g_x - \frac{\partial p_2}{\partial x} A\right)\right] + \frac{1}{2}(1-\delta)\,\rho D^2 U_b^2 C_b \delta_b \qquad (2.18\,a)$$

where $\rho U_b^2 \delta_b = \rho_2^2 U_{b_2}^2 \delta_{b_2}$ or $\rho_1^2 U_{b_1}^2 \delta_{b_1}$ depending on the particular case being considered. This alternative is necessary since one of the flows may have

zero velocity, with δ = 0 and nonzero force may exist at end x = L.

Substitution of equations (2.12), (2.14) and (2.18 a) into equation (2.9) leads to

$$\mu I \frac{\partial^5 y}{\partial x^4 \partial t} + EI \frac{\partial^4 y}{\partial x^4} + \rho_1 A \left(\frac{\partial}{\partial t} + U_{b_1} \delta_{b_1} \frac{\partial}{\partial x} \right)^2 y$$
$$+ \chi \rho_2 A \left(\frac{\partial}{\partial t} + U_{b_2} \delta_{b_2} \frac{\partial}{\partial x} \right)^2 y + \frac{1}{2} \rho_2 D U_{b_2} \delta_{b_2} C_{f_1} \left(\frac{\partial y}{\partial t} + U_{b_2} \delta_{b_2} \frac{\partial y}{\partial x} \right)$$
$$+ \frac{1}{2} \rho_2 D C_D \left(\frac{\partial y}{\partial t} + U_{b_2} \delta_{b_2} \frac{\partial y}{\partial x} \right) + \left[(m - \rho_2 A + \rho_1 A) g_x + \right.$$
$$\left. \frac{1}{2} \rho_2 U_{b_2}^2 \delta_{b_2} \lambda_2 A / D_h \right] \frac{\partial y}{\partial x} - \left\{ \left[(m - \rho_2 A + \rho_1 A) g_x + \frac{1}{2} \rho_2 U_{b_2}^2 \delta_{b_2} \right. \right.$$
$$\left. \lambda_2 A / D_h + \frac{1}{2} \rho_2 D U_{b_2}^2 \delta_{b_2} C_{f_1} \right] (L - x) + \delta \left[(1 - 2\nu) \overline{pA} + \overline{T} \right]$$
$$- \frac{L}{2} \left[(m - \rho_2 A + \rho_1 A) g_x + \frac{1}{2} \rho_2 U_{b_2}^2 \delta_{b_2} \lambda_2 A / D_h + \frac{1}{2} \rho_2 D U_{b_2}^2 \delta_{b_2} C_{f_1} \right]$$
$$\left. + \frac{1}{2} (1 - \delta) \rho D^2 U_b^2 C_b \delta_b \right\} \frac{\partial^2 y}{\partial x^2}$$
$$+ m \left(\frac{\partial^2 y}{\partial t^2} - g_y \right) = f(x, t) \qquad \text{(2.19 a)}$$

The following set of general boundary conditions can be used for the cylinder,

$$EI \frac{\partial^3 y}{\partial x^3} + k_0 y = EI \frac{\partial^2 y}{\partial x^2} - C_0 \frac{\partial y}{\partial x} = 0 \quad \text{at } x = 0$$
$$EI \frac{\partial^3 y}{\partial x^3} + k_L y = EI \frac{\partial^2 y}{\partial x^2} - C_L \frac{\partial y}{\partial x} = 0 \quad \text{at } x = L \qquad \text{(2.19 b)}$$

where k_0, k_L and C_0, C_L are linear and rotational spring constants respectively. Depending on the values of these all physical boundary conditions can

Equation (2.19 a) can be written in the form

$$\sum_{i=0}^{4}\sum_{j=0}^{2} \alpha_{ij} \frac{\partial^{i+j}}{\partial x^i \partial t^j} = f(x,t) \qquad (2.20\ a)$$

in which the constant term independent of x, y and t has been though of as included in f (x, t).

It can be shown that

$$\alpha_{41} = \mu I \; ; \quad \alpha_{40} = EI \; ; \quad \alpha_{02} = A(\rho_1 + \chi \rho_2) + m$$

$$\alpha_{11} = 2\rho_1 A U_{b_1} \delta_{b_1} + 2\chi \rho_2 A U_{b_2} \delta_{b_2}$$

$$\alpha_{01} = \tfrac{1}{2}\rho_2 D U_{b_2} \delta_{b_2} C_{f_1} + \tfrac{1}{2}\rho_2 D C_D$$

$$\alpha_{10} = [m + (\rho_1 - \rho_2)A] g_x + \tfrac{1}{2}\rho_2 U_{b_2}^2 \lambda_2 \delta_{b_2} A/D_h + \tfrac{1}{2}\rho_2 D U_{b_2}^2 C_{f_1} + \tfrac{1}{2}\rho_2 D U_{b_2} \delta_{b_2} C_D$$

$$\alpha_{20} = \rho_1 A U_{b_1}^2 + \chi \rho_2 A U_{b_2}^2 - \delta[(1-2\nu)\bar{p}A + \bar{T}] - \{m g_x - A[g_x(\rho_2 - \rho_1) - \tfrac{1}{2}\rho_2 U_{b_2}^2 \lambda_2 \delta_{b_2}/D_h] + \tfrac{1}{2}\rho_2 D U_{b_2}^2 \delta_{b_2} C_{f_1}\} [L(1 - \tfrac{\delta}{2}) - x] - \tfrac{1}{2}(1-\delta)\rho D^2 U_b^2 C_b \delta_b$$

All other coefficients ($\alpha_{12}, \alpha_{21}, \alpha_{22}, \alpha_{30}, \alpha_{31}, \alpha_{32}, \alpha_{42}, \alpha_{00}$) are considered to be zero.

II.3 Dimensional Parameters:

In order to bring equation (2.20 a) to a dimensionless form following dimensionless variables are introduced

$$\xi = \frac{x}{L} \qquad \eta = \frac{y}{L} \qquad \text{and} \qquad \tau = \left\{\frac{EI}{A(\rho_1 + \rho_2) + m}\right\}^{\frac{1}{2}} \frac{t}{L^2}$$

So that equation (2.20 a) reduces to

$$\sum_{i=0}^{4}\sum_{j=0}^{2} t_{ij} \frac{\partial^{i+j}\eta}{\partial \xi^i \partial \tau^j} = f_0(\xi, \tau) \qquad (2.21)$$

where

$$t_{40}=1\,;\quad t_{41}=\alpha=\left\{\frac{I}{E(m+\rho_1 A+\rho_2 A)}\right\}\frac{\mu}{L^2}$$

$$f_0(\xi,\tau)=\frac{L^3}{EI}f(\xi,\tau)\,;\quad t_{02}=1+(\chi-1)\beta$$

$$\beta=\rho_2 A/(m+\rho_1 A+\rho_2 A)$$

$$t_{11}=2u_1\delta_{b_1}\beta^{1/2}\rho_{12}^{1/2}+2\chi u_2\delta_{b_2}\beta^{\frac{1}{2}};\quad u_1=\left[\frac{\rho_1 A}{EI}\right]^{\frac{1}{2}}U_{b_1}L\,;$$

$$u_2=\left[\frac{\rho_2 A}{EI}\right]^{1/2}U_{b_2}L\;;\quad \rho_{12}=\rho_1/\rho_2$$

$$t_{01}=\tfrac{1}{2}u_2\delta_{b_2}c_f\beta^{1/2}\epsilon+\tfrac{1}{2}c\epsilon\beta^{1/2};\quad c_f=\frac{4}{\pi}C_f\,,\ c=\frac{4}{\pi}C_D L\left[\frac{\rho_2 A}{EI}\right]^{\frac{1}{2}};\quad \epsilon=\frac{L}{D}$$

$$t_{10}=\tfrac{1}{2}u_2^2c_f\epsilon+\tfrac{1}{2}u_2\delta_{b_2}c\epsilon+\gamma\cos\theta+\tfrac{1}{2}u_2^2\lambda_2\delta_{b_2}\epsilon h\quad\text{where}$$

$$h=D/D_h,\ \theta=\tan^{-1}(g_y/g_x),\ \gamma=(m+\rho_1 A-\rho_2 A)gL^3/EI$$

$$t_{20}=u_1^2+\chi u_2^2-\delta\left[(1-2\gamma)\pi+\Gamma\right]-\left\{\gamma\cos\theta+\tfrac{1}{2}u_2^2\lambda_2\delta_{b_2}\epsilon h\right.$$

$$\left.+\tfrac{1}{2}u_2^2\epsilon c_f\delta_{b_2}\right\}\left(1-\frac{\delta}{2}-\xi\right)-\tfrac{1}{2}(1-\delta)u^2c_{b_2}\delta_b$$

where $\Pi=(\rho_1-\rho_2)AL^2/EI$, $\Gamma=\bar{T}L^2/(EI)$;

$$c_b=\frac{4}{\pi}C_b$$

the last term in the expression for t_{20} is $-\frac{1}{2}(1-\delta)u_2^2c_{b_2}\delta_{b_2}$ or $-\frac{1}{2}(1-\delta)u_1^2c_{b_1}\delta_{b_1}$ depending on the particular case under consideration.

All other coefficients will have zero values.

Equation (2.19b) can be written in dimensionless form

$$\frac{\partial^3\eta}{\partial\xi^3}+K_0\eta=\frac{\partial^2\eta}{\partial\xi^2}-K_0'\frac{\partial\eta}{\partial\xi}=0\quad\text{at }\xi=0$$

$$\frac{\partial^3\eta}{\partial\xi^3}+K_1\eta=\frac{\partial^2\eta}{\partial\xi^2}-K_1'\frac{\partial\eta}{\partial\xi}=0\quad\text{at }\xi=1\qquad(2.22)$$

where

$$K_0 = k_0 L^3/(EI), \quad K_1 = k_1 L^3/(EI)$$

$$K_0' = C_0 L^2/(EI), \quad K_1' = C_1 L^2/(EI)$$

II.4 Response and Stability:

The equation of motion of a cylinder in axial flow, conveying fluid and subjected to an arbitrary force field has been obtained in article II.1. It may be written formally as

$$\mathcal{L}[\eta(\xi,\tau)] = f_0[\xi,\tau] \tag{2.23}$$

where $\mathcal{L}$ is a linear differential operator (equation 2.21). When the force field is generated by the pressure fluctuations on the surface of the cylinder, the force in a given direction is obtained by integrating around the periphery of the cylinder, i.e.

$$f_0(\xi,\tau) = \frac{DL^3}{2EI}\int_0^{2\pi} p(\xi,\theta_1,\tau)\cos\theta_1\, d\theta_1 \tag{2.24}$$

where p is the differential pressure acting over the surface of the cylinder. In order to obtain the response due to an arbitrary force field, the continuous system is transformed into a discrete one by seeking the solution of the type

$$\eta(\xi,\tau) = \sum_r \phi_r(\xi)\, q_r(\tau) \tag{2.25}$$

where $q_r(\tau)$ are the generalized coordinates and $\{\phi_r(\xi)\}$ constitutes complete set of eigenfunctions of the free vibration problem of a beam with

the same boundary conditions as the cylinder without any fluid.

Equation (2.21) then becomes

$$\sum_{r} \sum_{i=0}^{4} \sum_{j=0}^{2} t_{ij}\, \phi_r^{(i)}\, q_r^{(j)} = f_0[\xi, \tau]$$

In expanded form this becomes

$$\sum_{r} \{ t_{41} \lambda_r^4 \phi_r \dot{q}_r + \lambda_r^4 \phi_r q_r + t_{20} \phi_r'' q_r + t_{11} \phi_r' \dot{q}_r + t_{10} \phi_r' q_r + t_{01} \phi_r \dot{q}_r + t_{02} \phi_r \ddot{q}_r \} = f_0(\xi, \tau) \qquad (2.26)$$

where dots denote differentiation with respect to τ and primes those with respect to ξ.

λ_r are the beam eigenvalues corresponding to eigenfunctions ϕ_r satisfying,

$$\frac{d^4 \phi_r}{d\xi^4} = \lambda_r^4 \phi_r \quad , r = 1, 2, \cdots \qquad (2.27\ a)$$

For the boundary conditions considered herein $\{\phi_r\}$ is a self-adjoint set such that,

$$\int_0^1 \phi_r \frac{d^4 \phi_s}{d\xi^4} d\xi = \int_0^1 \phi_s \frac{d^4 \phi_r}{d\xi^4} d\xi \qquad (2.27\ b)$$

and

$$\int_0^1 \phi_r \phi_s d\xi = \delta_{rs} \qquad (2.27\ c)$$

where δ_{rs} is the Kronecker delta.

Multiplying equations (2.26) by ϕ_s, $s = 1, 2, \ldots$ and integrating between the limits 0 and 1 yields

$$\sum_{r} [M_{sr} \ddot{q}_r + C_{sr} \dot{q} + K_{sr} q_r] = Q_s \qquad (2.28)$$

where

$$M_{sr} = t_{02}\,\delta_{sr}$$

$$C_{sr} = t_{41}\,\lambda_r^4\,\delta_{sr} + t_{11}\int_0^1 \phi_r''\,\phi_s\,d\xi + t_{01}\,\delta_{sr}$$

$$K_{sr} = \lambda_r^4\,\delta_{sr} + \int_0^1 t_{20}\,\phi_r''\,\phi_s\,d\xi + t_{10}\int_0^1 \phi_r'\,\phi_s\,d\xi$$

$$Q_s = \int_0^1 \phi_s\,f_0(\xi,\tau)\,d\xi$$

Truncating the summation at r = n, equation (2.28) may be written in matrix form

$$M\ddot{\underset{\sim}{q}} + C\dot{\underset{\sim}{q}} + K\underset{\sim}{q} = \underset{\sim}{Q} \qquad (2.29)$$

n can be chosen to be large enough to determine the response within a desired accuracy. Matrix M is diagonal but C and K are asymmetric matrices due to the presence of Coriolis force terms. Equations (2.29) represent a set of coupled ordinary linear differential equations which is difficult to decouple unless matrix C is a linear combination of matrices M and K, which can occur only in particular cases. For a general case, equations (2.29) can be reduced to a system of first order differential equations as follows:

Pre-multiplying equation (2.29) by M^{-1}

$$\ddot{\underset{\sim}{q}} + M^{-1}C\dot{\underset{\sim}{q}} + M^{-1}K\underset{\sim}{q} = M^{-1}\underset{\sim}{Q} \qquad (2.30)$$

let $\underset{\sim}{z} \triangleq \begin{bmatrix} \underset{\sim}{q} \\ \dot{\underset{\sim}{q}} \end{bmatrix}_{2n\times 1}$

From equation (2.30) one gets $\dot{\underset{\sim}{z}} = B\underset{\sim}{z} + \underset{\sim}{F}$ (2.31)

where

$$B \triangleq \left[\begin{array}{c|c} 0 & I \\ \hline -M^{-1}K & -M^{-1}C \end{array}\right]_{[2n\times 2n]} \quad \underset{\sim}{F} \triangleq \left[\begin{array}{c} 0 \\ \hline M^{-1}\underset{\sim}{Q} \end{array}\right]_{[2n\times 1]}$$

where [0] is the null matrix and [I] is the unity matrix. Equation (2.31) represents a 2n dimensional linear time-invariant dynamical system with system matrix B. Matrix B is generally asymmetric and nonsingular. Premultiplying both sides of vector equation (2.31) by B^{-1}, which is presumed to exist,

$$D\dot{\underset{\sim}{Z}} = \underset{\sim}{Z} + D\underset{\sim}{F} \qquad (2.32)$$

where

$$D = B^{-1}$$

For the vector equation (2.32), if one seeks solution of the type

$$\underset{\sim}{Z} = e^{\mu\tau}\underset{\sim}{u}$$

the eigenvalue problem

$$[D\mu - I]\underset{\sim}{u} = [0] \qquad (2.33)$$

is obtained. The adjoint problem corresponding to equation (2.33) being,

$$[D^{T}\mu - I]\underset{\sim}{v} = [0] \qquad (2.34)$$

In general, the eigenvalues of equations (2.30) are distinct and it can be assumed that 2n eigenvalues of equations (2.33) and (2.34) and associated modal matrices A and N can be obtained such that

$N^T D A = J$ and $N^T A = L$ are diagnoal matri

Reverting now to the non-homogeneous equations (2.32) and letting

$$\underset{\sim}{Z} = A \underset{\sim}{\zeta} \tag{2.35}$$

equation (2.32) becomes

$$DA\dot{\zeta} = A\zeta + D\underset{\sim}{F}$$

premultiplying by N^T,

$$J\dot{\underset{\sim}{\zeta}} = L\underset{\sim}{\zeta} + \underset{\sim}{\Phi} \tag{2.36}$$

where

$$\underset{\sim}{\Phi} = N^T D \underset{\sim}{F}$$

Since matrices J and L are diagonal the system is decoupled. If generalized excitation force Φ is known in deterministic form, the response to the force field may be obtained as

$$\zeta_i(\tau) = \zeta_i(0)\, e^{\mu_i \tau} + \int_0^\tau e^{\mu_i(\tau-h)} \Phi_i(h)\, dh \tag{2.37}$$

and using equations (2.25), (2.31) and (2.35) can be transformed to dimensionless response $\eta(\xi, \tau)$. The first term on right hand side of equation (2.37) represents response due to initial conditions or free response alone. If the system has small perturbations from its quiescent state, eigenvalues μ_i will determine whether the response remains bounded. Eigenvalues μ_i will in general be complex and their real part determines the stability of the system.

When the force field is random but stationary and ergodic, wherein lies the chief interest of this work, the response statistics are obtained as follows.

The space time correlation function of the response is defined as

$$\psi_\eta(\xi,\xi_0,\tau_0) = \langle \eta(\xi,\tau), \eta(\xi+\xi_0,\tau+\tau_0)\rangle$$
$$= \lim_{T\to\infty}\frac{1}{T}\int_0^T \eta(\xi,\tau)\eta(\xi+\xi_0,\tau+\tau_0)\,d\tau$$

which, in view of equations (2.25) and (2.30) may be written as

$$\psi_\eta(\xi,\xi_0,\tau_0) = \lim_{T\to\infty}\frac{1}{T}\int_0^T \sum_{i,j}^{n} \phi_i(\xi) q_i(\tau)\,\phi_j(\xi+\xi_0) q_j(\tau+\tau_0)\,d\tau$$
$$= \lim_{T\to\infty}\frac{1}{T}\int_0^T \sum_{i,j}^{n} \phi_i(\xi)\,\phi_j(\xi+\xi_0) Z_i(\tau) Z_j(\tau+\tau_0)\,d\tau \qquad (2.38)$$

where n is the order of vector equation (2.30). Equation (2.38) can be transformed using Correlation Theorem to yield

$$\psi_\eta(\xi,\xi_0,\tau_0) = \sum_{i,j}^{n} \phi_i(\xi)\phi_j(\xi+\xi_0) \lim_{T\to\infty}\frac{1}{T}\int_{-\infty}^{\infty} Z_i(-\omega) Z_j(\omega)\, e^{i\omega\tau_0}\,d\omega \qquad (2.39)$$

where $\underset{\sim}{Z}(\omega)$ is the Fourier Transform of $\underset{\sim}{Z}(\tau)$. Next, taking Fourier Transform of equations (2.35) and (2.36), respectively,

$$Z_i(\omega) = \sum_{r=1}^{2n} A_{ir}\, \mathcal{Z}_r(\omega) \qquad (a)$$
$$(i\omega J_r - L_r)\,\mathcal{Z}_r(\omega) = \mathcal{F}_r(\omega) \qquad (b) \qquad (2.40)$$

and

where $\mathcal{Z}(\omega)$ is the Fourier Transform of $\underset{\sim}{\zeta}(\tau)$

Also it is convenient to define

$$H_r(\omega) = (i\omega J_r - L_r)^{-1} \tag{2.41}$$

Substitution of equations (2.40) and (2.41) in equation (2.39) gives,

$$\psi_n(\xi, \xi_0, \tau_0) = \sum_{i,j}^{n} \phi_i(\xi)\,\phi_j(\xi+\xi_0) \sum_{r,s}^{2n} A_{ir} A_{js} \lim_{T\to\infty} \frac{1}{2\pi T} \int_{-\infty}^{\infty} H_r(-\omega)\, H_s(\omega)\, \underline{\Phi}_r(-\omega)\, \underline{\Phi}_s(\omega)\, e^{i\omega\tau_0}\, d\omega \tag{2.42}$$

Defining generalized excitation cross spectral density,

$$G_{rs}(\omega) = \lim_{T\to\infty} \frac{1}{T}\, \underline{\Phi}_r(-\omega)\, \underline{\Phi}_s(\omega) \tag{2.43}$$

equation (2.42) may be rewritten as,

$$\psi_n(\xi, \xi_0, \tau_0) = \frac{1}{2\pi} \sum_{i,j}^{n} \phi_i(\xi)\,\phi_j(\xi+\xi_0) \sum_{r,s}^{2n} A_{ir} A_{js} \int_{-\infty}^{\infty} H_r(-\omega)\, H_s(\omega)\, G_{rs}(\omega)\, e^{i\omega\tau_0}\, d\omega \tag{2.44}$$

From which mean square response may be obtained by setting $\xi_0 = \tau_0 = 0$.

Thus,

$$\overline{\eta^2(\xi,\tau)} = \frac{1}{2\pi} \sum_{i,j}^{n} \phi_i(\xi)\,\phi_j(\xi) \sum_{r,s}^{2n} A_{ir} A_{js} \int_{-\infty}^{\infty} H_r(-\omega)\, H_s(\omega)\, G_{rs}(\omega)\, d\omega \tag{2.45}$$

Generalized excitation cross spectral density needs to be examined in detail

$$G_{rs}(\omega) = \lim_{T\to\infty} \frac{1}{T}\, \underline{\Phi}_r(-\omega)\, \underline{\Phi}_s(\omega)$$

$$= \lim_{T\to\infty} \frac{1}{T} \sum_{k,l}^{n} P_{r,n+k}\, P_{s,n+l}\, Q_k(-\omega)\, Q_l(\omega)$$

where $P = N^T D$, so that

$$G_{rs}(\omega) = \lim_{T\to\infty} \frac{1}{T} \sum_{k,\ell}^{n} P_{r,n+k}\, P_{s,n+\ell} \int_0^{\infty}\int_0^{\infty} \phi_k(\xi_1)\phi_\ell(\xi_2)\left[f_0(\xi_1,-\omega) f_0(\xi_2,\omega)\right] d\xi_1 d\xi_2 \quad (2.46)$$

In equation (2.46) the quantity in square brackets is the cross spectral density of dimensionless excitation on the cylinder. In order to study it further, consider the space time correlation function ψ_{f_0}, given by

$$\psi_{f_0}(\xi_1, \xi_2, \tau_0) = \lim_{T\to\infty} \frac{1}{T} \int_0^T f_0(\xi,\tau) f_0(\xi_2, \tau+\tau_0)\, d\tau$$

$$= \lim_{T\to\infty} \frac{1}{T} \frac{D^2 L^6}{4E^2 I^2} \int_0^T \int_0^{2\pi}\int_0^{2\pi} p(\xi_1,\theta_1,\tau)\, p(\xi_2,\theta_2,\tau+\tau_0) \cos\theta_1 \cos\theta_2\, d\theta_1 d\theta_2 d\tau$$

Interchanging the order of integration, which is permissible since integrals are assumed to converge

$$\psi_{f_0}(\xi_1,\xi_2,\tau_0) = \frac{D^2 L^6}{4E^2 I^2} \int_0^{2\pi}\int_0^{2\pi} \left[\lim_{T\to\infty} \frac{1}{T} \int_0^T p(\xi_1,\theta_1,\tau)\, p(\xi_2,\theta_2,\tau+\tau_0)\, d\tau\right] \cos\theta_1 \cos\theta_2\, d\theta_1 d\theta_2$$

$$= \frac{D^2 L^6}{4E^2 I^2} \int_0^{2\pi}\int_0^{2\pi} \psi_p(\xi_1,\xi_2,\theta_1,\theta_2,\tau_0) \cos\theta_1\cos\theta_2\, d\theta_1 d\theta_2 \quad (2.47)$$

Using Correlation Theorem, equation (2.47) can be transformed as

$$\lim_{T\to\infty} \frac{1}{2\pi T} \int_{-\infty}^{\infty} f_0(\xi_1,-\omega) f_0(\xi_2,\omega)\, e^{i\omega\tau_0}\, d\omega$$

$$= \frac{D^2 L^6}{4E^2 I^2} \int_0^{2\pi}\int_0^{2\pi} \lim_{T\to\infty} \frac{1}{2\pi T} \int_{-\infty}^{\infty} p(\xi_1,\theta_1,-\omega)\, p(\xi_2,\theta_2,\omega)\, e^{i\omega\tau_0}\, d\omega \cos\theta_1\cos\theta_2 d\theta_1 d\theta_2$$

Changing the order of integration

$$\lim_{T\to\infty}\frac{1}{2\pi T}\int_{-\infty}^{\infty} f_0(\xi_1,-\omega)\, f_0(\xi_2,\omega)\, e^{i\omega\tau_0}\, d\omega$$

$$= \int_{-\infty}^{\infty}\Bigg[\frac{D^2L^6}{4E^2I^2}\int_0^{2\pi}\int_0^{2\pi}\lim_{T\to\infty}\frac{1}{2\pi T}\, p(\xi_1,\theta_1,-\omega)\, p(\xi_2,\theta_2,\omega)$$

$$\cos\theta_1\cos\theta_2\, d\theta_1\, d\theta_2\Bigg]\, e^{i\omega\tau_0}\, d\omega$$

Comparing both sides

$$\lim_{T\to\infty}\frac{1}{T}\, f_0(\xi_1,-\omega)\, f_0(\xi_2,\omega) = \frac{D^2L^6}{4E^2I^2}\int_0^{2\pi}\int_0^{2\pi}\lim_{T\to\infty} p(\xi_1,\theta_1,-\omega)$$

$$p(\xi_2,\theta_2,\omega)\cos\theta_1\cos\theta_2\, d\theta_1 d\theta_2$$

$$= \frac{D^2L^6}{4E^2I^2}\int_0^{2\pi}\int_0^{2\pi}\Gamma_{pp}(\xi_1,\theta_1,\xi_2,\theta_2,\omega)\cos\theta_1\cos\theta_2\, d\theta_1 d\theta_2 \qquad (2.48)$$

where $\Gamma_{pp}(\xi_1,\theta_1,\xi_2,\theta_2,\omega)$ is the cross spectral density of the differential pressure. In the experimental results available so far, this quantity has been studied extensively.

Substituting equation (2.48) in equation (2.46)

$$\mathcal{L}_{rs}(\omega) = \frac{D^2L^6}{4E^2I^2}\sum_{k,\ell}^{n} P_{r,n+k}\, P_{s,n+\ell}\int_0^1\int_0^1 \phi_k(\xi_1)\,\phi_\ell(\xi_2)$$

$$\int_0^{2\pi}\int_0^{2\pi}\Gamma_{pp}(\xi_1,\xi_2,\theta_1,\theta_2,\omega)\cos\theta_1\cos\theta_2\, d\theta_1 d\theta_2 d\xi_1 d\xi_2$$

$$= \frac{D^2L^6}{4E^2I^2}\sum_{k,\ell}^{n} P_{r,n+k}\, P_{s,n+\ell}\, E_{k\ell}(\omega) \qquad (2.49)$$

where

$$E_{kl}(\omega) = \int_0^1 \int_0^1 \phi_k(\xi_1)\,\phi_l(\xi_2)\,\Gamma_p(\xi_1, \xi_2, \omega)\,d\xi_1\,d\xi_2 \qquad (2.50a)$$

and

$$\Gamma_p(\xi_1, \xi_2, \omega) = \int_0^{2\pi} \int_0^{2\pi} \Gamma_{pp}(\xi_1, \xi_2, \theta_1, \theta_2, \omega)\cos\theta_1 \cos\theta_2\,d\theta_1\,d\theta_2 \qquad (2.50b)$$

Thus, for the case when excitation is due to wall pressure fluctuations, the space time correlation function or spectral density of the response can be obtained if the wall pressure correlation function or cross spectral density is known, along with various coefficients used in expressing fluid forces on the cylinder. The latter must be specified in order to obtain either eigenvalues or response. The response obtained here is a linear mapping of random wall pressure field into idealized two dimensional response field. In the excitation considered here, the fluctuations in the wall shear stresses have been discounted since their component in the direction of motion of the cylinder, in any case, be negligible. In actual practice the motion will not be planar due to Coriolis forces and some torsional deformation will occur. In this formulation, other types of excitations, e.g. structure-borne vibration, can be accommodated easily. In this work, however, chief interest lies in studying stability and response due to turbulence originated excitation alone. Other types of excitation like structure-borne vibration, the

parametric one arising from pulsations in the flow rate and consequential wall pressure, are characteristics of each particular situation and therefore offer little motivation for the study.

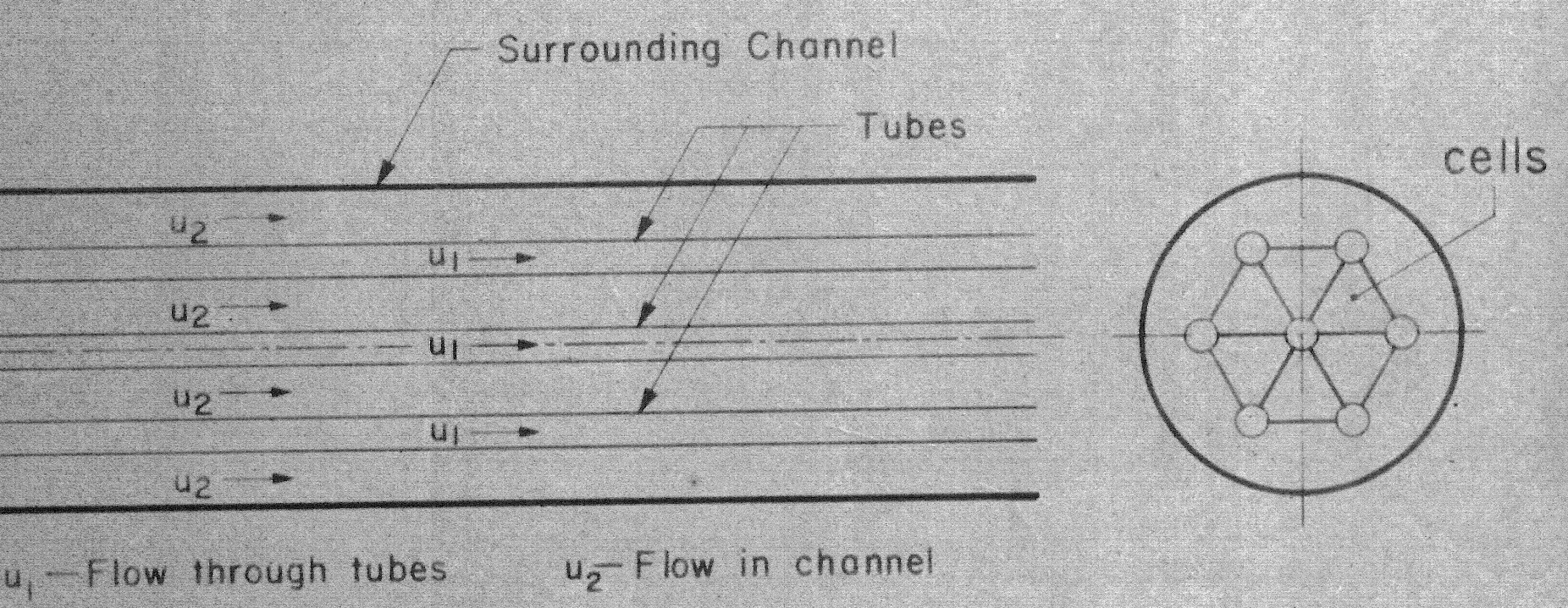

u_1 — Flow through tubes u_2 — Flow in channel

g. 2.1 Ideallized arrangement in parrallel flow heat exchanger

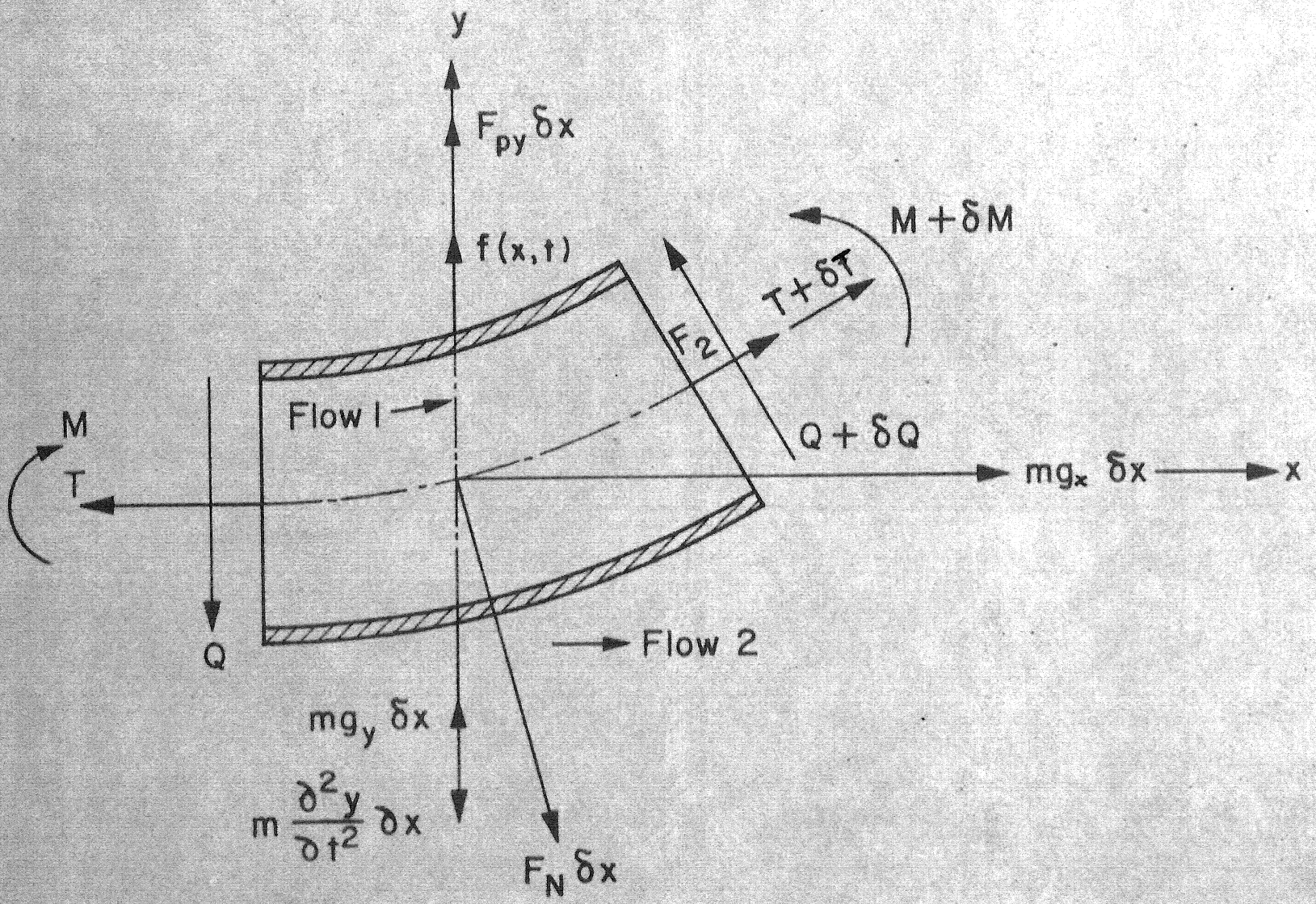

g. 2.2 (a) Forces and Moments on a Section of Cylinder

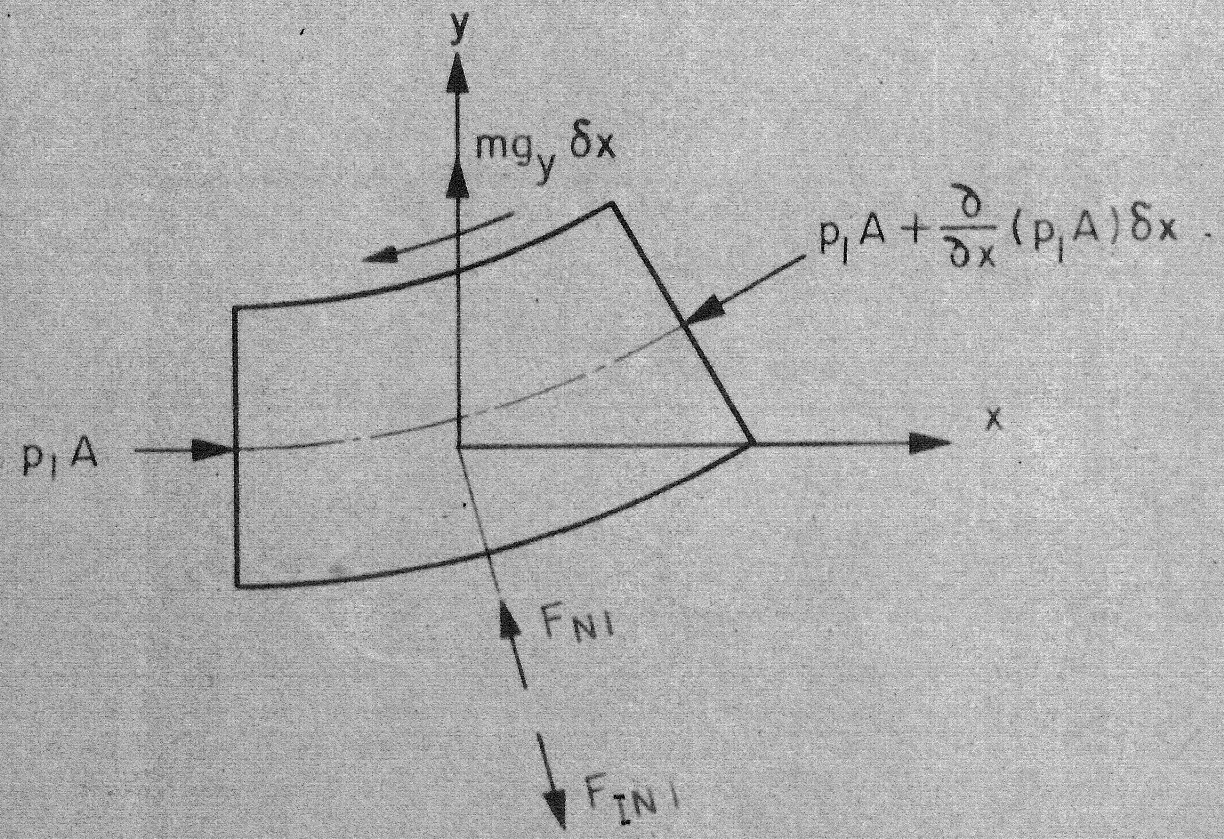

Fig 2.2(b) Forces on a section of inner fluid

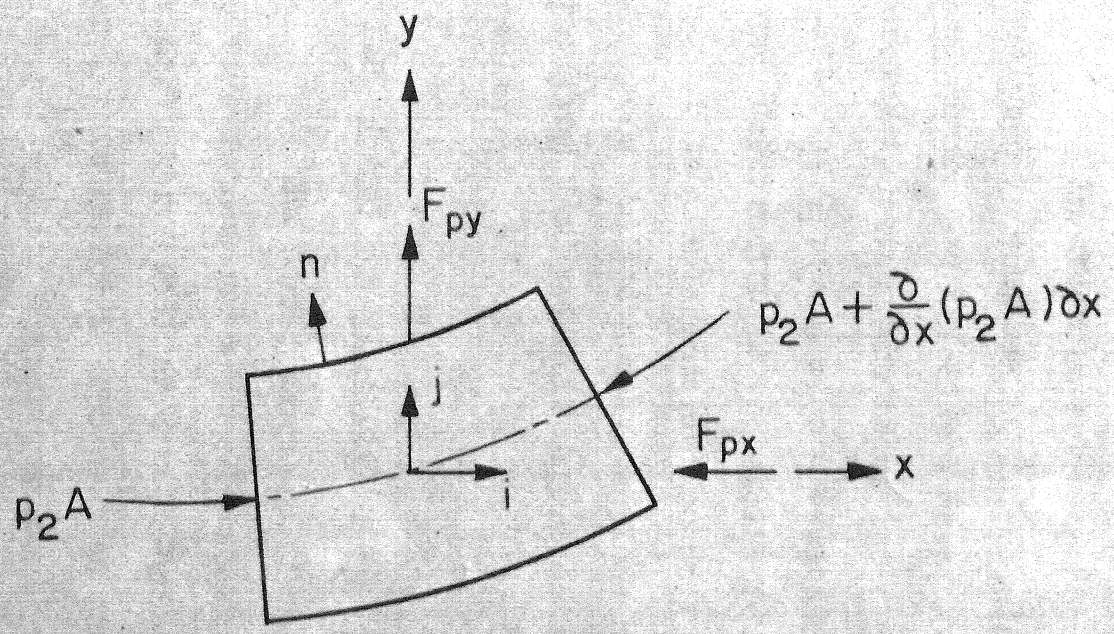

Fig. 2.3 Forces on a Section due to mean fluid pressure

CHAPTER III

THE FLUID INTERACTION PARAMETERS

III.1 Introduction:

In order to solve the equation of motion (2.20) developed in Chapter II, for obtaining free vibration frequencies and associated damping or response to arbitrary forcing function, one needs the fluid interaction coefficients C_d, C_f, χ, C_b and excitation f_o (or its statistical description if the excitation is random). In this chapter the fluid interaction coefficients C_d, C_f and χ have been studied and expressions have been derived for them from the available experimental and theoretical results.

III.2 Normal Drag Coefficient:

The Normal Drag Coefficient C_d has been introduced to take into account the viscous drag when the outer flow is negligibly small or zero. For a general case considered here, this factor will depend on the geometry of the flow passage and Reynolds number. For a general geometry this factor has not been studied in detail either theoretically or experimentally. In the absence of direct measurements one can obtain the average value of this

coefficient from the measurements of viscous damping due to stationary fluid or at small flow rates. Such measurements have been made by Chen and Wambsganss [67], Pavlica and Marshall [23, 32] and McCormic and Rippley [69]. Here an attempt has been made to derive the dependence of this coefficient on fluid flow induced damping measurements at small or zero flow rates. From the analysis, the coefficient C_d has been evaluated for annular flow geometry. For simplicity, the coefficient C_d will be assumed to be independent of Reynolds number. With these assumptions consider equation (2.21) with

$f_o = u_1 = \Pi = \Gamma = \gamma = 0$ and $\delta_{b_2} = 1$,

$$\alpha \frac{\partial^5 \eta}{\partial \xi^4 \partial \tau} + \frac{\partial^4 \eta}{\partial \xi^4} + t'_{11} \frac{\partial^2 \eta}{\partial \xi \partial \tau} + t'_{20} \frac{\partial^2 \eta}{\partial \xi^2} + t_{02} \frac{\partial^2 \eta}{\partial \tau^2} + t_{10} \frac{\partial \eta}{\partial \xi} + t_{01} \frac{\partial \eta}{\partial \tau} = 0 \qquad (3.1)$$

where the coefficients t' are evaluated with $u_1 = \Pi = \Gamma = \gamma = 0$, $\delta_{b_2} = 1$.

Let us assume a solution of the type

$$\eta(\xi, \tau) = F(\xi) e^{i\omega\tau} \qquad (3.2)$$

Substitution of equation (3.2) in equation (3.1) leads to

$$\alpha i\omega F^{IV} + F^{IV} + i\omega t'_{11} F' + t'_{20} F'' - \omega^2 t_{02} F + t_{10} F' + i\omega t_{01} F = 0 \qquad (3.3)$$

For the case when velocity $u_2 \to 0$, let

$$F = F_o + u_2 F_1 + u_2^2 F_2 + \cdots \qquad (a)$$

$$\omega = \omega_o + u_2 \omega_1 + u_2^2 \omega_2 + \cdots \qquad (b) \qquad (3.4)$$

$$\zeta = \zeta_o + u_2 \zeta_1 + u_2^2 \zeta_2 + \cdots \qquad (c)$$

where ζ is the damping factor associated with the first mode. Substituting equations (3.4 a,b) in equation (3.3) equating the coefficients of the terms containing u_2^o

$$i\alpha\omega_o F_o^{IV} + F_o^{IV} - t_{o2}\omega_o^2 F_o + \tfrac{1}{2} c\varepsilon\beta^{1/2} i\omega_o F_o = 0$$

or

$$F_o^{IV} - D_o^2 F_o = 0 \qquad (3.5)$$

where

$$D_o^2 = (t_{o2}\omega_o^2 - \tfrac{1}{2} i\omega_o \varepsilon\beta^{1/2} c)/(1+i\alpha\omega_o)$$

Equating the terms containing u_2^1,

$$i\alpha\omega_o F_1^{IV} + F_1^{IV} - t_{o2}\omega_o^2 F_1 + \tfrac{1}{2} ic\varepsilon\beta^{1/2}\omega_o F_1 = -i\alpha\omega_1 F_o^{IV}$$
$$-2i\chi\beta^{1/2}\omega_o F_o' + 2\omega_o\omega_1 t_{o2} F_o - \tfrac{1}{2} c\varepsilon F_o' - \tfrac{1}{2} i\omega_o c_f$$
$$\beta^{1/2}\varepsilon F_o - \tfrac{1}{2} i\omega_1 c\varepsilon\beta^{1/2} F_o$$

i.e.

$$F_1^{IV} - D_o^2 F_1 = [-i\alpha\omega_1 F_o^{IV} + (2\omega_o\omega_1 t_{o2} - \tfrac{1}{2} i\omega_o c_f\beta^{1/2}\varepsilon \qquad (3.6)$$
$$-\tfrac{1}{2} i\omega_1 c\varepsilon\beta^{1/2}) F_o - (2i\chi\beta^{1/2}\omega_o + \tfrac{1}{2} c\varepsilon) F_o'] / (1+i\alpha\omega_o)$$

Since F_o must satisfy the same boundary conditions as those for ϕ in equation (4.2)

$$D_{or} = \lambda_r^2, \quad r = 1, 2, \ldots$$

From this we obtain the first mode complex frequency, using equation (3.5)

$$\omega_{01} = \tfrac{1}{2}\left[i\left(\tfrac{1}{2} c\varepsilon\beta^{1/2} + 4\lambda_1^2\right) \pm \left\{4\lambda_1^4 - \left(\tfrac{1}{2} c\varepsilon\beta^{1/2} + 4\lambda_r^4\right)^2\right\}^{1/2}\right] / t_{o2}$$

The damping factor associated with the first mode at $u_2 = 0$ and for the case $\alpha = 0$ is now obtained as

$$\zeta_o = \frac{c\varepsilon\beta^{1/2}}{4\lambda_1^2\sqrt{t_{o2}}} \qquad \text{for all boundary conditions} \qquad (3.7)$$

Multiplying equation (3.6) by F_o and integrating with respect to ξ between the limits 0 and 1 leads to

$$\left[\left(2\omega_o\omega_1 t_{o2} - \tfrac{1}{2} i\omega_o c_f \beta^{1/2}\xi - \tfrac{1}{2} i\omega_1 c\varepsilon\beta^{1/2}\right)\int_o^1 F_o^2 dx\right] - \tfrac{1}{2}\left(2i\chi\beta^{1/2}\omega_o + \tfrac{1}{2}c\varepsilon\right) F_o^2\Big|_o^1 = 0$$

if $F(o) = F(1) = 0$, then for the case $\alpha = 0$, the contribution to the first mode complex frequency is given by

$$\omega_1 = \frac{\frac{1}{2}\varepsilon c_f \beta^{1/2}\omega_o}{2t_{o2}\omega_o - \frac{1}{2} ic\varepsilon\beta^{1/2}}$$

which gives the contribution to the damping factor associated with the first mode

$$\zeta_1 = \frac{c\varepsilon\beta^{1/2}}{4\eta_1^2\sqrt{t_{o2}}} \qquad (3.8)$$

If $F(0) = 0$ but $F(1) \neq 0$, then

$$\omega_1 = \frac{\frac{1}{2} i\varepsilon c_f \beta^{1/2}\omega_o + \frac{1}{2}\left(2i\chi\beta^{1/2}\omega_o + \frac{1}{2}c\varepsilon\right) F_o^2(1) \Big/ \int_o^1 F_o^2 dx}{2t_{o2}\omega_o - \frac{1}{2} ic\varepsilon\beta^{1/2}} \qquad (3.9)$$

From equation (3.9) it can be observed that the Coriolis force term can promote damping only when displacement at one end is nonzero.

In order to find the dimensionless parameter C and consequently viscous drag coefficient C_D, the first mode damping factor measurements by Chen and Wambsganss [67] were used. These measurements were made by a) bandwidth method, b) magnification method with constant force and c) magnification method with constant

isplacement. The dependence of the first mode damping factor on the velocity of flow was measured by applying external electromagnetic excitation to a cylindrical beam with clamped-clamped and pinned-pinned ends. The method of applying excitation did not disturb the flow and the displacement of the beam was observed by optical means for three different confinement ratios (n = 0.33, 0.5 and 1.0). For the annular flow geometry these experimental results were relied upon. The curves of the first mode damping factor against the velocity of the flow were approximated by a quadratic polynomial for the interval $u_2 = 0$ to 0.5, and an expression for C_D was obtained as

$$\frac{C_D D}{\nu_2} = \varepsilon\left(1120.5678\, d_{12}^2 - 681.13601\, d_{12} + 123.4916\right)$$

where d_{12} = radius ratio = $h/(1+h)$

$\bar{\nu}_2$ = dimensionless kinematic viscosity of the fluid

= kinematic viscosity $\cdot \sqrt{\frac{\rho_2 A}{EI}}$

The above expression is applicable to a single rod supported in a circular channel, for the range of confinement ratio $1.0 \geq h \geq 0.33$.

For an isolated cylinder ($d_{12} \rightarrow 0$) C_d was computed from cross flow normal drag coefficient, which for low Reynolds numbers, can be approximated as

$$C_D' \approx 10.0/Re$$

where Re = Reynolds number based on the diameter of the cylinder

C_D' = Drag coefficient = Drag Force $/\frac{1}{2}\rho U^2 DL$

from which

$$C_D \approx \frac{10.0}{D}\nu_2$$

so that

$$C \approx 12.72\,\varepsilon\,\bar{\nu}_2$$

where $\bar{\nu}_2$ = dimensionless kinematic viscosity of the fluid

$$= \nu_2\sqrt{\frac{\rho_2 A}{EI}}$$

Since C_D has been assumed to be independent of Reynolds number, following form of functional relationship has been assumed

$$\frac{C_D D}{\nu_2} = f(\varepsilon, h) \qquad \text{or constant}$$

In the above relationship the constant on the right hand side was assumed to be 10.0 for an isolated cylinder.

Since only a space averaged value of the coefficient C_D is required to account for the normal form drag, these expressions were thought to be adequate for further use.

III.3 Skin Friction Coefficient C_f

Overall friction factor λ has been measured by numerous researchers for various channel geometries. Direct measurement of the skin friction coefficient C_f is difficult. Both coefficients vary with Reynolds number but for Reynolds numbers greater than 10^5 the variation is small. The measurements of friction factor for annular flow by Lawn and Elliott [70] and Rehme [71] indicate that the overall friction factor is greater than that for a circular pipe of equal hydraulic diameter by upto 5% (depending on the radius ratio d_{12}), for all Reynolds numbers. The skin friction coefficients for inner and outer wall, C_{f_1} and C_{f_2} respectively, can be found if zero shear stress radius is known. Since the flow is radially asymmetric the radius of maximum shear stress and the one of maximum velocity differ, the difference being more for smaller radius ratios. Rehme [71] collected the experimental data of several other researchers for annular flow and found that these radii correlate as

$$d_m/d_2 = d_{12}^{0.343}$$

and

$$d_o/d_2 = d_{12}^{0.386}$$

where d_m = maximum velocity radius

d_o = zero shear stress radius

d_2 = diameter of outer cylinder

d_1 = diameter of inner cylinder

The skin friction coefficients can be estimated by using the laminar flow ratio

$$\frac{\tau_1}{\tau_2} = \frac{d_2(d_o^2 - d_i^2)}{d_1(d_2^2 - d_o^2)} \qquad (3.11)$$

using equivalent friction coefficient for the annulas

$$C_f = \frac{d_1 C_{f_1} + d_2 C_{f_2}}{d_1 + d_2}$$

one gets

$$\frac{C_{f_2}}{C_f} = \frac{1 - d_o^2/d_2^2}{1 - d_1/d_2}$$

which gives the inner wall friction coefficient C_{f_1}.

For computational purposes, the overall friction factor λ for confined flows was first found from Colebrook-White Relationship [58]

$$\frac{1}{\sqrt{\lambda}} = 1.74 - 0.87 \ln\left(\frac{2k}{d_h} + \frac{18.6}{Re\sqrt{\lambda}}\right) \qquad (3.12)$$

where k = equivalent surface roughness $= \frac{k_1 d_1 + k_2 d_2}{d_1 + d_2}$ for an annulas

$= \frac{k_2 d_2 + n_r k_1 d_1}{d_2 + n_r d_1}$ for a cluster of rods,

d_1 denoting rod diameter and d_2 the channel diameter.

The friction factor λ obtained by equation (3.12) was increased by 4% for annular flow geometry irrespective of radius ratio, since exact dependence of λ on radius ratio is not yet clearly established.

III.4 Added Mass Coefficient

The added mass for a body moving in a fluid arises from the hydrodynamic force required for accelerating the fluid replaced by the body. It is somewhat like a form drag in inviscid fluid. Generally, the added mass of a cylindrical rod is assumed to be equal to the mass of fluid replaced by the rod. This is true for a rod submerged in an infinite fluid. However, in a cluster of rods, the added mass is affected by adjacent rods and channel wall. The added mass increases with the increase in confinement. Chen and Wambsganss [67] have computed the added mass coefficient χ for a single rod in a channel. Chen [68] has shown that the added mass for a cluster of circular cylinders is a second order tensor. The added mass coefficients can be obtained in the form of a series solution. In general, the self added mass coefficient for the central rod in a cluster is much larger compared to the one for the same rod in an annulas of equal confinement ratio h. The results of Chen and Wambsganss show that the added mass coefficient is a strong function of confinement ratio h but weak function of sound velocity and frequency.

In this work, for the computational purposes, the added mass coefficient was computed using the expressions given by Chen and Wambsganss [67] for a single rod in a circular channel. For an isolated cylinder

this coefficient was taken to be unity while for a cluster of cylinders this coefficient was either assumed or taken to be the same as the one for an annulas of equal confinement ratio, since the explicit expressions for the added mass coefficients in terms of series solutions have not been given by Chen [68].

Since the response of the cylinder due to the flow originated excitation was not computed, the statistical model for the random pressure field at the wall was not necessary. Next chapter briefly outlines the computational method used to study the stability of the cylinders using the fluid interaction parameters studied in this chapter.

CHAPTER IV

COMPUTATIONAL APPROACH

This chapter briefly deals with the computational method used to obtain the numerical results.

IV.1 Characteristic Equations and Eigenfunctions:

Solution of the governing equation (2.23) using Galerkin Method requires the set of eigenfunction to be used as coordinate functions. These were computed from the "abbreviated" eigenvalue problem,

$$\frac{d^4\phi}{d\xi^4} = \lambda^4\phi \tag{4.1}$$

Subject to the boundary conditions (equation 2.22)

$$\left.\begin{aligned} \phi''' + K_0\phi = \phi'' - K_0'\phi' = 0 \quad \text{at } \xi = 0 \\ \phi''' + K_1\phi = \phi'' - K_1'\phi' = 0 \quad \text{at } \xi = 1 \end{aligned}\right\} \tag{4.2}$$

Eigenvalue problem defined by equation (4.1) and (4.2) is self adjoint and yields a set of eigenfunctions $\{\phi_r\}$ satisfying

$$\int_0^1 \phi_r \frac{d^4\phi_s}{d\xi^4}\, d\xi = \int_0^1 \phi_s \frac{d^4\phi_r}{d\xi^4}\, d\xi \tag{4.3}$$

and

$$\int_0^1 \phi_r \phi_s\, d\xi = M_r \delta_{rs} \tag{4.4}$$

For the actual computation solution of equation (4.1) is taken as

$$\phi(\xi) = C_1 \sin\lambda\xi + C_2 \cos\lambda\xi + C_3 \sinh\lambda\xi + C_4 \cosh\lambda\xi \qquad (4.5)$$

Substituting equation (4.5) into equations (4.2) one obtains a system of linear equations

$$\begin{bmatrix} -\lambda^3 & K_0 & \lambda^3 & K_0 \\ K_0' & \lambda & K_0' & -\lambda \\ K_1 \sin\lambda - \lambda^3 \cos\lambda & K_1 \cos\lambda + \lambda^3 \sin\lambda & K_1 \sinh\lambda + \lambda^3 \cosh\lambda & K_1 \cosh\lambda + \lambda^3 \sinh\lambda \\ -\lambda \sin\lambda - K_1' \cos\lambda & -\lambda \cos\lambda + K_1' \sin\lambda & \lambda \sinh\lambda - K_1' \cosh\lambda & \lambda \cosh\lambda - K_1' \sinh\lambda \end{bmatrix} \begin{bmatrix} C_1 \\ C_2 \\ C_3 \\ C_4 \end{bmatrix} = \begin{bmatrix} 0 \\ 0 \\ 0 \\ 0 \end{bmatrix} \qquad (4.6)$$

For nontrivial solution, setting the determinant of the coefficient matrix in equation (4.6) to zero yields the characteristic equation which may be written as

$$\Delta(K_0, K_0', K_1, K_1', \lambda) = 0 \qquad (4.7)$$

The roots of the transcendental equation (4.7) can be found for any desired number of eigenvalues. Once the eigenvalues are found C_n (n = 1, 2, 3) can be found in terms of C_4. In order to have definite numerical values for C_n, the orthonormality condition for the eigenfunctions can be imposed. Thus,

$$\int_0^1 \phi_i \phi_j \, d\xi = \delta_{ij} \qquad (4.8)$$

which simplifies further computation as well. For various standard boundary conditions equation (4.7) simplifies as follows:

1. Pinned-Pinned End Conditions: $(K_0 = K_1 = \infty ; K_0' = K_1' = 0)$

Characteristic equation $\Delta(\lambda) = \sin\lambda = 0$ (a)

eigenfunctions $\phi_r(\xi) = \sqrt{2}\sin r\pi\xi, \quad r = 1, 2, \cdots$ (b) (4.9)

2. Clamped-Clamped End Conditions: $(K_0 = K_1 = K_0' = K_1' = \infty)$

Characteristic equation $\Delta(\lambda) = 1 - \cos\lambda\cosh\lambda = 0$ (a)

and eigenfunctions (unnormalized), (4.10)

$$\phi(\xi) = C_1\sin\lambda\xi + C_2\cos\lambda\xi + C_3\sinh\lambda\xi + C_4\cosh\lambda\xi \quad \text{(b)}$$

where

$$C_4 = 1, C_2 = -1, C_3 = -C_1, \quad C_1 = \frac{\cos\lambda - \cosh\lambda}{\sin\lambda - \sinh\lambda}$$

3. Clamped-Free End Conditions: $(K_0 = K_0' = \infty, K_1 = K_1' = 0)$

Characteristic equation $\Delta(\lambda) = 1 + \cos\lambda\cosh\lambda = 0$ (a)

and eigenfunctions (4.11)

$$\phi(\xi) = C_1\sin\lambda\xi + C_2\cos\lambda\xi + C_3\sinh\lambda\xi + C_4\cosh\lambda\xi \quad \text{(b)}$$

where

$$C_4 = 1, C_2 = -1, C_3 = -C_1, \quad C_1 = \frac{\sinh\lambda - \sin\lambda}{\cos\lambda + \cosh\lambda}$$

4. Partially Fixed End Conditions: $(K_0 = K_1 = \infty)$

When ends are fixed in such a manner that the transverse displacement is completely restricted but slight rotation is permissible, the situation commonly found in practical assemblies like shell and tube heat exchangers, fuel rod bundles etc., this is appropriate boundary condition. For this case, characteristic equation

$$\Delta(\lambda) = \lambda(\sin\lambda\cosh\lambda - \cos\lambda\sinh\lambda)(K_0' + K_1') + 2\lambda^2\sin\lambda\sinh\lambda + K_0'K_1'(1 - \cos\lambda\cosh\lambda) = 0 \quad \text{(a)}$$

and eigenfunctions

$$\phi(\xi) = C_1 \sin\lambda\xi + C_2 \cos\lambda\xi + C_3 \sinh\lambda\xi + C_4 \cosh\lambda\xi \quad \text{(b)} \qquad (4.12)$$

where $C_4 = 1$, $C_2 = -1$

$$C_1 = [\cos\lambda - \cosh\lambda - 2\lambda(\sinh\lambda)/K_0'] / (\sin\lambda - \sinh\lambda)$$

and $$C_3 = 2\lambda/K_0' - C_1$$

when $K_0', K_1' \to \infty$, equations (4.12) simplify to corresponding equations (4.10), as they should.

5. <u>One End Partially Fixed, other Free</u>: ($K_0 = \infty, K_1 = K_1' = 0$)

This boundary condition can be used for a cylinder free at one end and fixed at the other end in such a way that the transverse displacement is prevented while allowing some rotation.

For this case characteristic equation is given by

$$\Delta(\lambda) = \lambda^3(\sin\lambda\cosh\lambda - \cos\lambda\sinh\lambda) - K_0'(1 + \cos\lambda\cosh\lambda) = 0 \quad \text{(a)}$$

and eigenfunctions by (4.13)

$$\phi(\xi) = C_1 \sin\lambda\xi + C_2 \cos\lambda\xi + C_3 \sinh\lambda\xi + C_4 \cosh\lambda\xi \quad \text{(b)}$$

where $C_4 = 1$, $C_2 = -1$

$$C_1 = \left(\cos\lambda + \cosh\lambda + \frac{2\lambda\sinh\lambda}{K_0'}\right) / (\sin\lambda + \sinh\lambda)$$

and $$C_3 = 2\lambda/K_0' - C_1$$

Equations (4.13) simplify to corresponding equations (4.11) when $K_0' = \infty$, as they should.

In this work only five end conditions of the above type were studied. The eigenvalues were computed using a combination of internal halving and linear interpolation method since eigenvalues are well separated. The coefficients $\{C_n\}$ were normalized according tc equation (4.8).

IV.2 Galerkin Matrices:

For computing Inertia, stiffness and damping matrices appearing in equation (2.28) one needs to compute the integrals $\int_0^1 \phi_i' \phi_j \, d\xi$, $\int_0^1 \phi_i'' \phi_j \, d\xi$, and $\int_0^1 \xi \phi_i'' \phi_j \, d\xi$, the last one due to appearance of a linear term in in the expression for the coefficient t_{20} in equation (2.21). These were obtained using exact closed form formulae without resorting to numerical quadrature. In order to retain the desired precision, the eigenvalues λ_i, i = 1, 2, ... and coefficients C_r, r = 1, 2, ... were computed using double precision arithmetic. In order to expedite and thus economise the computation, following relations for boundary conditions of type 1, 2 and 4 were used.

$$G^1_{ji} = \int_0^1 \phi_j' \phi_i \, d\xi = -\int_0^1 \phi_i' \phi_j \, d\xi = -G^1_{ij} \qquad \text{(a)}$$

$$G^2_{ji} = \int_0^1 \phi_j'' \phi_i \, d\xi = \int_0^1 \phi_j'' \phi_i \, d\xi = G^2_{ij} \qquad \text{(b)}$$

$$G^3_{ji} = \int_0^1 \xi \phi_j'' \phi_i \, d\xi = \int_0^1 \xi \phi_i'' \phi_j \, d\xi + 2\int_0^1 \phi_i' \phi_j \, d\xi \quad (c) \qquad (4.14)$$
$$= G^3_{ij} + 2 G^1_{ij}$$

IV.3 System Matrix and Eigenvalues:

The fluid parameters such as coefficients C, C_f, λ and χ were computed as described in chapter III and dynamic matrix B appearing in equation (2.31) was computed using these. It was then inverted using Gauss-Jordan technique so that the eigenvalues to be computed would appear in the desired sequence. For computing the complex eigenvalues of the Matrix D two different methods were used. When both real and imaginary parts of all the eigenvalues were nonzero a method which is a combination of Mises power method and Hotelling's deflation technique [72, 73], appropriately specialized for complex eigenvalues and eigenvectors, was used. The matrix deflation technique requires construction of sweeping matrix. It was computed using Gauss Jordan technique for matrix inversion, to retain the significance in desired eigenvalues and eigenvector. Magnitude of the eigenvector was controlled during every iteration so that the quantities did not grow rapidly and precision was

retained. Since only first three modes were considered power method proved fast; further while computing eigenvalues.one obtains the modal matrices for the system and adjoint system as well. This enables the computation of response due to arbitrary force field by modal analysis.

When an eigenvalue was pure real or imaginary the eigenvalues were computed by a different method. The computational procedure switched to this method as soon as one of the eigenvalues approached close to real or imaginary axis. In this method [74] the eigenvalues were computed by QR double step method and eigenvectors by inverse iteration. The matrix was first scaled by a sequence of similarity transformations so that the absolute sums of corresponding rows and columns are roughly equal. The scaled matrix was then normalized so that Euclidean norm equals unity. The main part of the computational procedure consisted of the reduction of the matrix to upper-Hessenberg form by means of similarity transformations using Householder's method. Then the QR double step iteration was performed on the Hessenberg matrix until all elements of the subdiagonal converge to zero or in modulus less than $2^{-27} \| H \|_E$. The eigenvalues were then extracted from this reduced form. For computing the eigenvector inverse iteration was performed on the upper Hessenberg matrix until the

absolute value of the largest component of the right hand side vector was greater than $2^{27}/(100\ n)$ where n was the order of the matrix. After this bound was achieved one more step was performed but at each step if the computed residuals were greater in absolute value than those of the previous step then the vector of the previous step was accepted as the computed eigenvector.

The principal aim of the computational program was to compute the response due to turbulent flow induced excitation, therefore Galerkin method was used in spite of other simpler and faster methods to compute the eigenvalues alone. The stability study was thought of as a part of the general programme for the study of flow induced vibration of cylindrical structural elements.

CHAPTER V

RESULTS AND DISCUSSION

V.1 Introduction:

This chapter deals with the numerical results obtained for some of the cases of practical interest. Dimensionless complex frequencies of the lowest three modes have been found as functions of the velocity of internal or external flow. The mechanism underlying the onset of various types of instabilities has been discussed from the analytical point of view. The significance of Coriolis forces has been examined.

In all the figures of this chapter, square roots of real and imaginary frequencies have been plotted on a linear scale and only magnitudes of imaginary part of the complex frequencies have been considered, so that frequencies of all three modes can be shown in a compact figure for convenience of scaling the results. In cases where parameters have been mentioned, they were held constant irrespective of varying Reynolds number. For all these studies dimensionless viscosity has been taken to be 10^{-5} and densities of inner and outer fluid to be equal. Wherever necessary, the loci of the roots which lie on axis or overlap each other are shown schematically along the axis, for the sake of clarity.

V.2 Isolated Pinned-Pinned Cylinder

Figure (5.1) shows the loci of the dimensionless complex frequencies of a pinned-pinned cylinder with external velocity, u_2, as parameter. The other parameters are $\beta = 0.1, \epsilon c_f = \delta = \chi = 1, \alpha = h = \gamma = \Gamma = \Pi = c = 0$ (see reference 48, figure 3). It can be seen that small flow velocities act to damp free oscillations of the cylinder. As the flow velocity increases the system may become unstable in all the three modes. The locus of the first mode bifurcates on the Re (ω) axis, one branch receeding from the origin and other approaching and eventually crossing it at $u_2 \approx 3.14$; this evidently indicates buckling instability - ($\omega = 0$). The instability associated with the second mode, on the other hand, which occurs at $u_2 \approx 5.99$, is oscillatory, As the velocity is increased further, the locus of the second mode bifurcates on the Re (ω) axis at $u_2 \approx 6.27$. At slightly higher flow velocity, $u_2 \approx 6.33$, the positive branches of first and second mode loci coalesce and leave the Re (ω) axis at a point where Re (ω) > 0, indicating the onset of coupled mode flutter. The other branches of these modes behave similarly, leaving the axis where Re (ω) < 0. Since the frequencies were computed for $u_2 \leq 9$ the third-mode buckling observed in reference [48], (which occured at $u_2 \approx 9.46$) does not appear in Fig.(5.1). The second mode flutter, which sets in at $u_2 \approx 5.99$ is

notably absent in Fig.(3)of reference [48], according to which the system loses stability in the second mode first by buckling and then by coupled-mode flutter as opposed to ordinary flutter. These differences are due to correct manner of accounting for the frictional forces in the present investigation.

When fluid parameters are allowed to vary, similar results were obtained, as shown in Figure(5.2), except that the critical velocities are different, evidently due to the inclusion of parameter **c**, which has been taken equal to zero for Figure (5.1).

In order to study the effect of internal flow the cylinder corresponding to Figure(5.1)has been considered as a tube with internal flow with velocity $u_1 = 0.5$. The complex frequencies of the lowest three modes are shown in Figure (5.3). The fluid parameters were held constant. It can be observed that the dynamical behaviour is similar, but the critical velocities are now smaller. The results, when the fluid parameters are allowed to vary with the flow velocity, are shown in Figure (5.4). From Figures (5.3) and (5.4), it is obvious that the internal flow destabilizes the cylinder. Parameters of Figures (5.5) and (5.6) correspond to those of Figures (5.3) and (5.4) respectively, except that the direction of the internal flow is reversed. The character of the frequency diagrams is

similar but the critical flow velocities for oscillatory type of instabilities are higher. The internal flow in direction opposite to the outer flow, thus, appears to stabilize the cylinder; critical velocities for buckling however remain unchanged.

The dynamic behaviour discussed above is not unique. The complex frequencies for a pinned-pinned cylinders with u_2 as parameter and $\beta = 0.48$, $\epsilon_f = 1$, $c = \alpha = h = \gamma = \Gamma = \Pi = 0$ are shown in Figure(5.7). In this case too, it can be seen that small flow velocities tend to damp the free motions of the system. As the velocity is gradually increased, however, the loci of first mode frequency bifurcate on the Re (ω) axis, one of the branches crossing origin at $u_2 \approx 3.14$ (as for the case when $\beta = 0.1$), indicating the onset of buckling instability. As the velocity is further increased the second mode gets less damped and the loci eventually cross the Re (ω) axis, indicating loss of stability by ordinary flutter, at $u_2 \approx 6.27$. Almost simultaneously, one of the branches of the first mode crosses the origin, two branches coalesce and leave the Re (ω) axis at a point where Re (ω) < 0. Thus the flow velocity which corresponds to loss of stability in the second mode is approximately the one for which the first mode regains stability. The coupled mode flutter occuring for the case when $\beta = 0.1$ is now absent. In

reference [48] this case has been studied with slightly lower value of ϵC_f such that $\epsilon C_f = 0.25$. In Figure 4 of reference [48], ordinary flutter of second mode does not appear and system loses stability in common mode flutter, the role of second mode being replaced by second branch of the first mode loci. This difference can be attributed both to higher value of ϵC_f in this study and to correction in the representation of the frictional forces.

Results obtained for the same cylinder when fluid parameters were varied, are shown in Figure(5.8). Internal fluid has been assumed to be stationary. It can be seen that the general character of the frequency diagram does not change except that the critical velocity for first mode buckling is slightly greater than 3.14. The velocity at which the second mode flutter sets in does not significantly change. Parameters in Figures (5.9) and (5.10) correspond to those of Figures (5.7) and (5.8) with the difference that the internal velocity is 0.5 in the same direction as the external velocity. The critical velocity for the buckling instability is now reduced while the critical velocity for oscillatory instability remains approximately the same as in Figures (5.7) and (5.8). Thus internal flow destabilizes the cylinder. Figures (5.11) and (5.12) correspond to Figures (5.9) and (5.10) but the direction of the internal

flow is now reversed. It is seen that the character of the dynamical behaviour is similar but critical velocities are lower compared to the case when internal flow is absent and the reversal in the direction of the internal flow further destabilizes the cylinder.

V.3 Pinned-Pinned Cylinder in Cluster:

Next, the dynamical behaviour of a pinned-pinned cylinder with increasing flows in a cluster can also be examined. If the internal flow is absent, this case can be considered pertinent to the fuel bundle assembly in a nuclear reactor. If internal flow is present this case represents the kind of situation in a parallel flow heat exchanger.

A complex frequency diagram is shown in Figure (5.13), corresponding to the parameters $\beta = 0.1$, $\epsilon c_f = 0.25$, $h = 1.5$, $\chi = 4$, $\delta = 1$, $u_1 = c = \gamma = \Gamma = \pi = 0$. It can be noted that the dynamical behaviour is quite similar to that of an isolated cylinder (refer to Figures 5.1 - 5.6). However, the flow induced damping is smaller in this case and the instabilities occur at much lower values of flow velocities. Accordingly, the onset of coupled mode flutter appears twice with buckling instability interposed in between. The low value of critical velocity for buckling in first mode, $u_2 = 1.57$ is especially noteworthy. The onset of

second-mode flutter at $u_2 \approx 3.095$ is absent in Figure(5) of reference [48], presumably because of different manner of representation of frictional forces. Similar argument can be given for the second appearance of the common mode flutter. The critical velocities (1.57, 3.1, 3.14, 4.715) for various instabilities show that the close spacing severely destabilizes the cylinder in a cluster. This comes from the effect of increased added mass as will be discussed later. Figures (5.14) and (5.15) show the complex frequencies when the external and internal flow is in the same and opposite directions respectively. Internal flow velocity u_1 is held constant and external flow velocity u_2 has been varied. Internal flow is seen to reduce the critical velocity for buckling in first mode (1.55 as against 1.57). Irrespective of the direction, however, the critical velocities for second mode flutter and the first and second common-mode flutter are now lower. Thus internal flow further destabilizes the cylinder subjected to external flow. This result is of practical importance since, in order to improve the heat transfer in parallel flow heat exchanger, higher flow velocities are employed. The effect of the added mass on buckling instability can be examined by considering Figure(5.16), where the fluid parameters were allowed to vary. Since the added mass coefficient was computed for an equivalent annulus, its value is much

lower (χ = 2.125 as against χ = 4 in Figure 5.13). The dynamical behaviour is now quite different. Instabilities associated with first and second mode are of buckling type rather than oscillatory and occur at higher velocities u_2 = 1.83 and 3.66 respectively. Internal flow in same and reversed direction (Figures 5.17 and 5.18) reduce these values to approximately 1.82 and 3.645 and 1.81 and 3.642 respectively. The third mode remains damped for the range of flow velocities considered.

V.4 Cantilever Cylinder:

The complex frequency diagram for the case of an isolated cantilever cylinder has been shown in Figure (5.19). The parameters correspond to those of Figure 6 of reference [55]. However, free end has been considered blunt and fluid parameters have been held constant. It can be seen that for low values of flow velocity the free motions of the cylinder are damped. As the flow velocity is gradually increased the first mode locus crosses Im(ω) axis at $u_2 \approx 0.395$, indicating the onset of flutter. The first mode loci bifurcate on Re (ω) axis, one branch approaching the origin and the other receding away. The cylinder loses stability in the second mode by flutter, at $u_2 \approx 4.8$. The third mode loci remain in the stable region for the range of velocity considered and imaginary parts of the

frequencies of the third mode monotonically increase with flow velocity.

The complex frequency diagram, shown in Figure (5.20) has been obtained by allowing the fluid parameters to vary. General character of the complex frequency diagram appears to be similar as that of Figure (5.19) except that the critical velocity for the onset of first mode flutter is now increased and subcritical damping is larger; the velocity for the second mode flutter to set in is, however, unaffected.

The dynamical behaviour of the same cylinder when the direction of the flow is reversed, i.e. towards fixed end, can be examined from Figures (5.21) and (5.22) which correspond to figures (5.19) and (5.20) as far as other parameters are concerned. It can be seen that the loci of all modes leave the $I_m(\omega)$ axis into unstable region, for small flow velocities. Thus, flow induced damping becomes negative. It is interesting to note that the first mode regains stability at $u_2 = 0.41$, but loses stability by buckling at $u_2 \approx 1.25$. Second mode, similarly, regains stability at $u_2 \approx 3.33$. Third mode however remains unstable for the range of velocities considered. In case of cantilever cylinders subjected to steady flow towards fixed end the flow appears to destabilize the cylinder for the flow velocities within the range considered here.

For this case, when fluid parameters have been allowed to vary, the results shown in Figure (5.22) were obtained. It is of interest that the onset of the first mode flutter now disappears and first mode instability is of buckling type. The second mode loses stability by flutter at $u_2 \approx 0.15$ but regains it at $u_2 \approx 3.1$; however, the third mode remains unstable for the velocities within the range considered for these results.

The results obtained for cantilever cylinders are particularly striking; flutter instabilities associated with cantilever cylinder are the result of frictional and inviscid hydrodynamic forces both of them being of non-conservative type in this case. Before examining the mechanism underlying these instabilities it will be convenient to examine the effect of flows on the dynamic behaviour of pipes.

V.5 Pinned-Pinned Pipe:

Figure(5.23)shows the complex frequencies of the lowest three modes of a pinned-pinned pipe with internal flow velocity as parameter, for $\beta = 0.1$, $\epsilon = 40$, $\xi = 1$ and $\alpha = h = \gamma = \Pi = \Gamma = u_2 = 0$. Pipe has been considered to be immersed in an infinite fluid. Fluid parameters were computed as discussed in Chapter III, resulting in non-zero value for $\dot{c}$, the viscous drag

coefficient. It can be seen that small flow velocities damp the free motions and as the external fluid is stationary, the damping, which is proportional to real part of the complex frequency, is constant and roughly equal for all the three modes. The imaginary parts of the frequencies of all three modes decrease with the increase in velocity till those of first mode reach and bifurcate on the Re (ω) axis. One of the branches, then crosses the Im(ω) axis, at $u_1 \approx \pi$, which indicates the onset of buckling. Further increase in velocity causes the two branches to receed away from the origin while the second mode loci approach close to the Re (ω) axis. At $u_1 \approx 6.08$ two btanches of the first mode start approaching the origin. At slightly higher flow velocity second mode loci reach and bifurcate on Re (ω) axis. The pipe loses stability by buckling in the second mode at $u_1 \approx 2\pi$. With further increase in velocity two branches of the second mode receed away from origin till at $u_1 \approx 6.39$ they coalesce with the branches of the first mode loci and leave the Re (ω) axis where Re (ω) is positive and negative, indicating the onset of coupled mode flutter.

In Figure 3(a) of reference [55] the coupled-mode flutter for the same case starts at $u_1 \approx 6.38$, and has been reported there for the first time. Figure(5.24) shows the dynamical behaviour for this case when external flow velocity is 0.5, where the second mode loci

have been drawn on $I_m(\omega)$ axis for the sake of clarity, since they overlap those of the first mode. The flow induced damping for small flow velocities is increased due to external flow. General character of the frequency diagram is similar to the case when external fluid was stationary; however, all the critical velocities are reduced. This observation is of practical interest since this case pertains to parallel flow heat exchanger.

The complex frequency diagram of the lowest three modes for the pipe considered in Figure(5.23)(with the mass ratio β changed to 0.5) is shown in Figure(5.25). The presence of stationary fluid results in non-zero values for the parameters χ, c_f and c. The dynamic behaviour shown is different than the one shown in Figure 5.23. It is noted that once again the first mode frequency vanishes at $u \approx \pi$. However, $u = 2\pi$ does not correspond to buckling in the second mode, but rather it is the point where the system loses stability by coupled mode flutter. It is interesting to note that similar results have been obtained in reference [48] for the case of an isolated pinned-pinned cylinder, for $\beta = 0.48$, $\epsilon c_f = 0.25$, $\delta = \chi = 1$, $c = \alpha = \lambda = \gamma = \Pi = \Gamma = u_1 = 0$. The role of the second mode in Figure(5.23)is assumed in this case by the second branch of the first mode, without affecting the overall stability characteristics of the system in a radical way;

this interchange in the roles of contiguous modes has been previously found to occur in the case of cantilever pipe [37] .

The dynamic behaviour, when external velocity is 0.5 in the same direction as that of the internal flow (refer to Figure 5.26) is not significantly different, but critical velocities for buckling and coupled mode flutter are reduced, evidently due to frictional forces associated with external flow. Reversal in the direction of external flow (refer to Figure 5.27) does not cause significant change in the general behaviour excepting that the critical velocity for buckling is slightly reduced (3.09 as against 3.11 in Figure 5.26).

V.6 Clamped-Clamped Pipe

Finally the case of a pipe with clamped-clamped ends may be examined. The results are shown in Figure (5.28), corresponding to parameters $\Gamma = \Pi = \alpha = \gamma = u_2 = 0$, $\beta = 0.5$ and $\epsilon = 40$. It is seen that the general character of the results is similar to those obtained for a pinned-pinned pipe, shown in Figure (5.25). The velocities at which system loses stability by buckling and common mode flutter are higher due to the nature of end conditions.

V.7 Comparison Between Cylinders and Pipes

The similarities and differences in the results for pipes and cylinders with different end conditions can now be examined together in general terms. General behaviour of the complex frequencies with increasing flow for pinned-pinned pipes and cylinders is similar except that for pipes second mode flutter does not set in, at least for the range of parameters of this study. The difference between systems of high and low mass ratio β is worth considering. For small values of β the system buckles in the first mode both for pipes and cylinders; but the second mode loses stability by flutter in case of cylinder and by buckling in the case of pipe. The loss of stability by coupled-mode flutter is common to pipe and cylinder. For larger values of β, second mode instability is notably absent in the case of a pipe while in the case of a cylinder, common mode flutter is absent. The coupled mode flutter was also found to set in for thin pipes studied by Paidoussis [43], Weaver and Unny [49] and Weaver and Myklatun [50]. The results for clamped-clamped pipes are similar to those for pinned-pinned cylinders. For supported systems flow induced damping at small flow velocities is caused only by external flow. The dynamical behaviour discussed above also holds for the cylinder or pipe in a cluster but higher added mass

coefficient destabilizes the system [48]. The character of the instabilities highly depends on the added mass, as shown by the results with low and high added mass coefficients. Thus the geometry and spacing between the cylinders are parameters of equal importance in clusters.

The effect of flow on the free motions of cantilever cylinder results in oscillatory instabilities of all the three modes studied. This can be attributed to the frictional and inviscid hydrodynamic forces, as the system is inherently non conservative. The effect of two flows in all the cases considered seems to destabilize the system, the effectiveness of destabilization being dependent on the relative direction of the flows, for systems with symmetric supports.

V.8 The Mechanism of Instability

Having seen the numerical results obtained for cylinders and pipes subjected to internal and external flows the mechanism causing various instabilities may now be considered from the analytical point of view.

V.8.1 Buckling Instabilities

The mechanism underlying buckling instabilities may be shown by considering the static equilibrium of the cylinder with both ends supported, which is assumed to

have momentarily frozen taking an arbitrary bowed shape y (x). Eliminating the time-dependent terms in equation (2.20) and considering excitation f (x, t) to be absent, one obtains

$$\alpha_{40} \frac{d^4 y}{dx^4} + \alpha_{10} \frac{dy}{dx} + \alpha_{20} \frac{d^2 y}{dx^2} = 0 \qquad (5.1)$$

where $\alpha_{40} = EI$

$$\alpha_{10} = [m + (\rho_1 - \rho_2)A] g_x + \tfrac{1}{2} \rho_2 U_{b_2}^2 \lambda \delta_{b_2} A/D_h + \tfrac{1}{2} \rho_2 D U_{b_2}^2 (f + \tfrac{1}{2} \rho_2 D U_{b_2} \delta_{b_2} C_D$$

$$\alpha_{20} = \rho_1 A U_{b_1}^2 + \chi \rho_2 A U_{b_2}^2 - \delta [(1-2\nu)\overline{pA} + \overline{T}] - \{ mg_x - A [g_x(\rho_2 - \rho_1) - \tfrac{1}{2} \rho_2 U_{b_2}^2 \lambda_2 \delta_{b_2} / D_h] + \tfrac{1}{2} \rho_2 D U_{b_2}^2 \delta_{b_2} C_f \} [L(1 - \tfrac{\delta}{2}) - x] - \tfrac{1}{2} (1-\delta) \rho D^2 U_b^2 \delta_b C_b$$

For sufficiently high fluid velocity the forces represented by the terms $\rho_1 A U_{b_1}^2 \frac{d^2 y}{dx^2}$ and $\chi \rho_2 A U_{b_2}^2 \frac{d^2 y}{dx^2}$ may overcome the flexural and tensile restoring forces $EI \frac{d^4 y}{dx^4}$ and $-\delta \overline{T} \frac{d^2 y}{dx^2}$ respectively, resulting in a monotonic increase in the amplitude of y (x). It may further be noted that the centrifugal forces due to inner and outer flow add irrespective of their directions, resulting in lower critical velocity for buckling when both the flows are present. In case of pipes carrying fluid, when gravity is ignored, equation (2.21)

simplifies to (with time dependent terms eliminated),

$$\frac{d^4\eta}{d\xi^4} + \upsilon^2 \frac{d^2\eta}{d\xi^2} = 0 \qquad (5.2)$$

where

$$\upsilon^2 = u_1^2 - \delta\left[(1-2\nu)\Pi + \Gamma\right]$$

The above equation admits solutions of the type

$$\eta(\xi) = \sum_{j=1}^{4} A_j e^{i\gamma_j \xi}$$

with $\gamma_1 = \gamma_2 = 0$, $\gamma_3 = \upsilon$, $\gamma_4 = -\upsilon$. Hence the solution can be rewritten in the form

$$\eta(\xi) = A_1 + A_2\xi + B_1 \cos\upsilon\xi + B_2 \sin\upsilon\xi \qquad (5.3)$$

Substituting the boundary conditions (equations (2.22), for simply supported pipes) for non-trivial solution one gets a vanishing determinant which yields

$$\upsilon^4 \sin\upsilon = 0 \qquad (5.4)$$

Since $\upsilon = 0$ is a trivial solution, one obtains $\upsilon = j\pi$ where $j = 1, 2, \ldots$. This, of course, is the familiar Euler's result if pipe is considered as an equivalent column subjected to a compressive load $\beta_1 A U_{b_1}^2 \frac{\partial^2 y}{\partial x^2}$ thus in case of $u = \pi = 0$, one has $\Gamma = -(j\pi)^2$, the compressive load at the end of the pipe for the onset of buckling. In case of clamped-clamped pipes critical values of υ are found corresponding to the zeros of

$$2(1 - \cos\upsilon) - \upsilon \sin\upsilon = 0 \qquad (5.5)$$

Physically, one may regard υ^2 as an effective compressive load. Alternatively, and more appropriately for the case of a flowing fluid, $\upsilon^2 \frac{\partial^2\eta}{\partial\xi^2}$ may be regarded

as a generalized centrifugal force. When this force overcomes the flexural restoring force, the pipe buckles.

V.8.2 Flutter Instabilities

For oscillatory instabilities, the condition of neutral stability is one of the dynamic equilibrium where, in the course of one cycle of oscillation, the energy transfer from fluid to cylinder and vice versa exactly balances. When the former exceeds the latter (since the fluid stream may be regarded as a source of infinite energy) the amplitude increases without limit. In the opposite case, the oscillations are damped.

Considering equation (2.19 a), one finds that the rate of work done on the cylinder in the course of free periodic motions may generally be written as

$$\frac{dW}{dt} = -\int_0^L EI\,\dot{y}\,y^{IV}\,dx - \int_0^L \dot{y}\,\rho_1 A\left(\frac{\partial}{\partial t} + U_{b_1}\delta_{b_1}\frac{\partial}{\partial x}\right)^2 y\,dx$$
$$-\int_0^L \chi\rho_2 A\,\dot{y}\left(\frac{\partial}{\partial t} + U_{b_2}\delta_{b_2}\frac{\partial}{\partial x}\right)^2 y - \tfrac{1}{2}\rho_2 D\left(C_D + U_{b_2}\delta_{b_2}C_f\right)$$
$$\int_0^L \dot{y}\left(\dot{y} + U_{b_2}\delta_{b_2}y'\right)dx \qquad (5.6)$$

and over one period of oscillation t_1, the work done ΔW, with the cylinder returning to its original position is given by

$$\Delta W = -\int_0^{t_1}\left[\dot{y}\left\{EI\,y''' + \rho_1 A U_{b_1}\delta_{b_1}\left(\dot{y} + U_{b_1}\delta_{b_1}y'\right) + \chi\rho_2 A U_{b_2}\delta_{b_2}\right.\right.$$
$$\left.\left.\left(\dot{y} + U_{b_2}\delta_{b_2}y'\right)\right\}\right]_0^L dt - \tfrac{1}{2}\rho_2 D\left(C_D + U_{b_2}\delta_{b_2}C_f\right)\int_0^{t_1}\int_0^L$$
$$\left(\dot{y}^2 + U_{b_2}\delta_{b_2}\,\dot{y}y'\right)dx\,dt \qquad (5.7)$$

Applying the boundary conditions, one obtains for cantilever cylinders

$$\Delta W = -\int_0^{t_1} \rho_1 A U_{b_1} \delta_{b_1} (\dot{y}^2 + U_{b_1} \delta_{b_1} \dot{y} y')\Big|_{x=L} dt - \int_0^{t_1} \chi \rho_2 A U_{b_2} \delta_{b_2} (\dot{y}^2 + U_{b_2} \delta_{b_2} \dot{y} y')\Big|_{x=L} dt - \frac{1}{2} \rho_2 D (C_D + U_{b_2} \delta_{b_2} C_f) \int_0^{t_1} \int_0^{L} (\dot{y}^2 + U_{b_2} \delta_{b_2} \dot{y} y') dx dt \tag{5.8}$$

and for cylinders with both ends supported

$$\Delta W = -\frac{1}{2} \rho_2 D (C_D + U_{b_2} \delta_{b_2} C_f) \int_0^{t_1} \int_0^{L} (\dot{y}^2 + U_{b_2} \delta_{b_2} \dot{y} y') dx dt \tag{5.9}$$

If $\Delta W < 0$, motion will be damped; while if $\Delta W > 0$ the oscillations will grow, i.e. the system will be unstable by flutter [29]. From equation (5.2) it is evident that in the absence of hydrodynamic drag effects, in case of supported cylinders, $\Delta W = 0$. Thus the hydrodynamic forces are of purely conservative type. It is, therefore, evident that the existence of flutter for supported cylinders depends on the presence of frictional forces as the system is inherently conservative. This explains the onset of instability by ordinary flutter in case of supported cylinders and pipes when the external flow is present; on the other hand, cantilever cylinders may become unstable entirely by the action of inviscid hydrodynamic forces. It is not surprising that a small correction in the viscous terms of the equation of motion should have a profound effect on the dynamical behaviour of cylinders where the system is inherently conservative.

The onset of amplified oscillations corresponds to a change in the character of the mode at a specified flow velocity as determined by the conservative forces in the system; frictional effects, however small, cause the amplification of the oscillation, whereas before the change occured they caused damping. This change in the character of the mode is essentially like the change from class B to class A behaviour discussed by Benjamin [15].

Inspecting equation (5.9) more closely, one observes that the condition of neutral stability ($\Delta W = 0$) requires that

$$\int_0^L \dot{y}^2 dx = - U_{b_2} \delta_{b_2} \int_0^L \overline{\dot{y}\, y'}\, dx \qquad (5.10)$$

For the right hand side of equation (5.10) to be nonzero, different parts of the cylinder must vibrate in quadrature, and this is an effect that can only be produced by the action of the flow. If the solution is represented as the sum of a standing and a travelling wave, it can be seen that the right hand side of equation (5.10) depends only on the amplitude of the travelling wave component; furthermore, the phase velocity of this component must be in the direction of the flow for the right hand side of equation (5.10) to be positive.

In the case of cantilever cylinders, from equation (5.8), it can be observed that the energy transfer between

the fluid stream and the cylinder may be caused both by inviscid and viscous hydrodynamic forces. Benjamin [11] has considered the mechanism of energy transfer in the related problem of fluid flowing in an articulated pipe system. He found that over one complete period of oscillation t_1, the energy gained by pipes when the down stream end is free, is given by

$$\Delta W = - \int_0^{t_1} M_i U \left(\dot{\underset{\sim}{R}}^2 + U \underset{\sim}{\tau} \cdot \dot{\underset{\sim}{R}} \right) dt \qquad (5.11)$$

where M_i is the mass per unit length of the contained fluid and $\underset{\sim}{\tau}$ and $\underset{\sim}{R}$ are the tangential and position vectors at the end of the last pipe. Similarly between equation (5.11) and the first two terms of equation (5.8) is striking. In the case of cantilever cylinders, the oscillatory instabilities can occur independently of the friction forces. When $C_D = C_f = 0$, the equation (5.8) gives

$$\Delta W = - \int_0^{t_1} \rho_1 A U_{b_1} \delta_{b_1} \left(\dot{y}^2 + U_{b_1} \delta_{b_1} \dot{y} y' \right)\Big|_{x=L} dt - \int_0^{t_1} \chi \rho_2 A U_{b_2} \delta_{b_2} \left(\dot{y}^2 + U_{b_2} \delta_{b_2} \dot{y} y' \right)\Big|_{x=L} dt \qquad (5.12)$$

It is evident that when U_b is small, the first term in each integrand predominates over the second and vibrations are damped. For sufficiently high fluid velocity, however, if $\dot{y}$ and y' are sufficiently out of phase to give a negative average value to $\dot{y}\, y'$, it is

possible for ΔW to become positive, in which case oscillations are amplified. Thus for amplified vibration, for the greater part of a cycle the free end of the cylinder must slope backwards to its motion, i.e. a dragging motion must occur. ΔW as given by equation (5.12) is the work done by nonconservative hydrodynamic forces. Equation (5.12) also shows that for the oscillatory instability the directions of the two flows are important in case of cantilever cylinders. This is particularly clear from the numerical results.

V.8.3 Coupled-Mode Flutter:

The coupled-mode flutter at sufficiently high flow velocity was shown to occur in the case of thin pipes conveying fluid. The dynamics of this was studied using shell theory to describe the motion of the pipe [43, 46, 49, 50]. The coupled mode flutter was obtained for thicker pipes only recently [55]. The existence of the coupled-mode oscillatory instabilities is connected to the presence of Coriolis forces which are operative only when mass ratio $\beta \neq 0$. He confirmed this by calculating the frequencies for a simply supported pipe with $\beta = 0$. Due to the effect of Coriolis forces the "critical" flow velocities obtained by Euler's method of equilibrium do not always correspond to thresholds of instabilities, as

indicated by the results obtained using dynamic method. The systems with supported ends considered in the present study are subject to inactive Coriolis forces and therefore, are gyroscopic conservative systems. Accordingly, the static method gives only the first critical velocity which corresponds to buckling in the first mode; beyond this point systems cease to be positive definite, and only the dynamic method is capable of giving all higher critical velocities and their correct physical interpretation. From equation (5.9) it is seen that in the absence of frictional forces, $\Delta W = 0$ for conservative systems considered here. On closer examination, this argument implies that the critical point for flutter cannot be a point of neutral stability. The critical condition for coupled-mode flutter is not a point of neutral stability as it corresponds to coincidence of two frequencies and hence to growing oscillations of the form $y(x,t) = f(x)(a+bi)e^{\omega t}$. Therefore one may arrive at a conclusion that, apart from buckling in the absence of frictional forces the gyroscopic conservative systems can only be subject to coupled mode flutter. The presence of ordinary flutter for these systems then can only be connected to the hydrodynamic drag forces. Recently Shieh [64] has drawn similar conclusions for gyroscopic conservative systems in general.

The existence of Coriolis force in the system gives rise to phase difference and mode coupling. Coriolis force terms introduce asymmetry in damping matrix C and inertia matrix K of equation (2.28) and make the problem non-self-adjoint. As shown by Chen [40], Coriolis forces do not dissipate or supply any energy. Coriolis forces contribute to damping only when displacement at one of the ends of the cylinder is nonzero. For simply supported pipe or cylinder, from equation (4.14),

$$G^{1}_{nj} = 0 \quad \text{for} \quad n, j = \text{even} \quad \text{or} \quad n, j = \text{Odd}$$

This relationship implies that there is no coupling between even-even modes or odd-odd modes. Physically this means that the motion in odd modes will excite the motion in even modes only, and vice versa. For the fundamental mode of pipes or cylinders with supported ends, this can be explained as follows: the displacement being symmetric about the centre of the span, the angular velocities of left and right half span of the beam are in opposite directions. The fluid motion being unidirectional, gives rise to the antisymmetric Coriolis force which excites only antisymmetric modes. The motion of these modes in turn produces a symmetric Coriolis force which induces symmetric motion. This is the reason why Coriolis force causes mode coupling and phase difference. This further explains to some extent, the mechanism giving rise to coupled mode flutter at higher flow velocities.

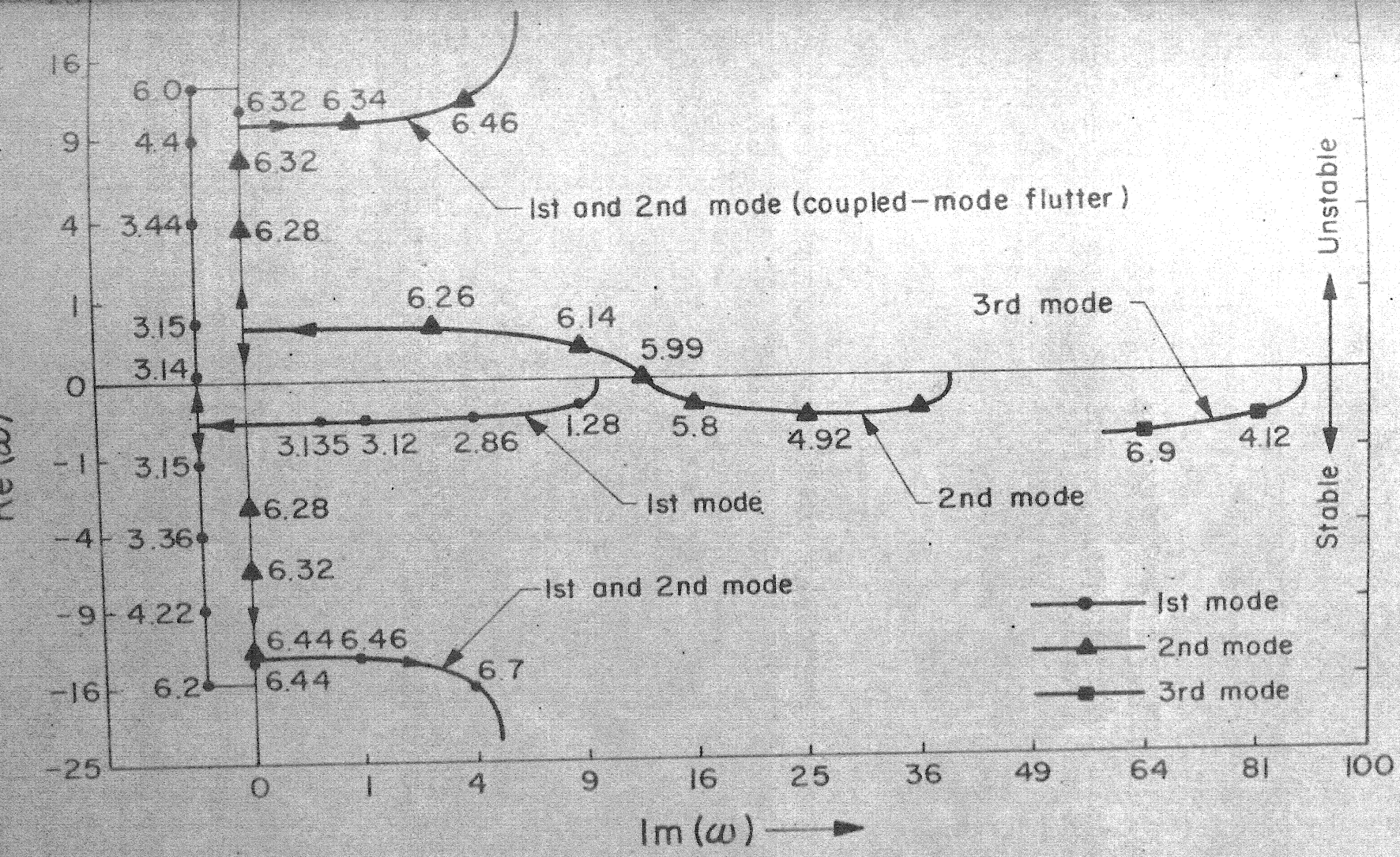

Fig. 5.1 Argand diagram of the complex frequencies, ω, of the lowest three modes of an isolated pinned-pinned cylinder, as functions of u_2, for $\beta = 0.1$, $\epsilon C_f = 1$, $\delta = \chi = 1$, $c = \alpha = h = \gamma = \Pi = \Gamma = u_1 = 0$

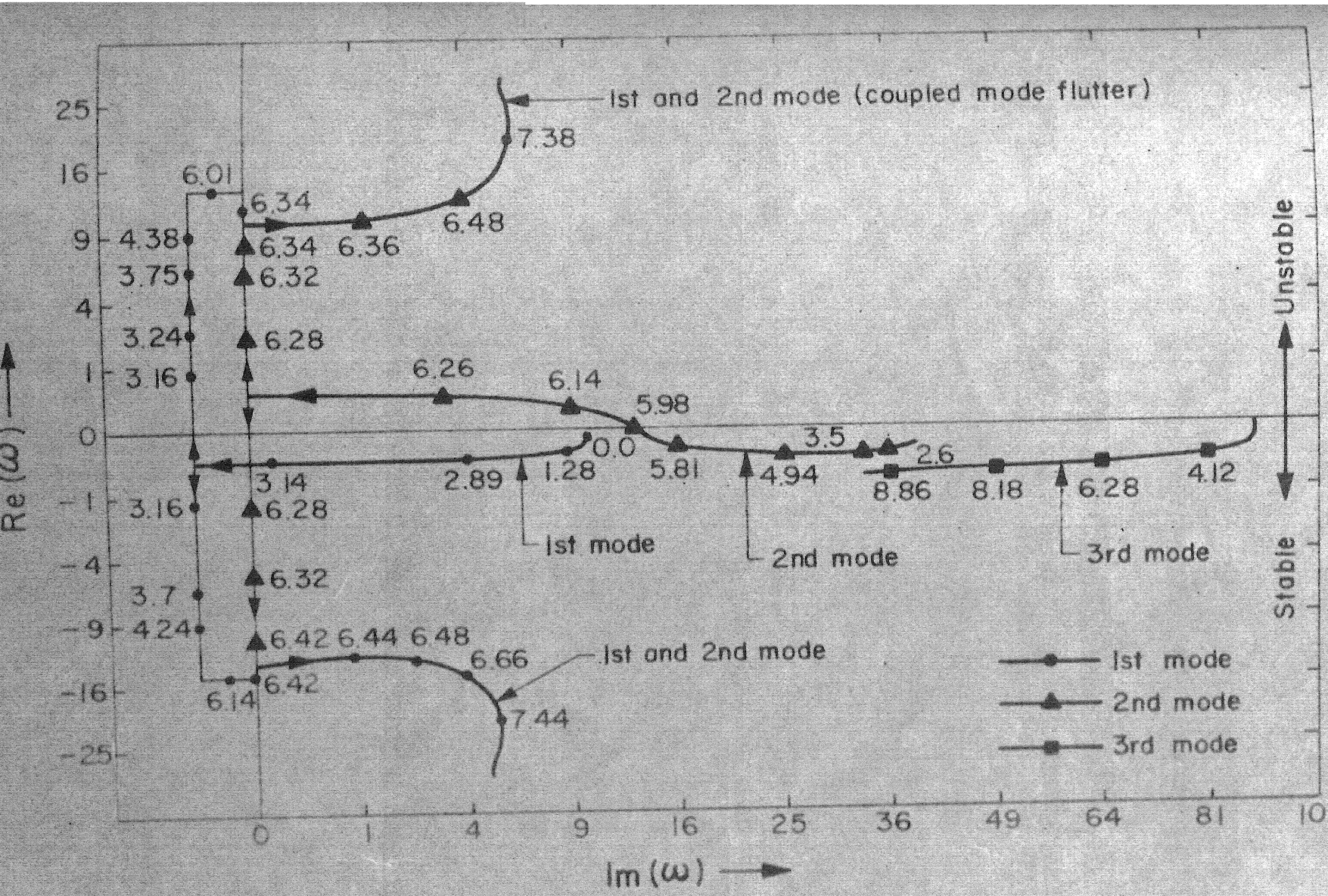

Fig.5.2 Argand diagram of the complex frequencies, ω, of the lowest three modes of an isolated pinned-pinned cylinder,

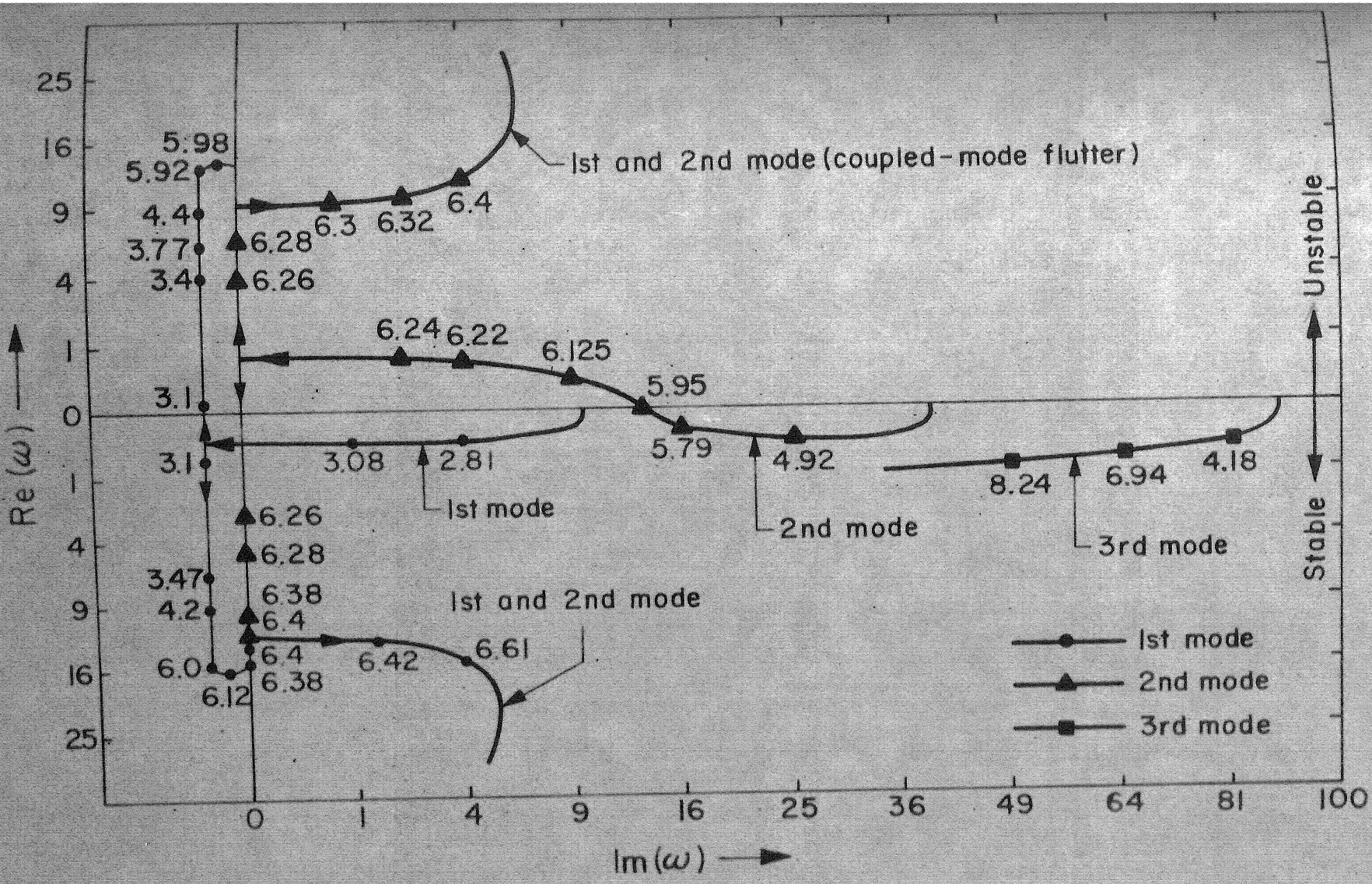

g.5.3 Argand diagram of the complex frequencies, ω, of the lowest three modes of an isolated pinned-pinned cylinder as functions of u_2, for $\beta = 0.1$, $\epsilon C_f = 1$, $\delta = \chi = 1$, $c = \alpha = h$

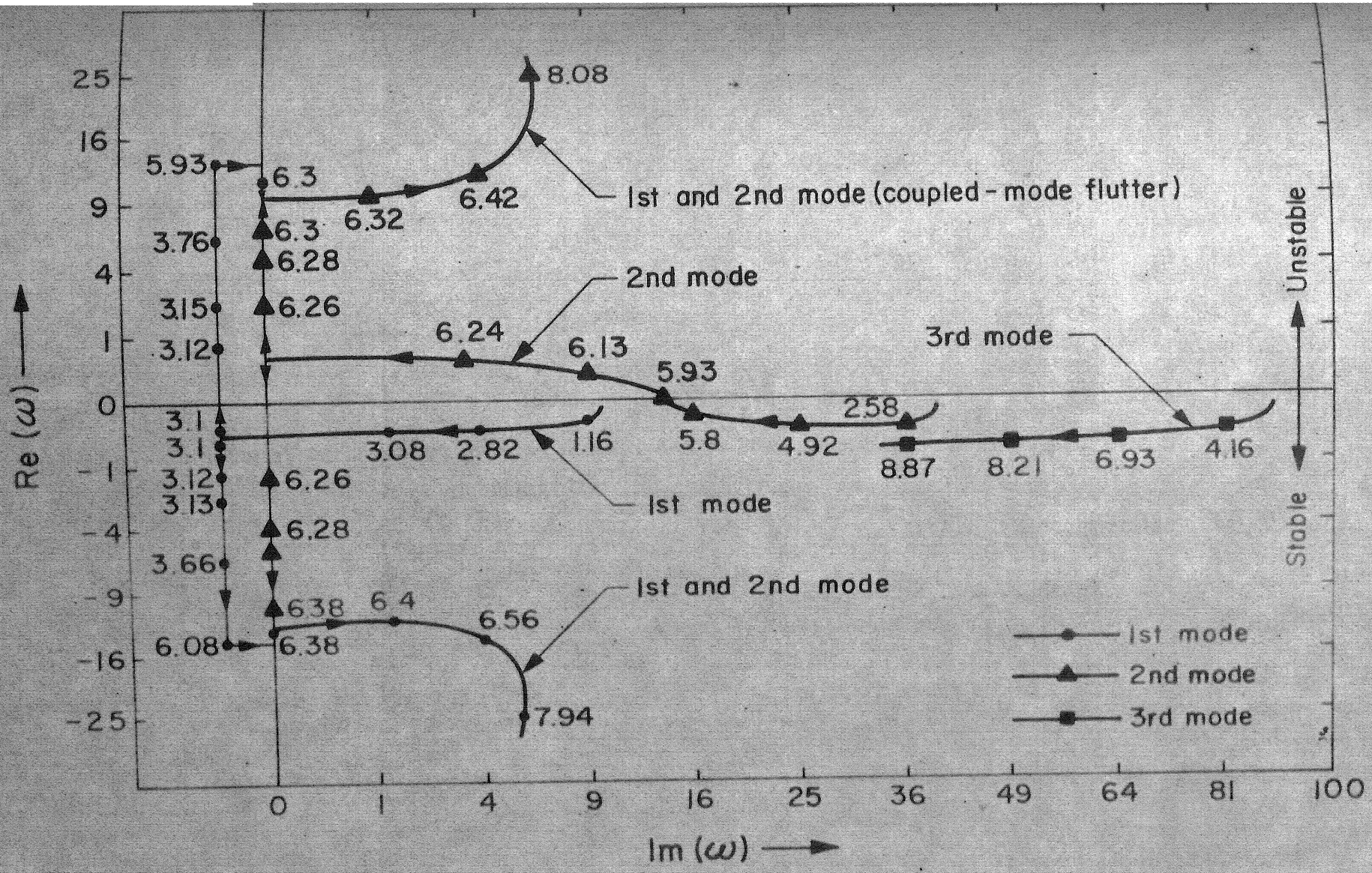

Fig.5.4 Argand diagram of the complex frequencies, ω, of the lowest three modes of an isolated pinned-pinned cylinder as functions of U_e, for $B = 0.1$, $\delta = 1$, $\alpha = h = \nu = \Pi = \Gamma$

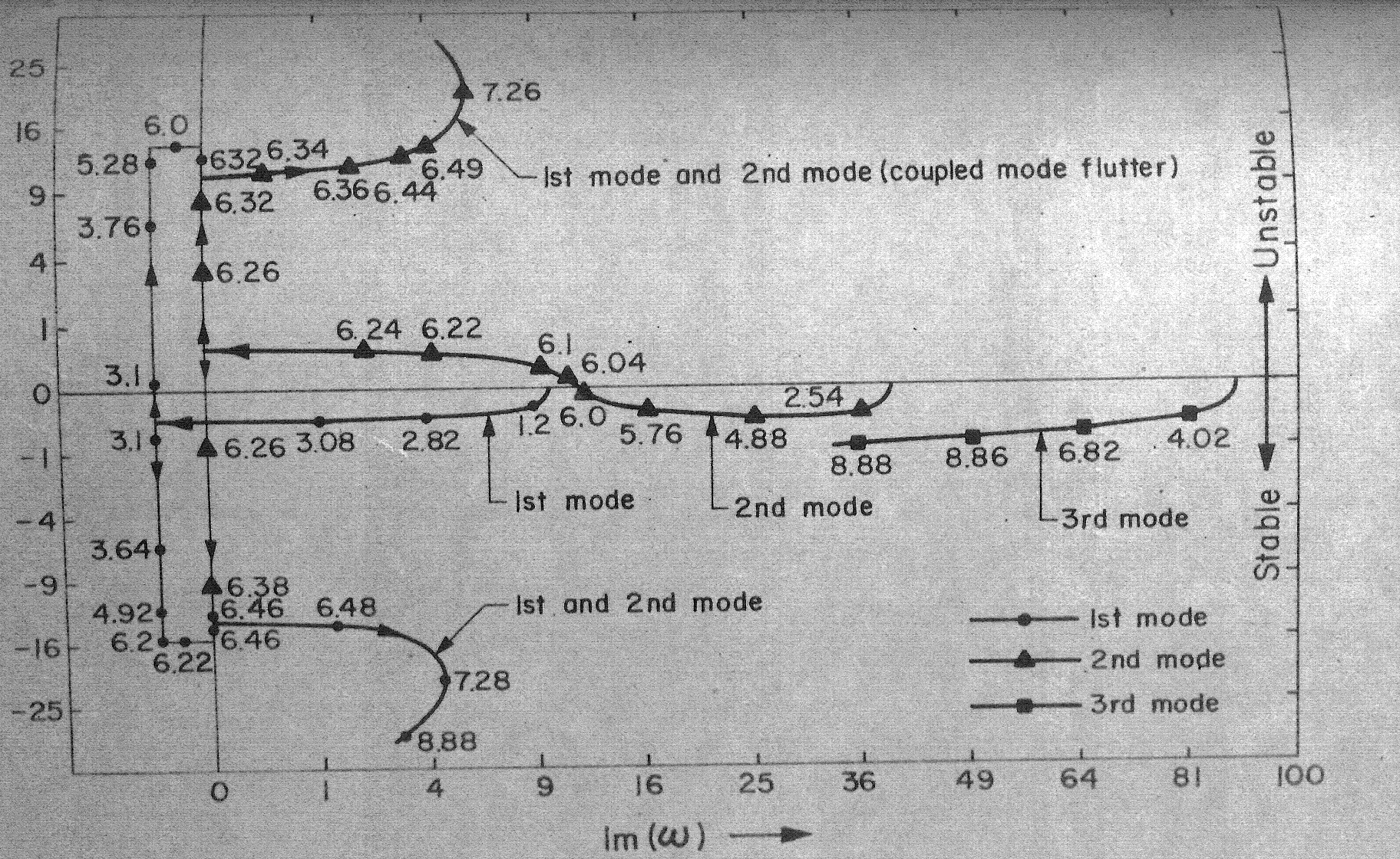

ig. 5.5 Argand diagram of the complex frequencies, ω, of the lowest three modes of an isolated pinned-pinned cylinder as a function of u_2, for $\beta = 0.1$, $\epsilon C_f = 1$, $\delta = \chi = 1$, $c = \alpha = h$

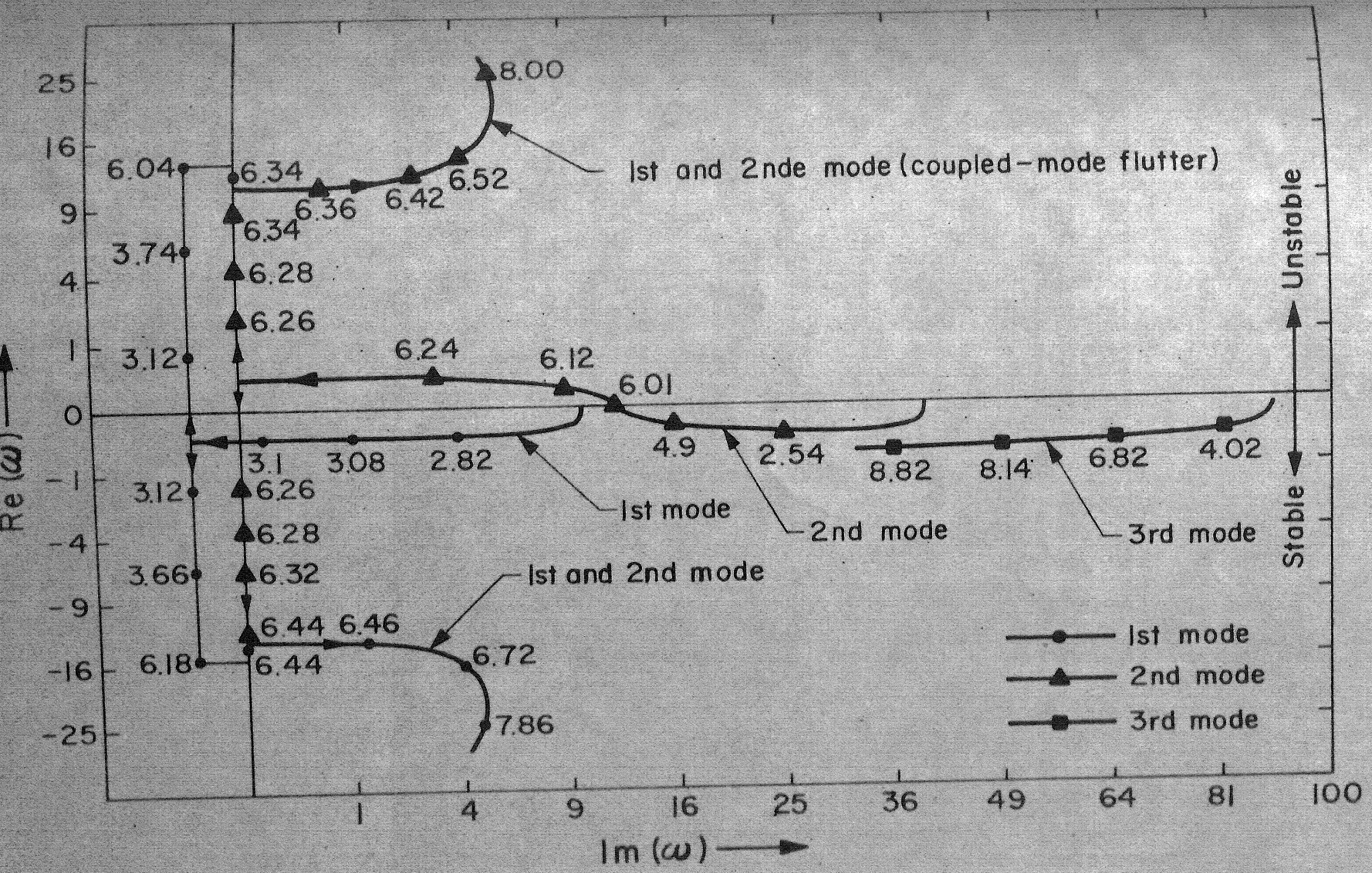

Fig. 5.6 Argand diagram of the complex frequencies, ω, of the lowest three modes of an isolated pinned-pinned cylinder as functions of u_3, for $B = 0.1$, $\delta = \chi = 1$, $\alpha = h = \nu = \Pi = \Gamma = 0$

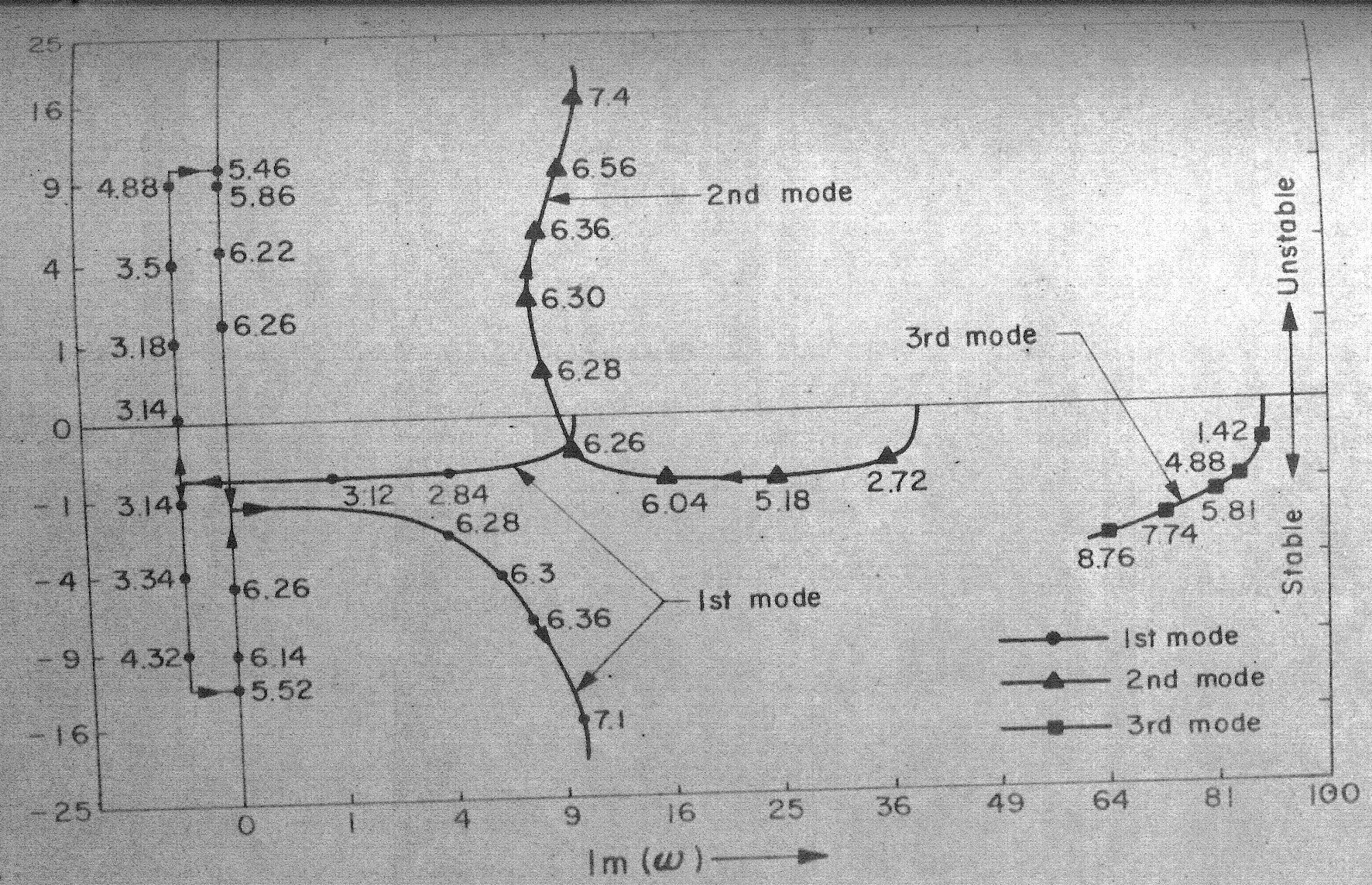

g. 5.7 Argand diagram of the complex frequencies, ω, of the lowest three modes of an isolated pinned-pinned cylinder, as functions of u_2, for $\beta = 0.48$, $\epsilon C_f = 1$, $\delta = \chi = 1$, $c = \alpha =$

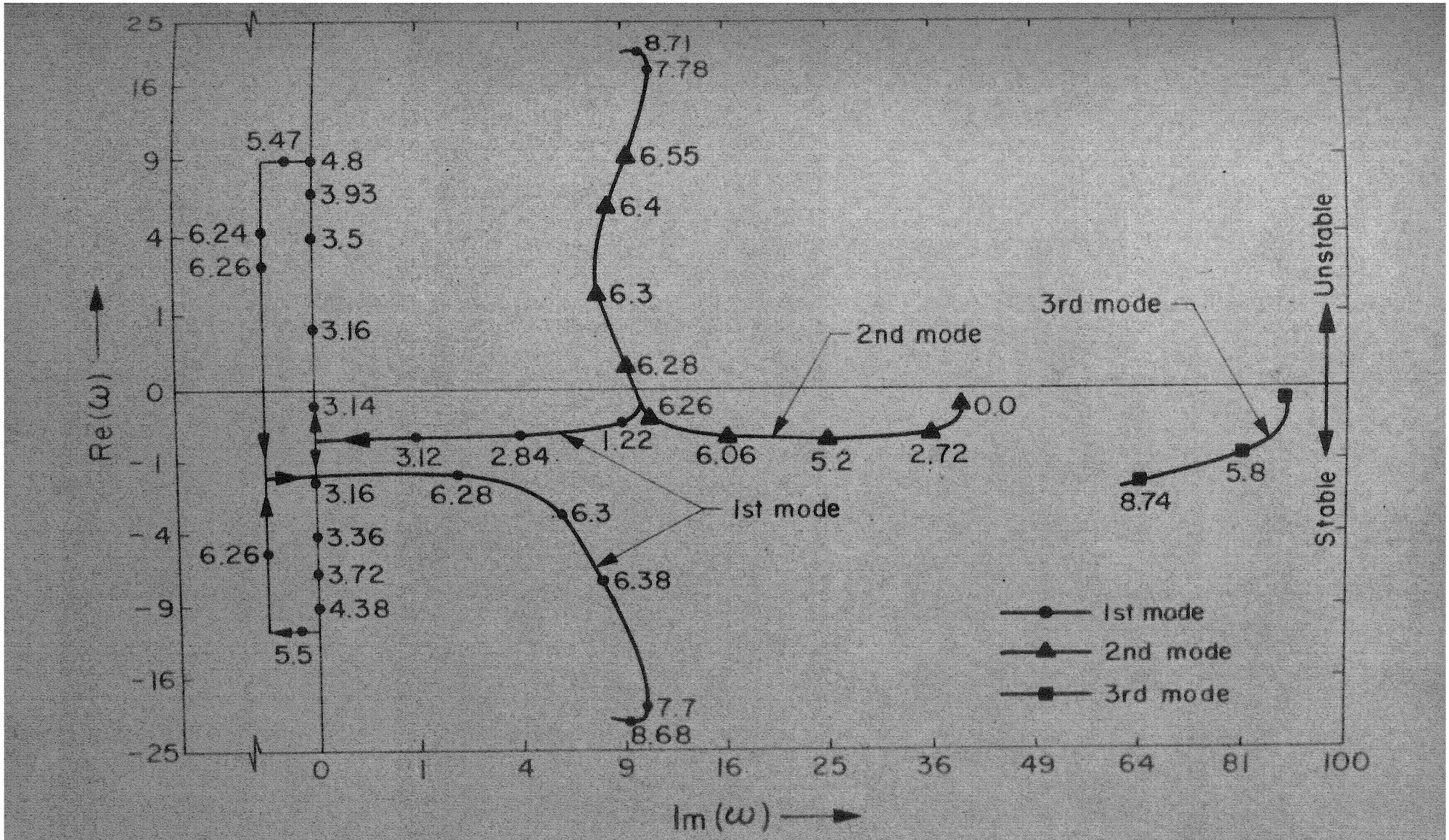

Fig.5.8 Argand diagram of the complex frequencies, ω, of the lowest three modes of an isolated pinned-pinned cylinder, as a function of u_2, for $\beta = 0.48$, $\epsilon = 40$, $\delta = \chi = 1$, α, h, γ, $\Pi = \Gamma = 0$, $\overline{\nu}_2 = 10^{-5}$, $u_1 = 0$

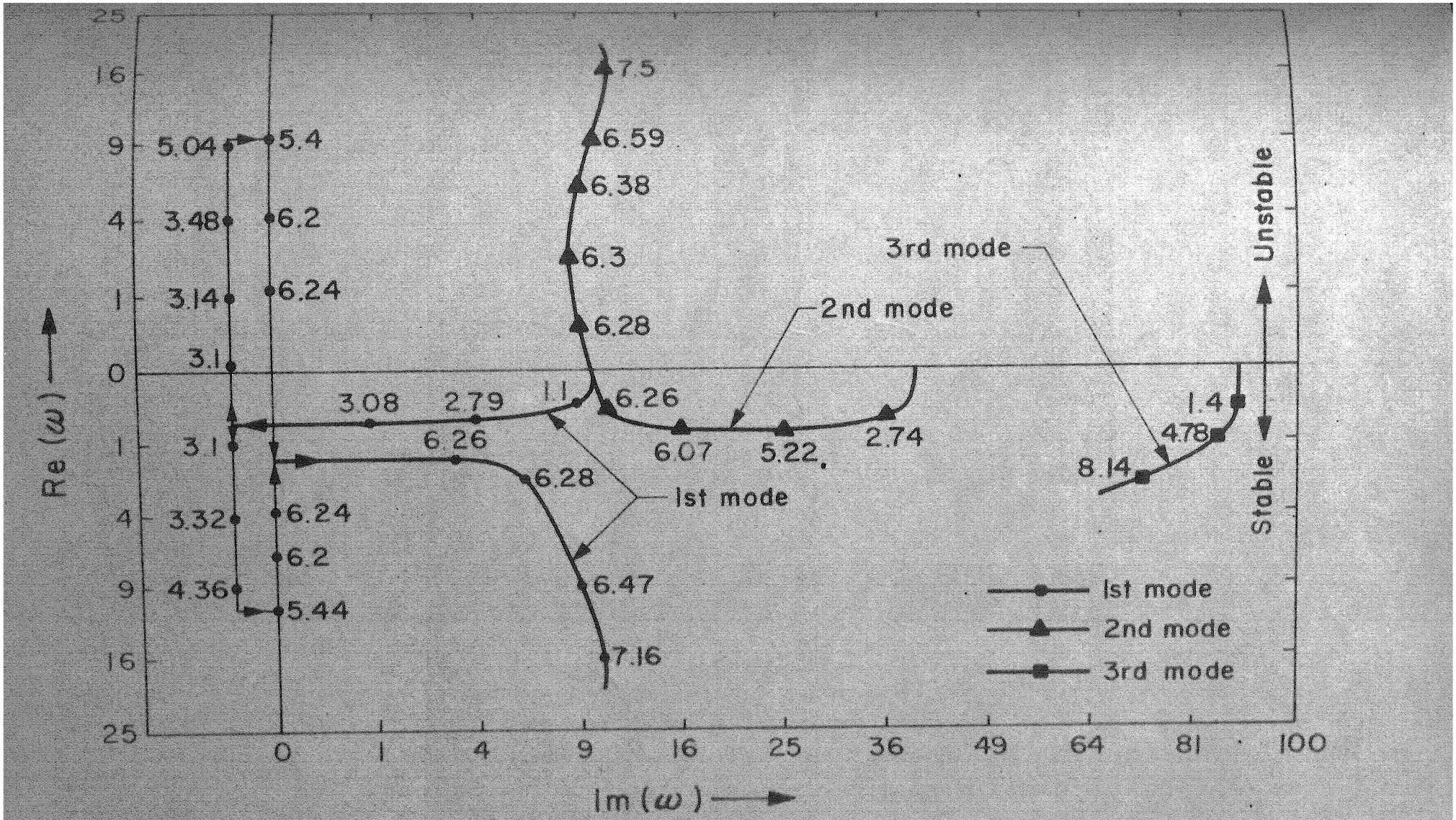

Fig. 5.9 Argand diagram of the complex frequencies, ω, of the lowest three modes of an isolated pinned-pinned cylinder as functions of u_2, for $\beta = 0.48$, $\epsilon = 40$, $\delta = \chi = 1$, $\alpha = h = \gamma = \Pi = \Gamma = 0$, $u_1 = +0.5$

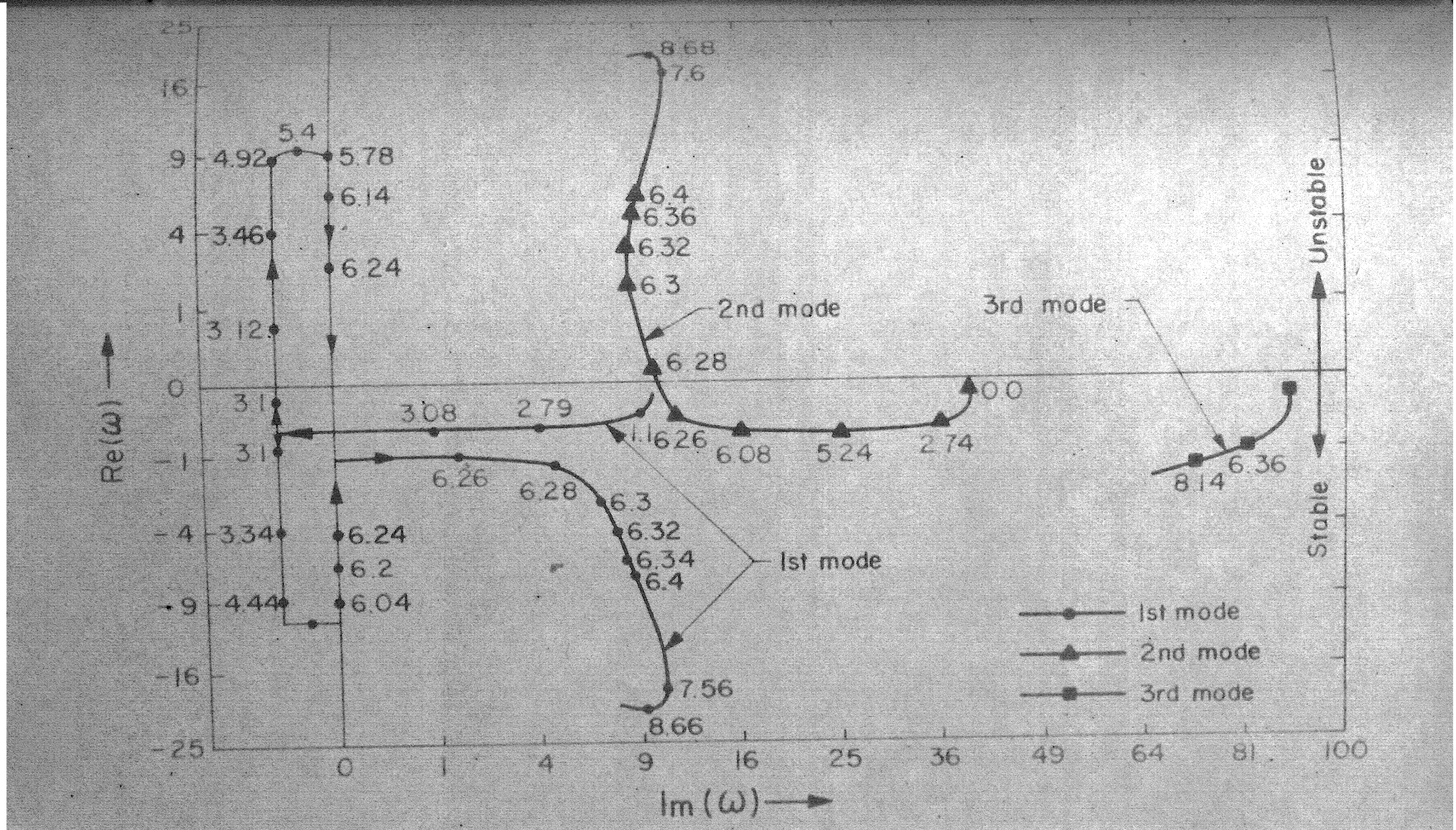

Fig.5.10 Argand diagram of the complex frequencies, ω, of the lowest three modes of an isolated pinned-pinned cylinder, as function of u_2, for $\beta = 0.48$, $\bar{\nu}_2 = 10^{-5}$, $\epsilon = 40$, $\delta = \chi = 1$, $c = \alpha = h = \gamma = \Pi = \Gamma = 0$, $u_1 = +0.5$

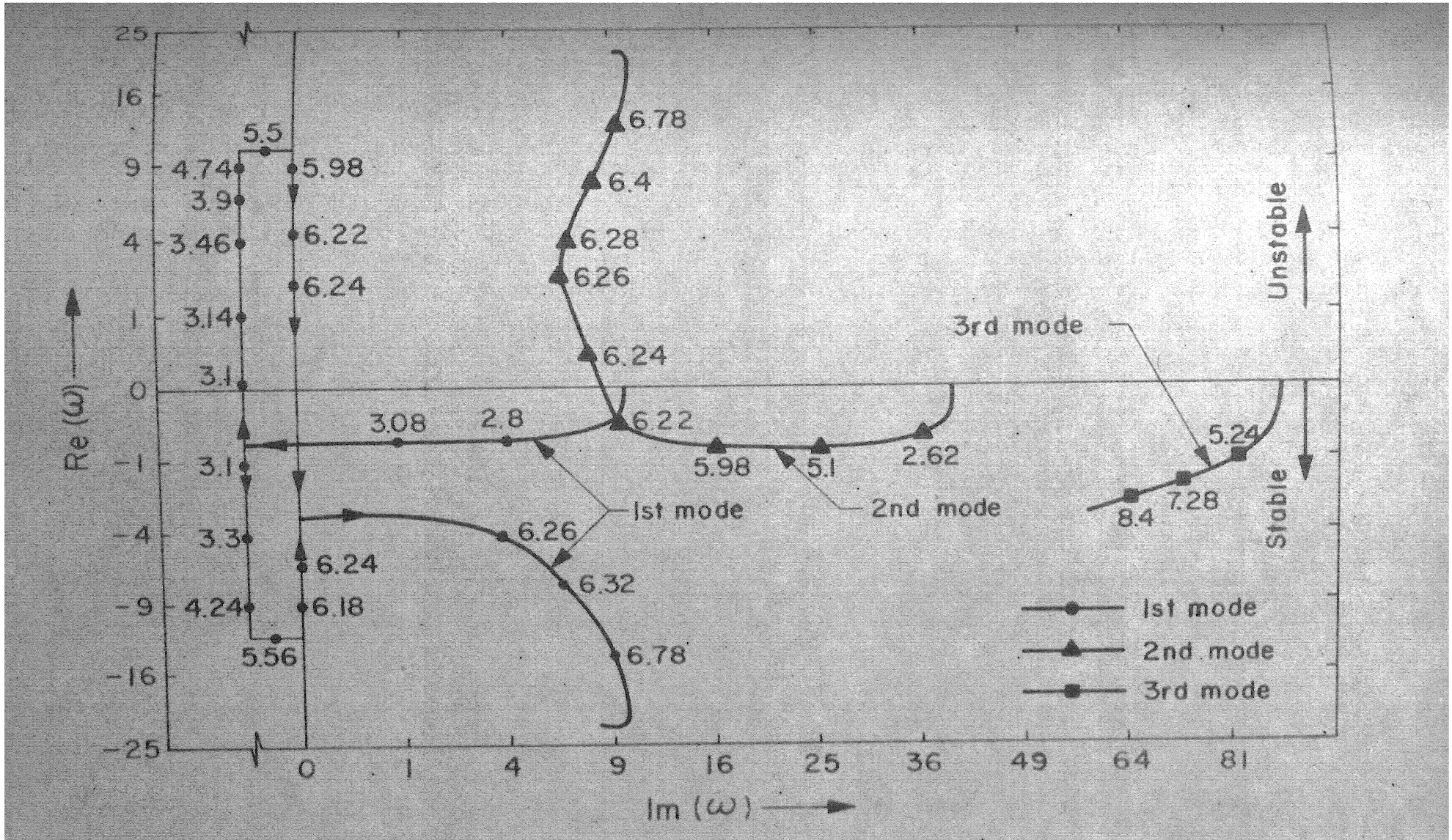

Fig. 5.11 Argand diagram of the complex frequencies, ω, of the lowest three modes of an isolated pinned-pinned cylinder, as function of u_2, for $\beta = 0.48$, $\epsilon C_f = 1.0$, $\delta = \chi = 1$, $c = \alpha = h = \gamma = \Pi = \Gamma = 0$, $u_1 = -0.5$

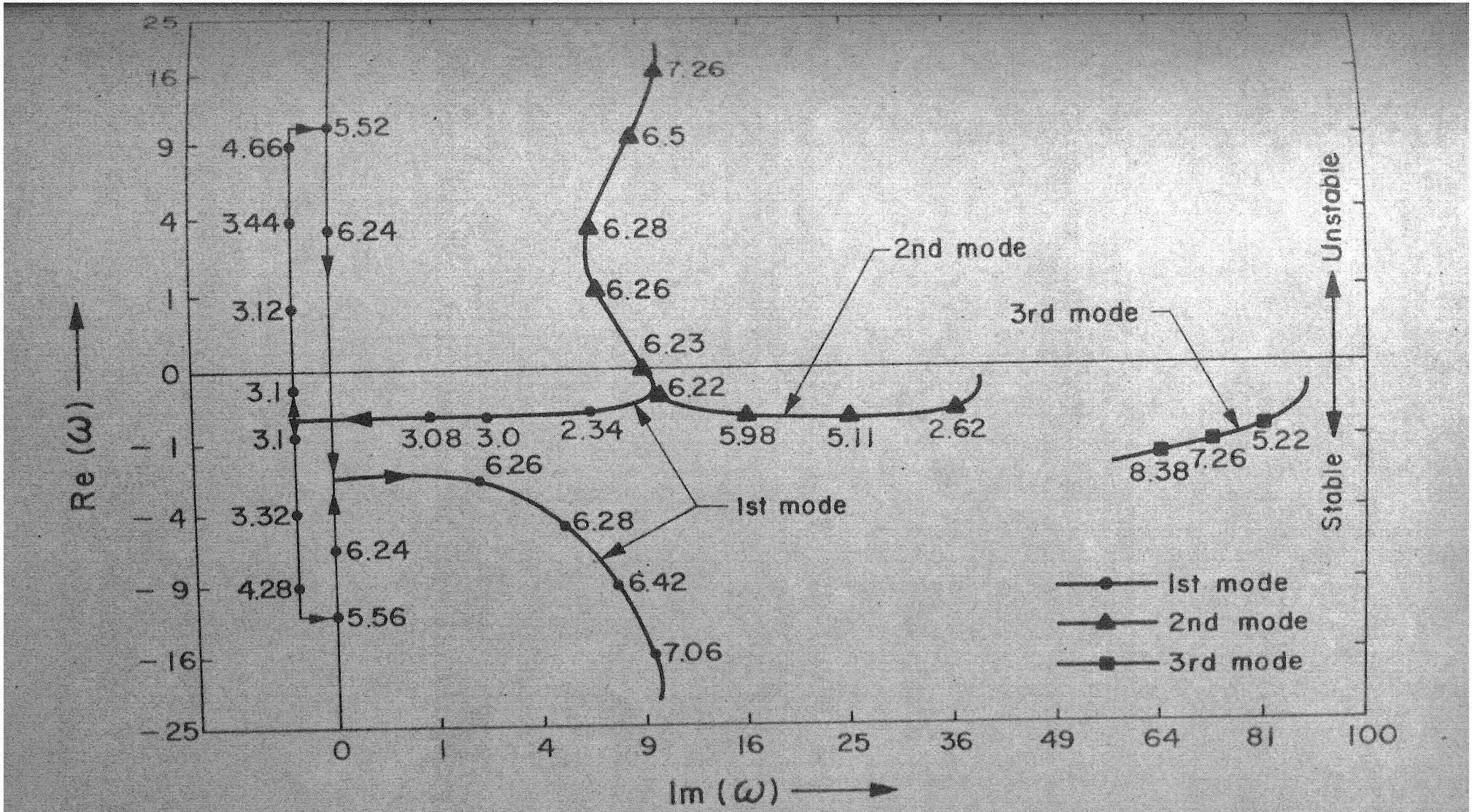

Fig. 5.12 Argand diagram of the complex frequencies, ω, of the lowest three modes of an isolated pinned-pinned cylinde as functions of u_2, for $\beta = 0.48$, $\epsilon = 40$, $\delta = \chi = 1$ $\alpha = h = \nu = \Pi = \Gamma = 0$, $u_1 = -0.5$

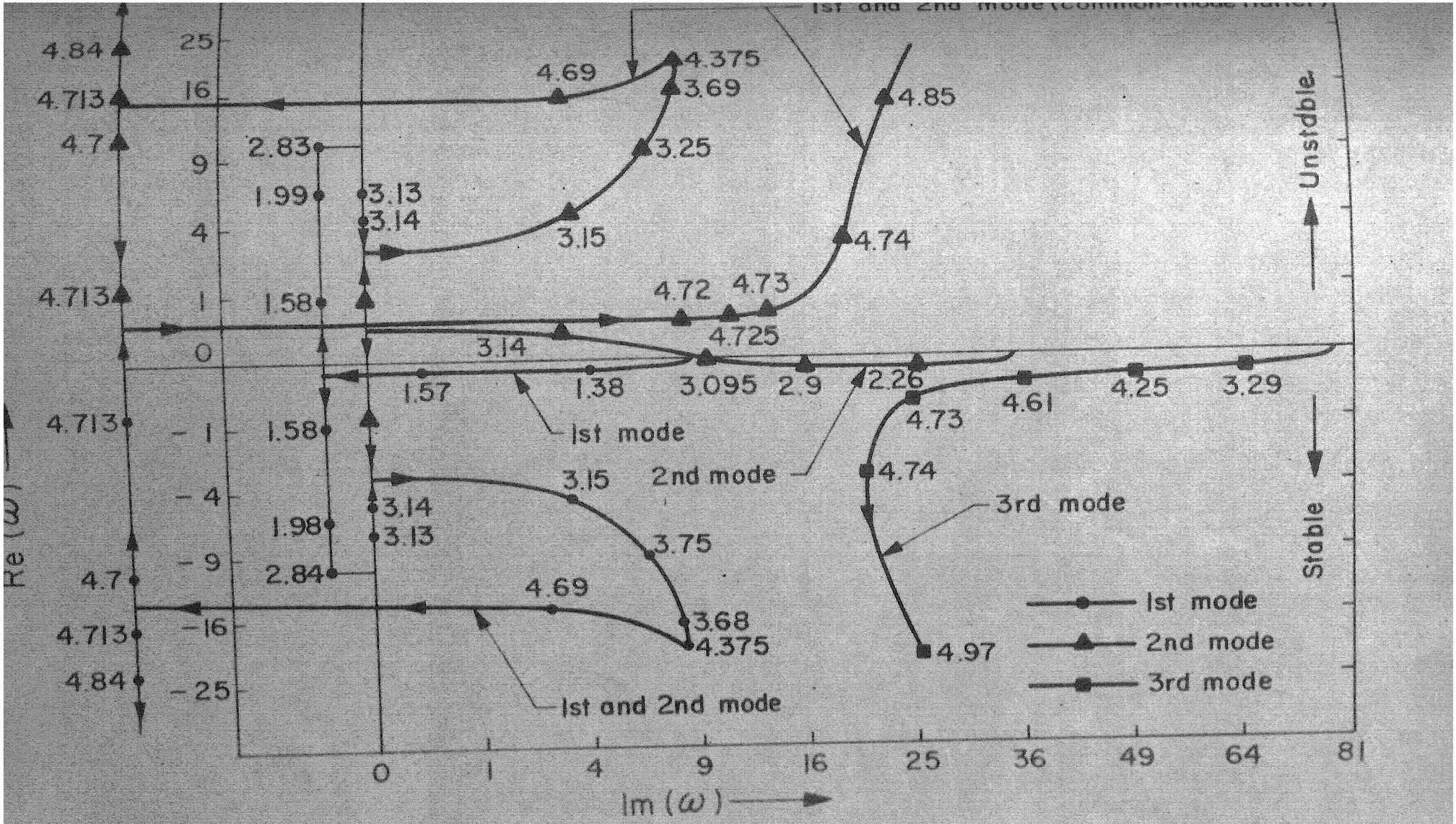

Fig.5.13 Argand diagram of the complex frequencies, ω, of the lowest three modes of a pinned-pinned cylinder in cluster, as functions of u_2, for $B = 0.1$, $\epsilon C_f = 0.25$, $h = 15$, $\chi = 4$, $\delta = 1$, $u_1 = c = \alpha = \nu = \Pi = \Gamma = 0$

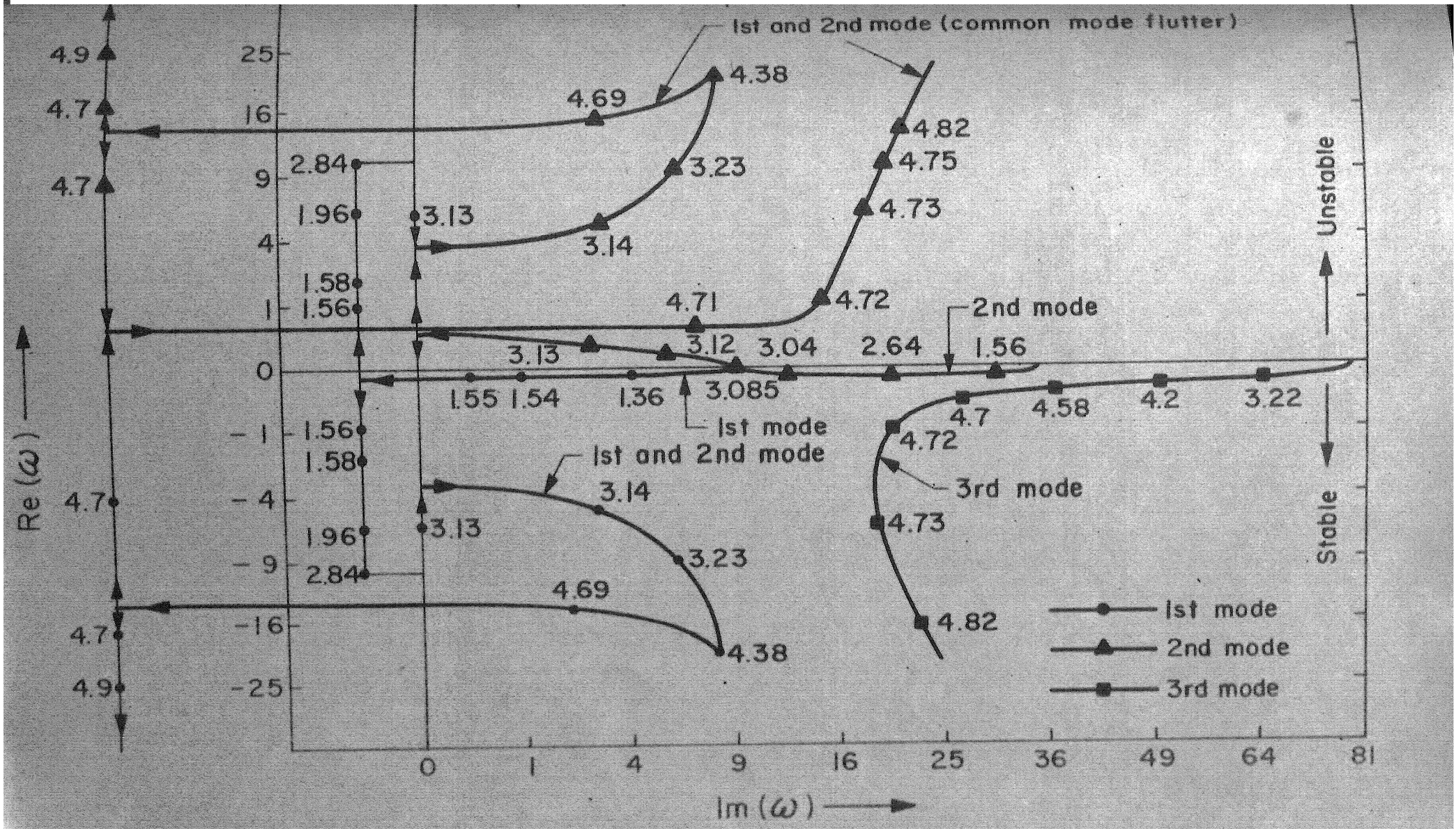

Fig. 5.14 Argand diagram of the complex frequencies, ω, of the lowest three modes of a pinned-pinned cylinder in cluster as functions of u_2, for $\beta = 0.1$, $\epsilon C_f = 0.25$, $h = 1.5$, $\chi = 4$, $\delta = 1$, $c = \alpha = \nu = \Pi = \Gamma = 0$

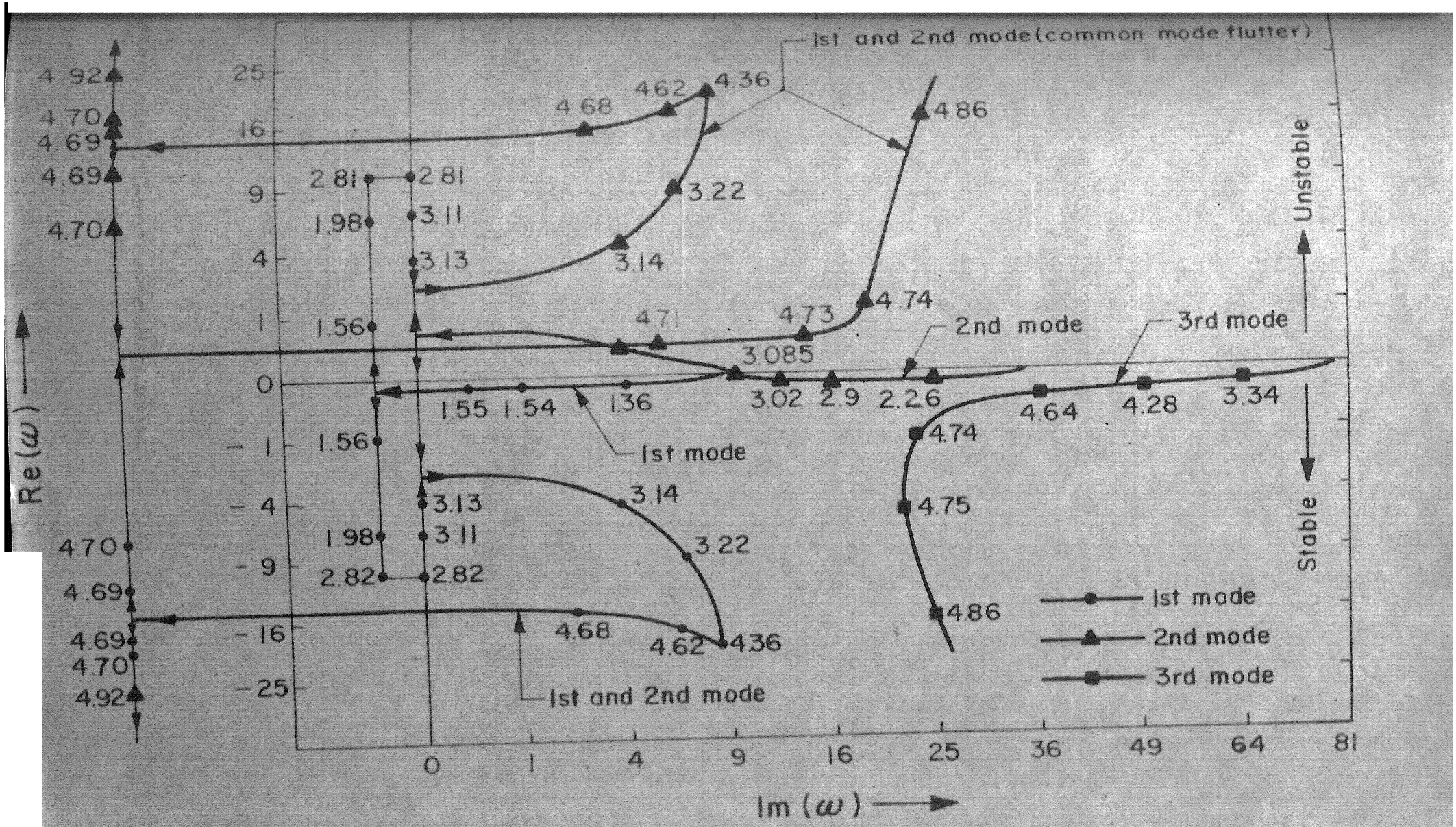

Fig. 5.15 Argand diagram of the complex frequencies, ω, of the lowest three modes of a pinned-pinned cylinder in a cluster, as functions of u_2, for $\beta = 0.1$, $\epsilon C_f = 0.25$, $h = 1.5$, $\chi = 4$, $\delta = 1$, $c = \alpha = \nu = \Pi = \Gamma = u_1 = 0$

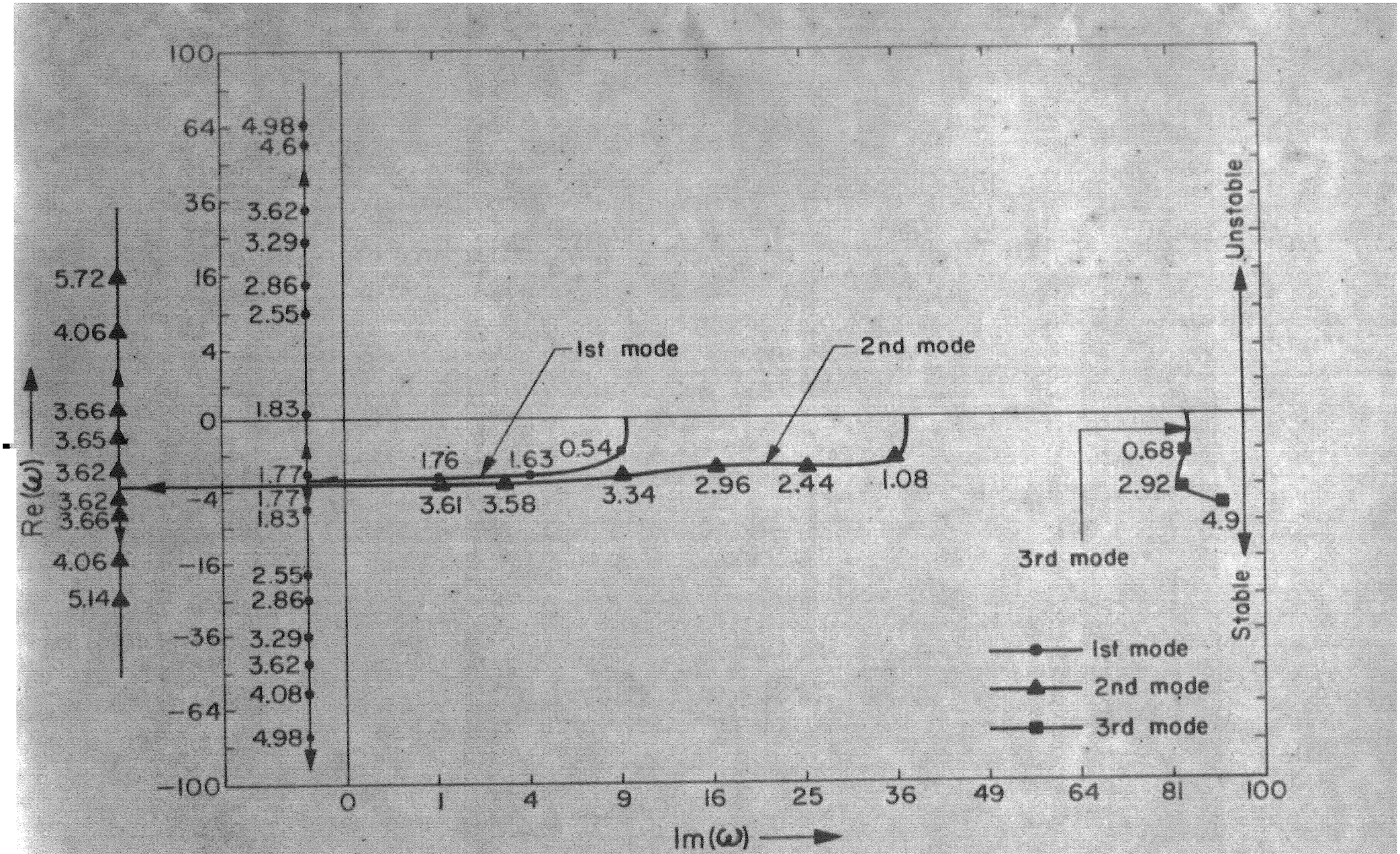

Fig.5.16 Argand diagram of the complex frequencies, ω, of the lowest three modes of a pinned-pinned cylinder in cluster, as functions of u_2, for $\beta=0.1$, $h=1.5$, $\delta=1$, $u_1=\alpha=\gamma=\Pi=\Gamma=0$

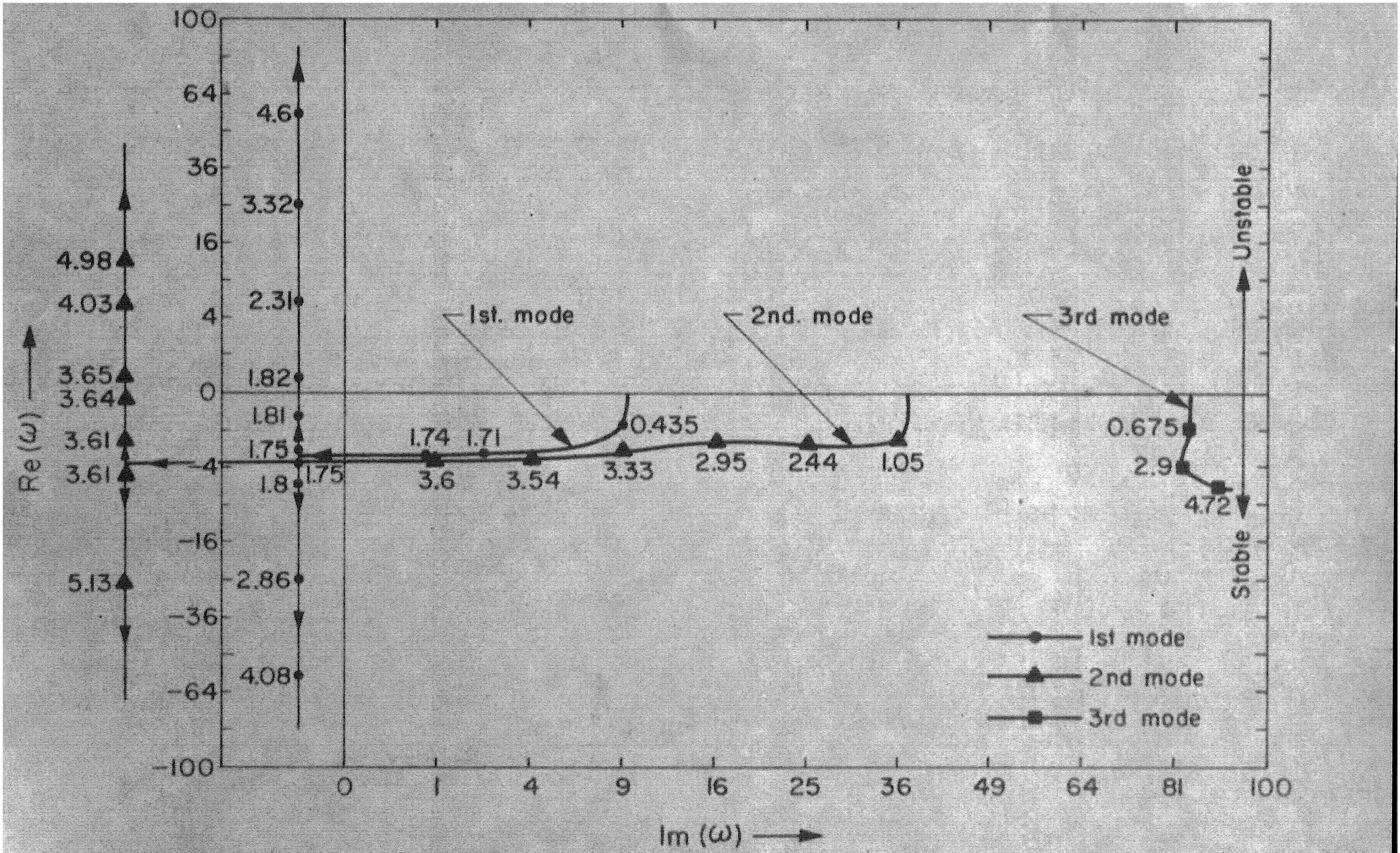

Fig.5.17 Argand diagram of the complex frequecies, ω, of the lowest three modes of a pinned-pinned cylinder in cluster as functions of u_2, for $B=0.1, h=1.5, \delta=1, \alpha=\gamma=\Pi=\Gamma=0, u_1=+0.5$

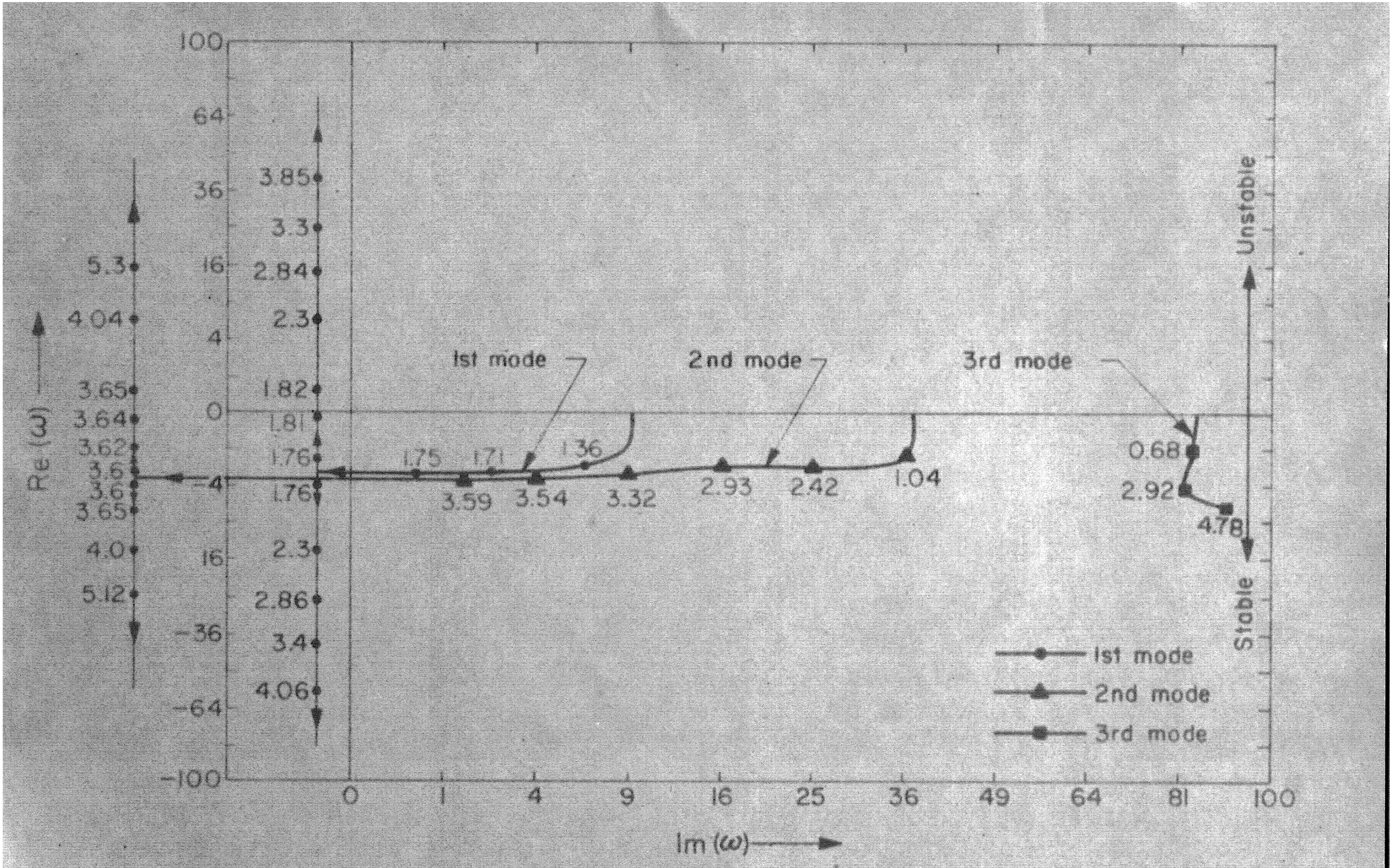

Fig.5.18 Argand diagram of the complex frequencies, ω, of the lowest three modes of a pinned-pinned cylinder in a cluster, as functions of u_2, for $B=0.1, \epsilon=40, h=1.5, S=1, \alpha=\gamma=\Pi=\Gamma=0, u_2=-0.5$

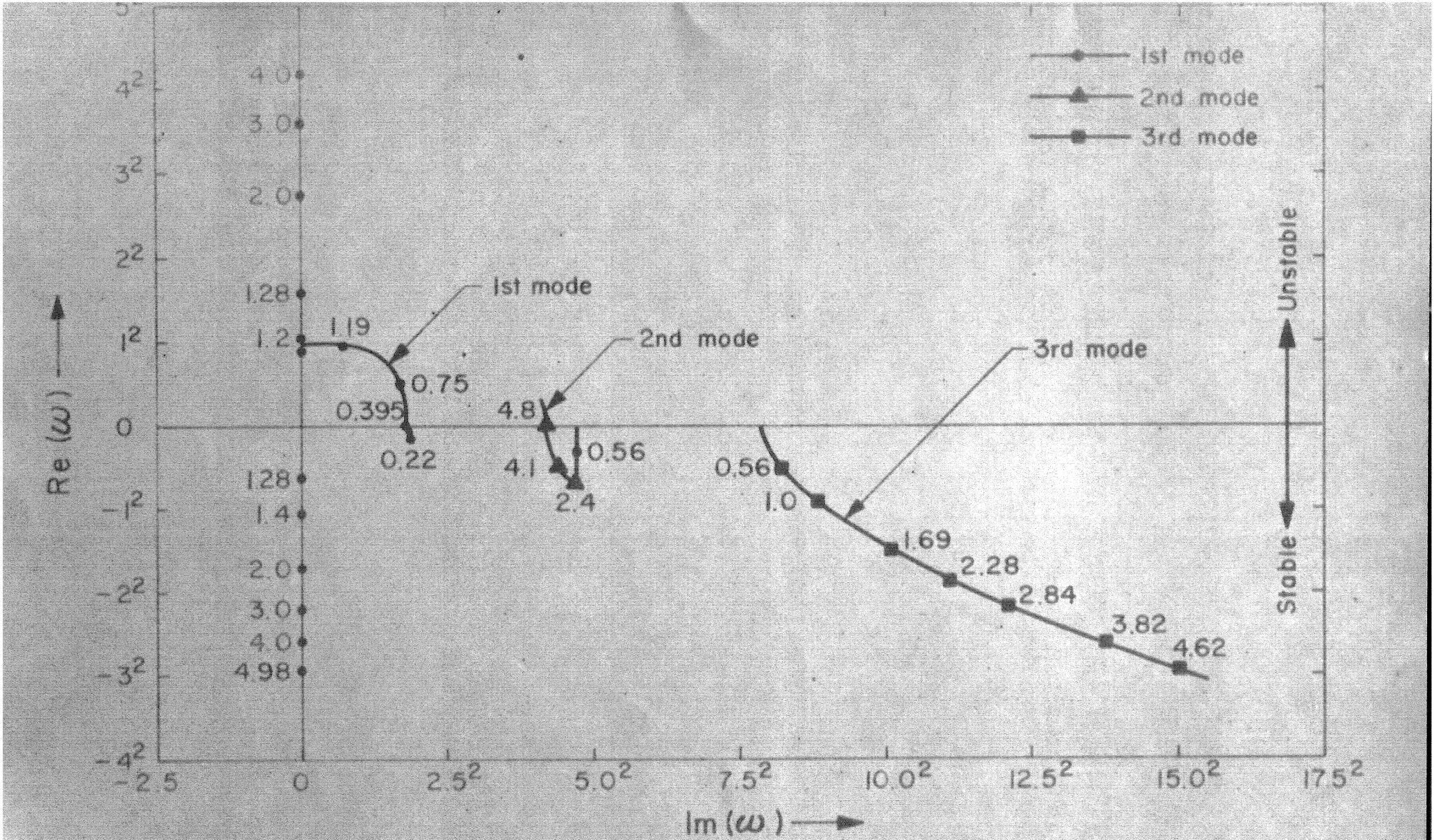

Fig.5.19 Argand diagram of the complex frequencies, ω of the lowest three modes of an isolated cantilevered cylinder, as functions of u_2, for $\beta = 0.5, \epsilon C_f = 1, \chi = 1, c = \alpha = \nu = \Pi = \Gamma = u_1 = \delta = c_b = 0$

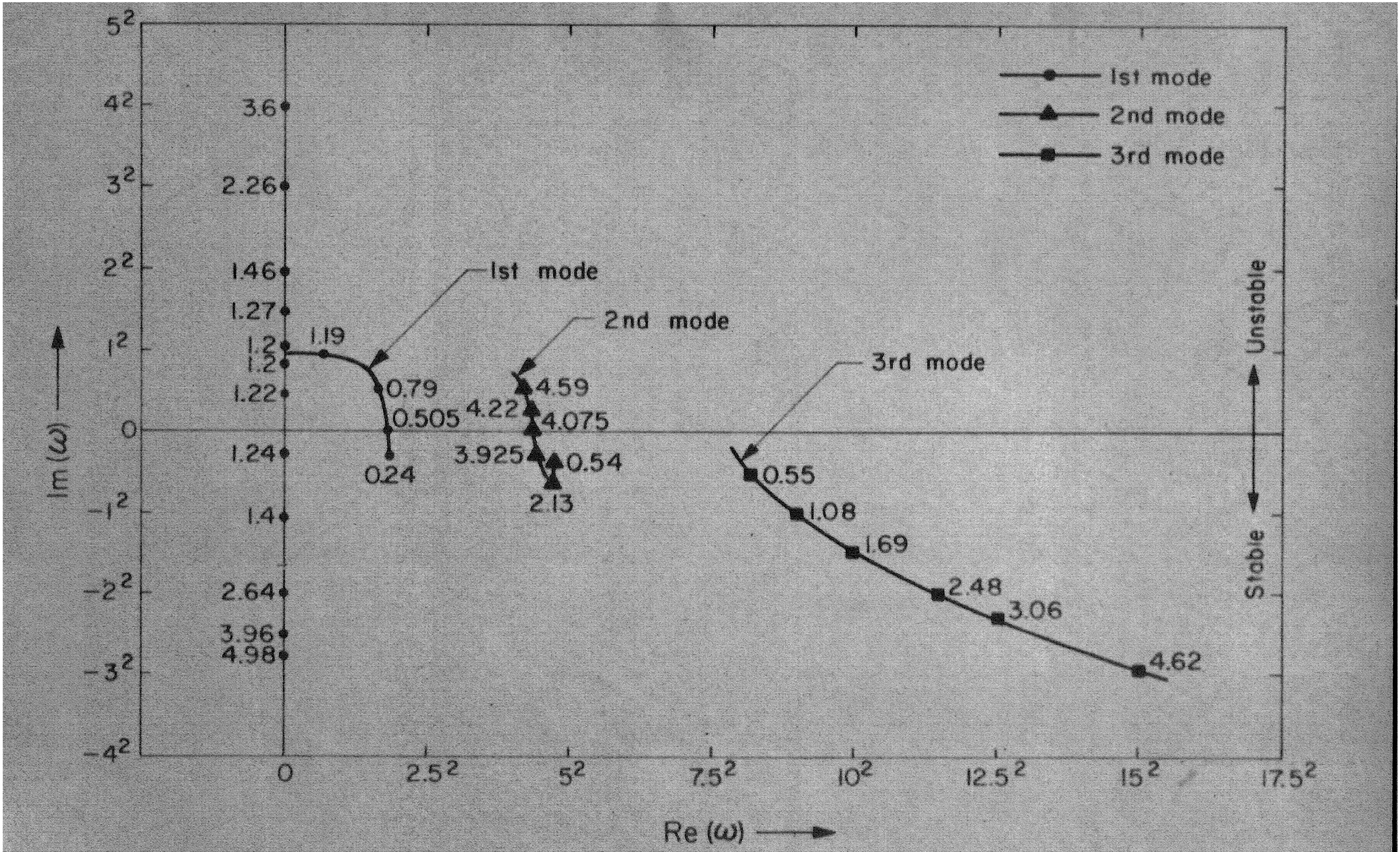

Fig.5.20 Argand diagram of the frequencies, ω, of the lowest three modes of an isolated cantilever cylinder as functions of u_2, for $B=0.5, \epsilon=40, \delta=0, \chi=1, c_b=\Upsilon=\Pi=\Gamma=u_1=0$

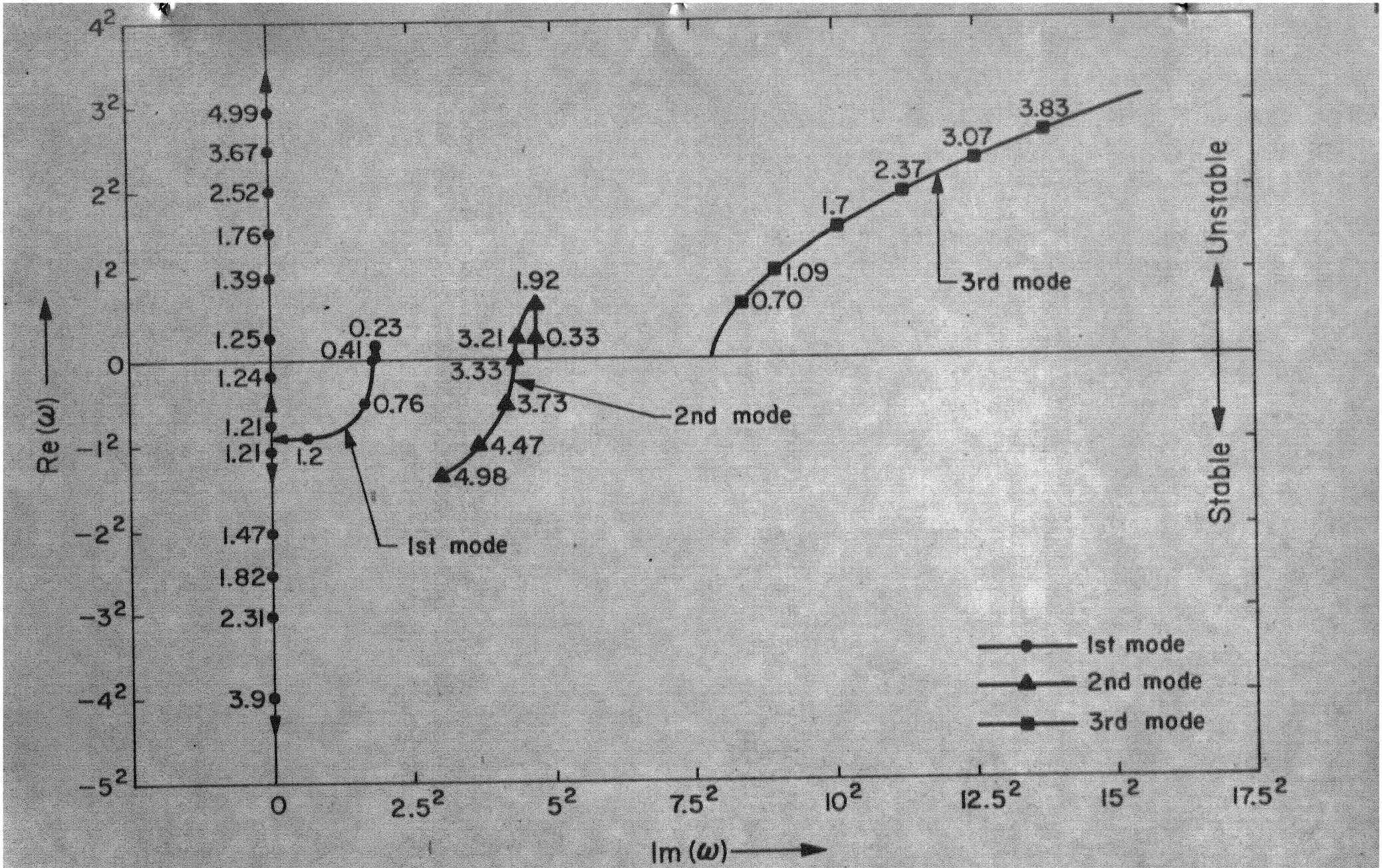

Fig.5.21 Argand diagram of the complex frequencies, ω, of the lowest three modes of an isolated cantilever cylinder, as functions of u_2, for $\beta=0.5, \epsilon C_f=1, \delta=0, \chi=1, c=\gamma=\Pi=\Gamma=0, \delta c_b=-1$

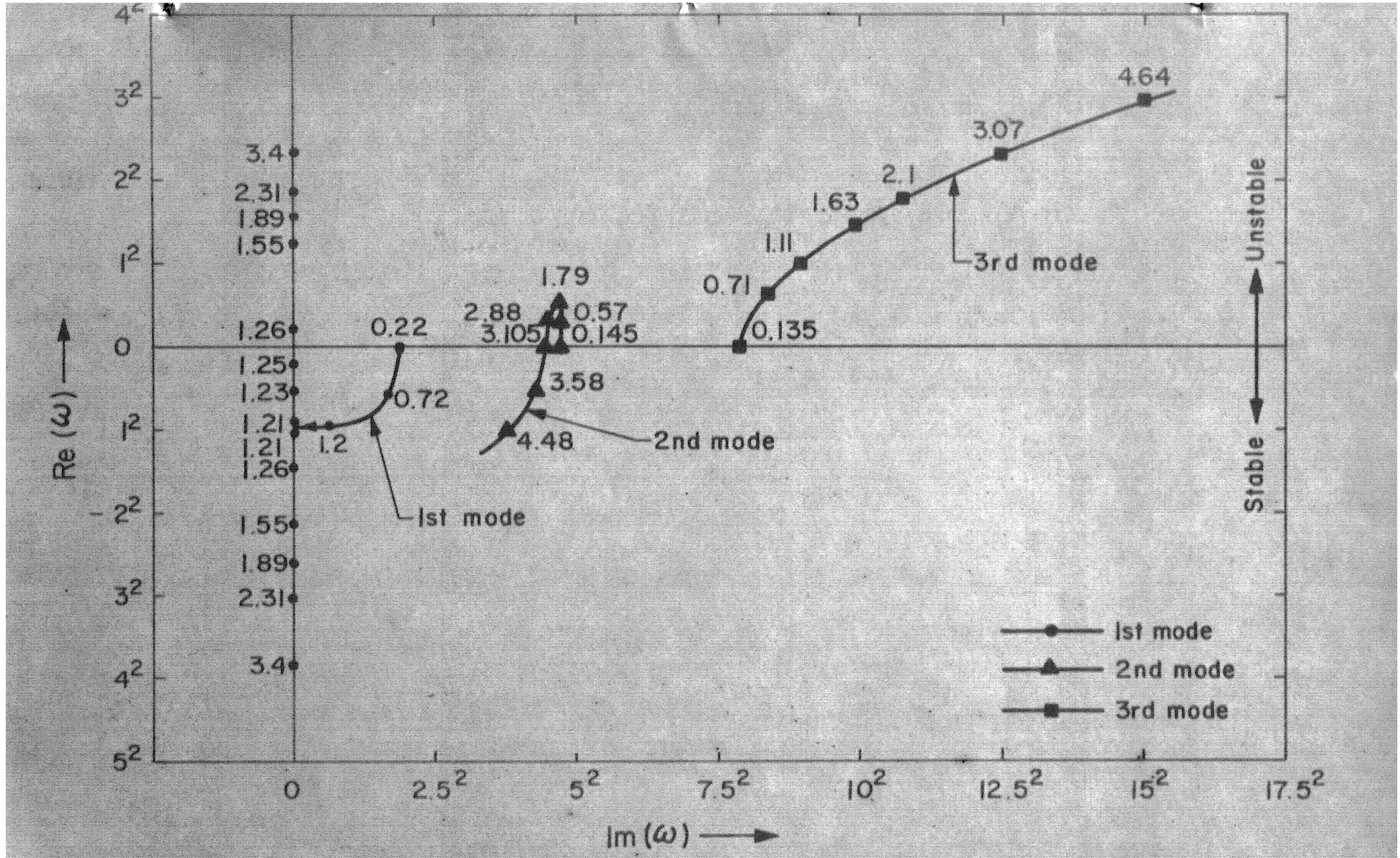

Fig. 5.22 Argand diagram of the complex frequencies, ω, of the lowest three modes of an isolated cantilevered cylinder, as functions of u_2, for $\beta = 0.5$, $\epsilon = 40$, $\delta = 0$, $c_b = \gamma = \Pi = \Gamma = 0$, $\delta_{b_2} = -1$

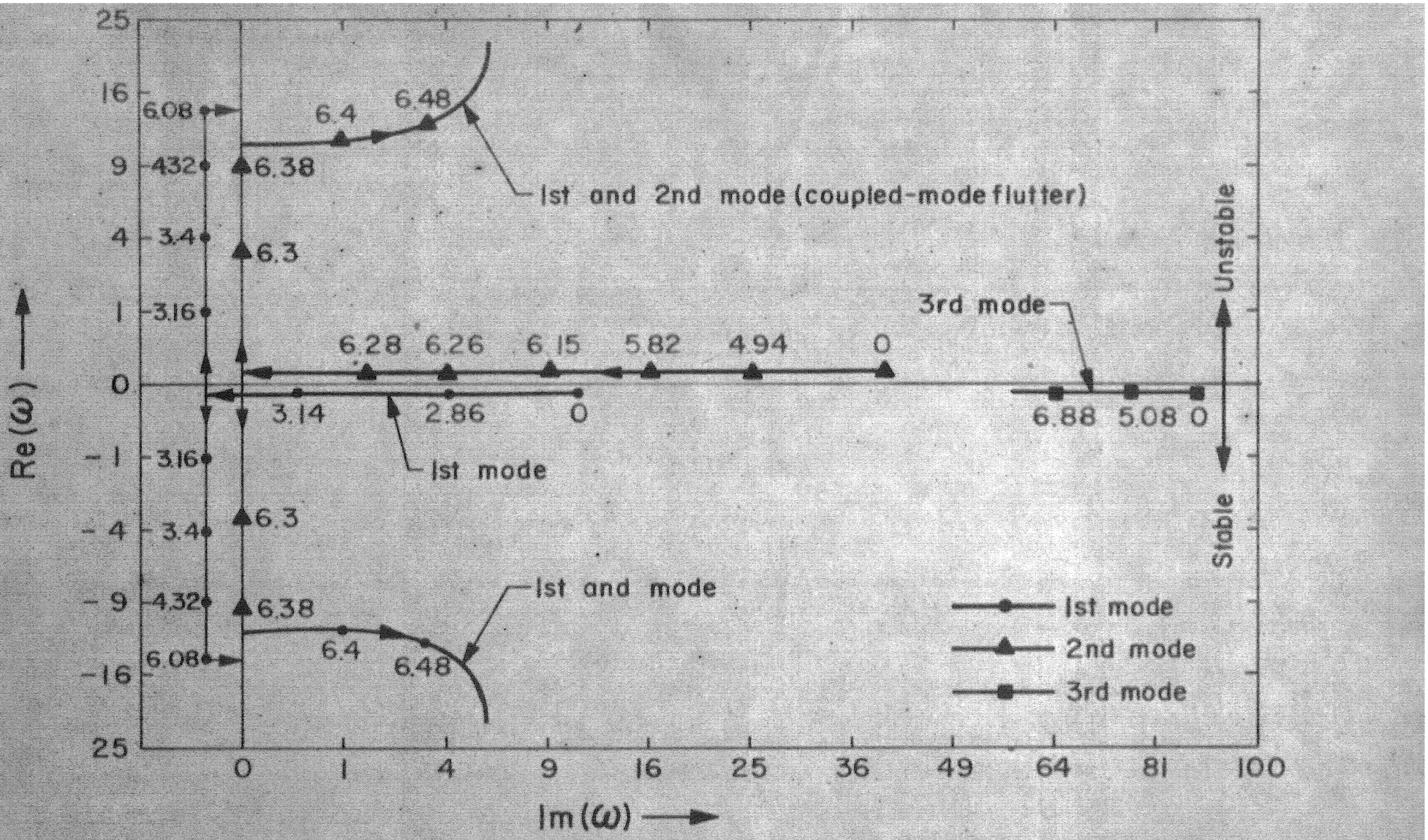

Fig. 5.23 Argand diagram of the complex frequencies, ω, of the lowest three modes of a pinned-pinned pipe, as functions of u_1, for $\beta = 0.1$, $\epsilon = 40$, $\delta = 1$, $\alpha = h = \gamma = \Pi = \Gamma = u_2 = 0$

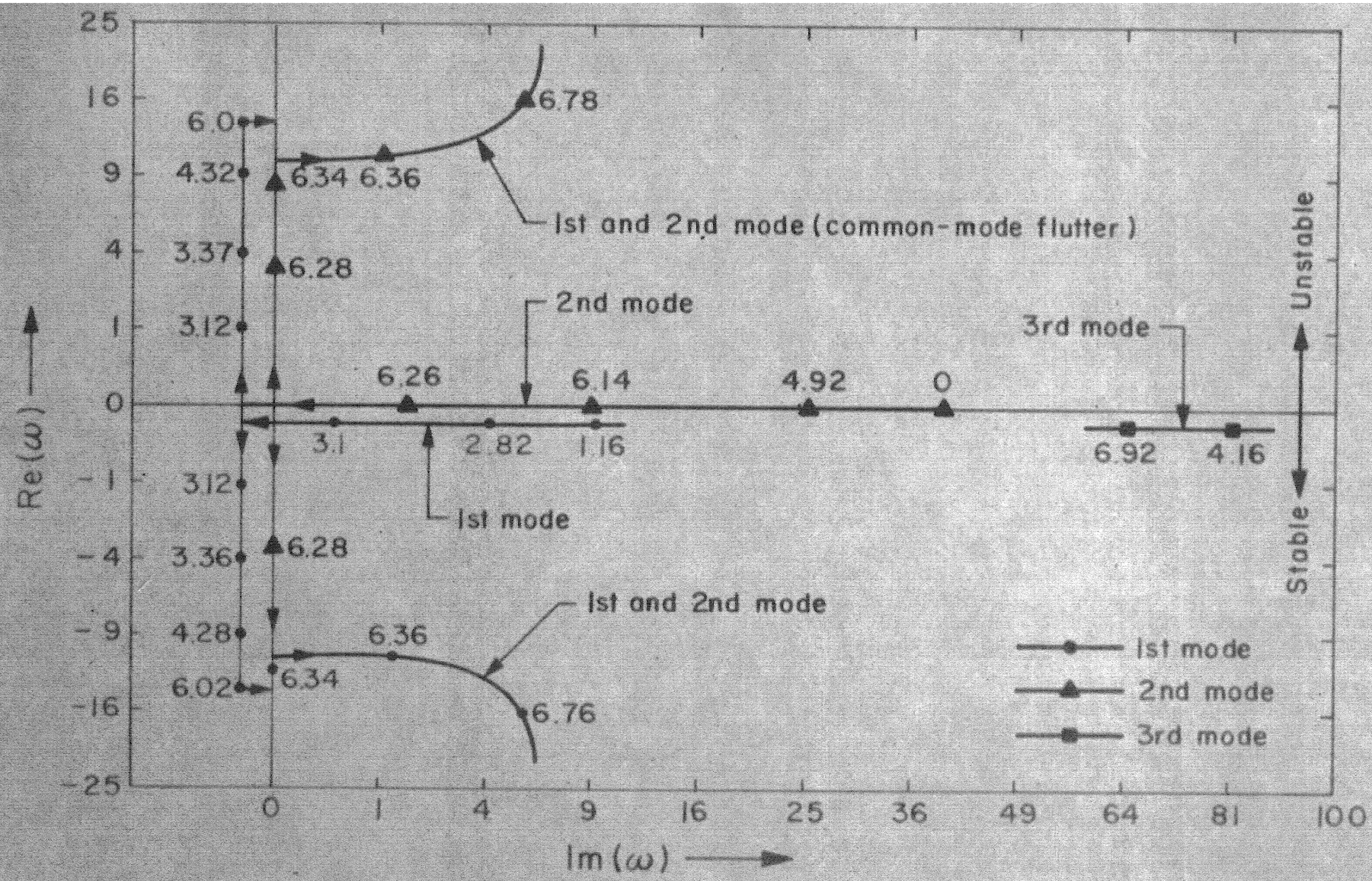

Fig. 5.24 Argand diagram of the complex frequencies, ω, of the lowest three modes of a pinned-pinned pipe, as functions of u_1, for $\Gamma = \Pi = \alpha = \gamma = 0$, $u_2 = 0.5$, $\epsilon = 40$, $\beta = 0.1$,

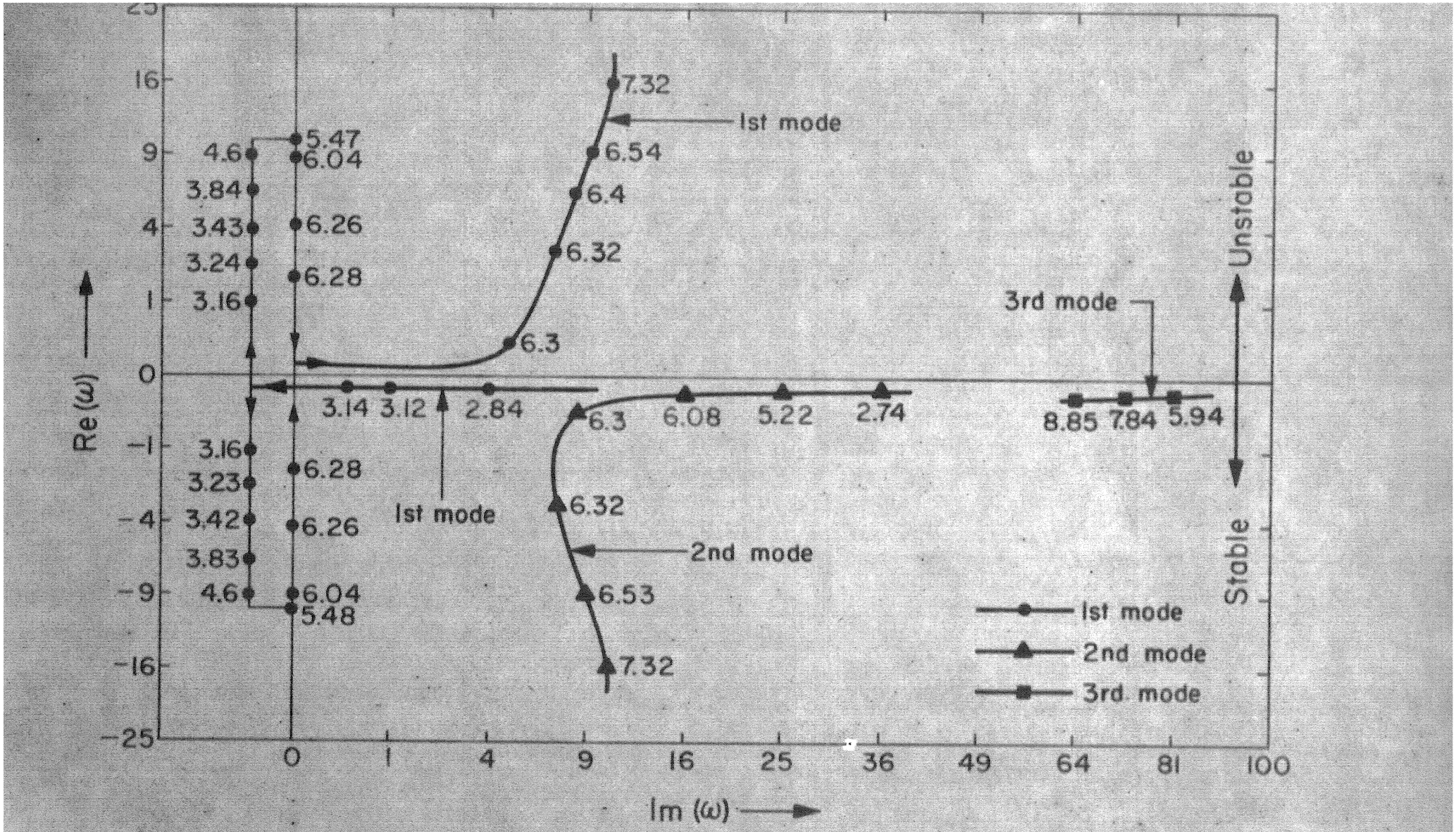

Fig.5.25 Argand diagram of the complex frequencies, ω, of the lowest three modes of a pinned-pinned pipe, as functions of u_1, for $\beta=0.5$, $\alpha=\gamma=\delta=\Pi=\Gamma=h=u_2=0$, $\epsilon=40$

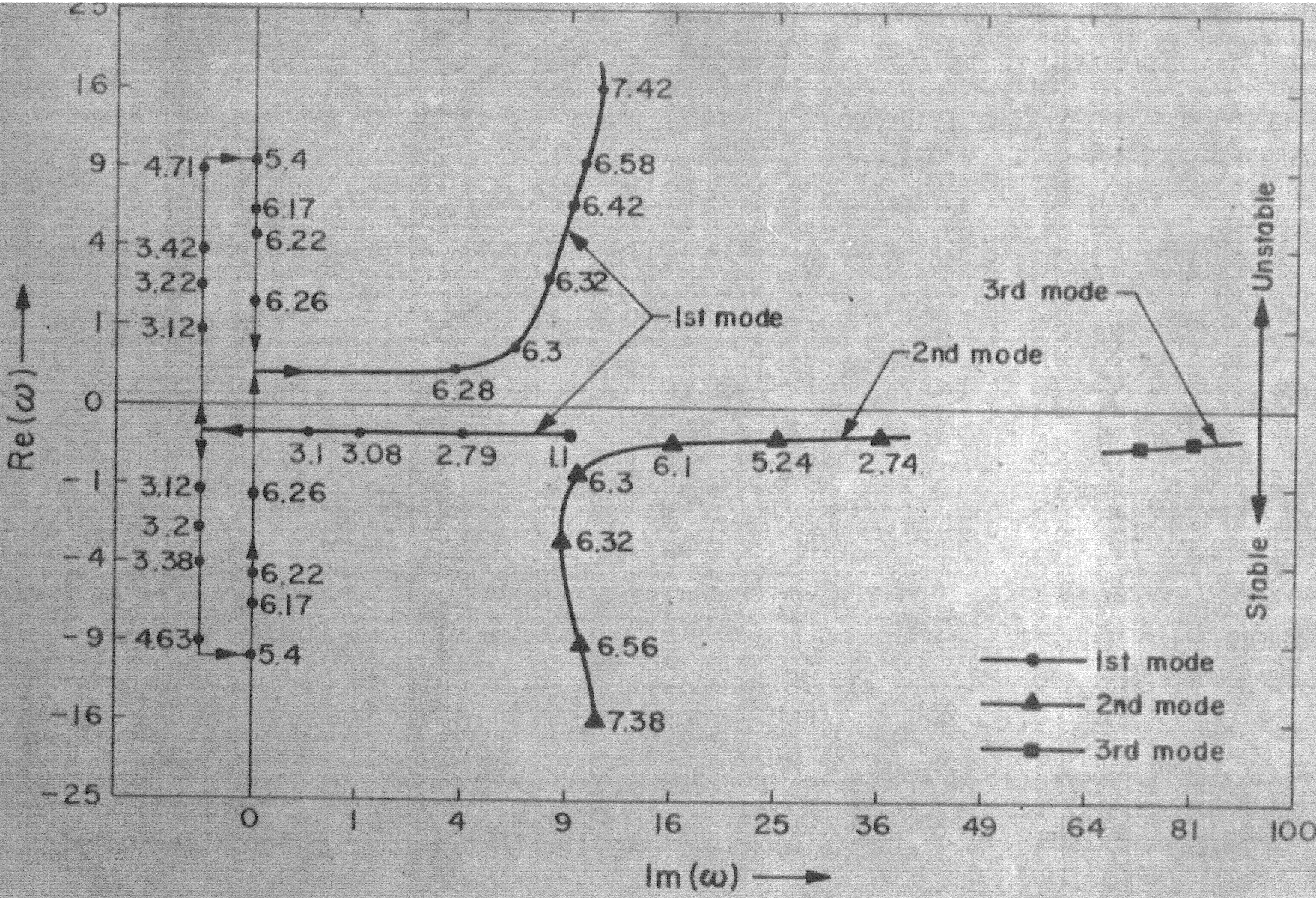

Fig. 5.26 Argand diagram of the complex frequencies, ω, of the lowest three modes of a pinned-pinned pipe, as functions of u_1, for $\beta = 0.5$, $\epsilon = 40$, $\alpha = \gamma = \Gamma = \delta = h = 0$ $x = 1$, $u_2 = +0.5$

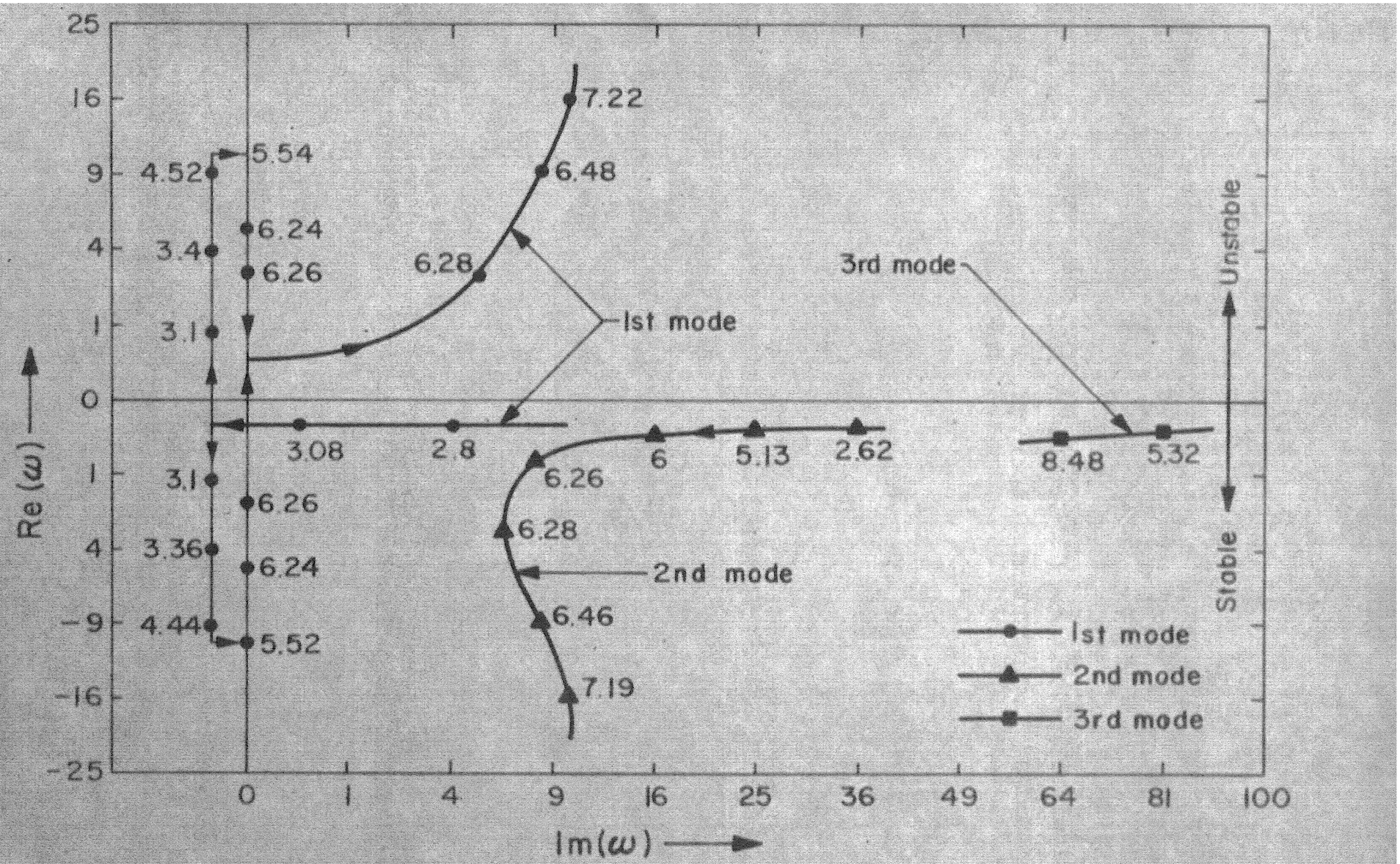

Fig. 5.27 Argand diagram of the frequencies, ω, of the lowest three modes of a pinned-pinned pipe, as functions of u_1, for $\beta = 0.5$, $\Pi = \Gamma = \alpha = h = 0$, $\epsilon = 40$, $u_1 = -0.5$

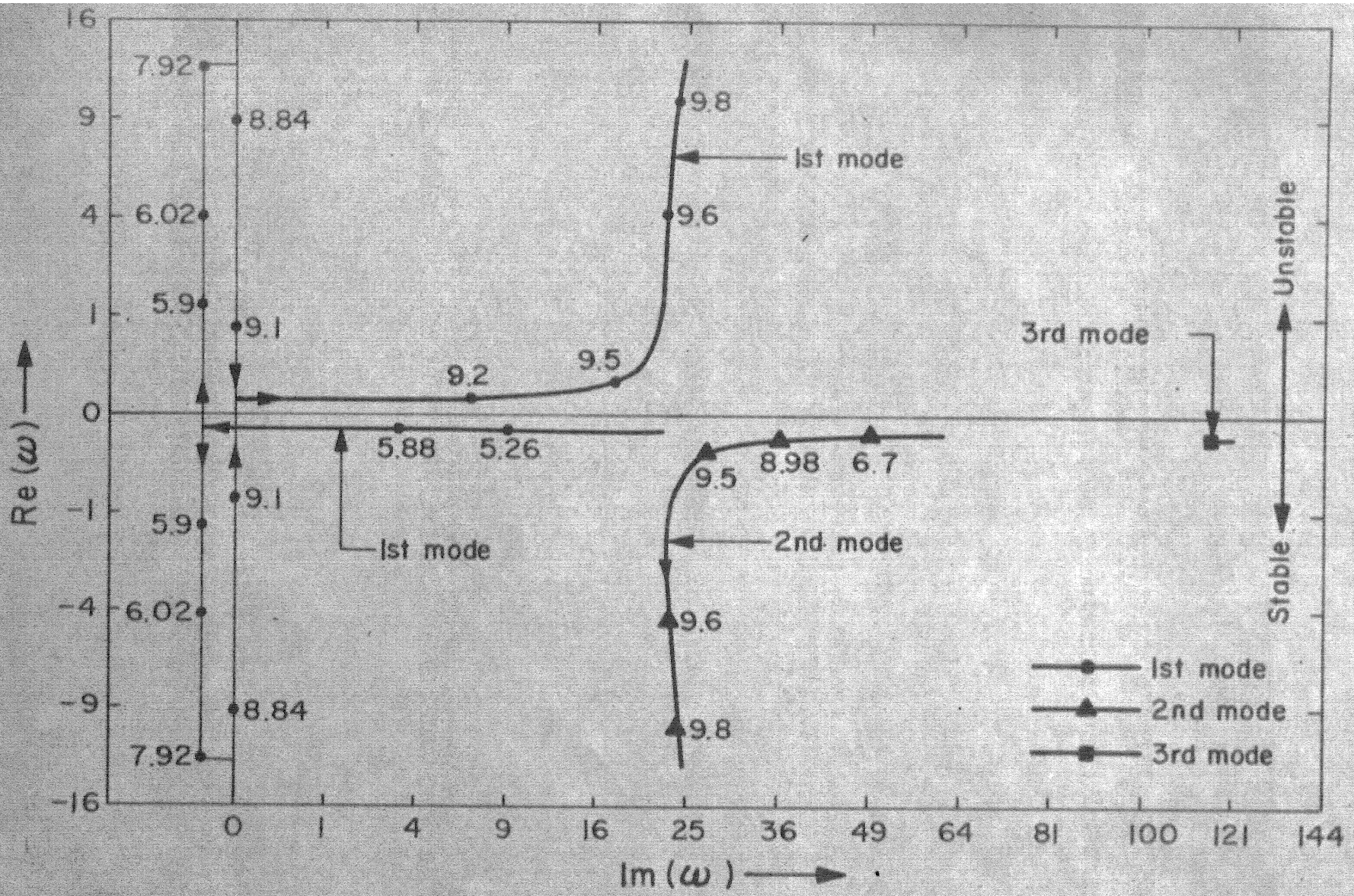

Fig.5.28 Argand diagram of the complex frequencies, ω, of the lowest three modes of a clamped-clamped pipe as functions of u_1, for $u_2 = \Gamma = \Pi = \alpha = \gamma = 0$, $\beta = 0.5$, $\epsilon = 40$

CHAPTER VI

CONCLUSIONS

VI.1 Summary and Results

In this chapter the results obtained in Chapter V have been summarized and they are reexamined in the context of theory developed in Chapter II and objectives set out in article I.4.

1. As a first step in understanding the mechanism of parallel flow induced vibration, mathematical model governing small transverse vibrations of cylinders conveying fluid and subjected to external steady flow has been set up taking into account gravity, pressurization, internal dissipation and direction of the flows. The equation of motion as derived in the present study corrects an error in the representation of frictional forces, considered in previous formulations [48, 61]. Galerkin method has been used to obtain the complex frequencies of the cylinders with different end conditions. The orthonormal eigen functions of a simple beam with identical boundary conditions in the absence of fluid have been used as coordinate functions for Galerkin's expansion.

2. In the case of pinned-pinned (simply supported) cylinders and pipes small flow velocities tend to damp the free motion, as the flow velocity is gradually increased, the cylinders and pipes are subject to buckling. As velocity is increased further, cylinders lose stability by flutter while in the case of pipes the second instability is by buckling in the second mode if the mass ratio is small and by coupled mode flutter if mass ratio is high. With still higher flow velocity, coupled-mode flutter has been found to occur in the case of cylinders as well as pipes, especially when mass ratio is high.

3. When the cylinder or pipe is a part of a cluster of identical cylinders or pipes the close spacing results in increased virtual mass, which has been found to act as destabilizing agent. Further, for clusters, in addition to ordinary flutter the coupled-mode flutter has been found to occur twice with buckling instability interposed in between. When the virtual mass coefficient is comparatively small, on the other hand, only buckling instabilities in the first and second mode have been obtained for sufficiently high flow velocities. Similarity in the character of these instabilities and those in the case of supported pipes with low mass ratio may be noted.

4. The presence of second flow (internal flow in case of cylinders and external flow in case of pipes) has been found to lower the critical velocities in general. The severity of the destabilization effect being dependent on the directions of the two flows. The effect on critical velocities for buckling is less compared to that on the velocities for the onset of flutter.

5. In case of cantilever cylinders subjected to only external flow towards the free end, small flow velocities have been found to damp the free motion. However, the flutter involving first mode soon sets in, followed by one involving second mode. When the direction of the external flow is towards fixed end, the flow induces negative damping for small velocities. As velocity is increased further the cylinder regains stability ($u_2 \approx 0.41$) and looses it again ($u_2 \approx 1.25$) by divergence involving first mode. Similarly, second mode regains stability, at still higher velocity ($u_2 \approx 3.33$); however third mode frequencies remain in the unstable region for the range of velocities under consideration.

6. The divergence type of instability has been shown to be due to inviscid centrifugal force of the fluid, which overcomes the elastic and tensile restoring forces at sufficiently high flow velocities. This

explains destabilization effect of added mass in case of clusters and that due to the presence of both internal and external flows in the case of pipes and cylinders. The direction of the internal flow does not affect the critical velocity for buckling.

7. Instability by ordinary flutter is caused by viscous forces due to external flow alone in the case of supported systems and by inviscid hydrodynamic forces in addition to viscous forces in the case of cantilever cylinders and pipes. For oscillatory instabilities the direction of the external flow is important when internal flow is also present. The correction in the viscous terms of equation of motion has resulted in ordinary flutter instability in case of cylinders and pipes with external flow. In case of cantilever cylinder, which constitutes an inherently nonconservative system, the oscillatory instabilities are due to hydrodynamic forces.

8. The coupled mode flutter has been explained to be the result of inactive Coriolis force which introduces mode coupling and phase difference. The static method to obtain critical velocities for buckling in higher modes fails due to the presence of gyroscopic Coriolis force, the system no longer remaining positive definite.

In the parameter space, the critical point for the flutter cannot be a point of neutral stability. In the absence of frictional forces supported pipes and cylinders can only be subject to coupled-mode flutter since the systems are conservative.

VI.2 Future Work:

1. The results concluded so far constitute the first step towards the solution of response to the flow induced excitation which may consist of either fluctuations in the wall pressure due to turbulence or parametric excitation due to pulsations in the flow rate as discussed in Chapters I and III. The conditions, under which the bounded solution for the motion cannot be obtained, have only been examined in the present work. The next step is to seek the solution of the response problem. If the excitation is parametric, the stability problem has to be solved for unsteady flow velocity. In particular, when velocity has a small harmonic perturbation superimposed on a steady mean value, the primary and secondary instability regions need to be investigated in the context of corrected viscous interaction and presence of internal and external flows.

2. It may be noted that though the mathematical model formulated in the present work takes an account of gravity, internal dissipation, pressurization and spacing between the cylinders in a cluster, detailed parametric study has not been taken up. Further work on this topic should take up the study of the effect of these parameters, in addition to the structural and fluid coupling between the cylinders, on the dynamic behaviour of the cluster as a whole.

3. The present study, as mentioned in Chapter I, had to be diverted and restricted to the investigation of stability analysis only due to the non-availability of reliable analytical or experimental data. This is due to difficulties in the measurement of small scale pressure fluctuations in complicated flow geometries of practical interest. Analytically, the pressure fluctuations can be obtained as mentioned earlier but the method is uneconomical; furthermore it would be more convenient to obtain the response of the cylinder directly using simulation technique rather than pressure fluctuations. It may be appreciated that if the excitation contains deterministic unsteady forces or force field in addition to random but stationary forcing function, as in turbulence induced excitation due to pulsatile flow of a fluid, no satisfactory

method exists for obtaining the response. Considering all these difficulties immediate need of approximate methods for obtaining the response exists. This is also one of the reasons for large volume of research activity on stability problem compared to the one on response problem. An alternative offered by experimental measurements of the response itself, though useful for particular system is not sufficiently attractive due to difficulties in extrapolating the results. Under the circumstances the measurement of pressure fluctuations and simulation are the only feasible methods. In theory, one can obtain the response coupled with flow dynamics, even when flow velocity contains unsteady components. This way, even though the solution is obtained by computationally uneconomical methods, one has a satisfaction of obtaining a meaningful solution.

REFERENCES

1. Bourrières F.J., 1939
"Sur un phènomene d'oscillation auto-entretenue en mècanique des fluides rèels."
Publications Scientifiques et Techniques du Ministère de l'Air, No. 148

2. Ashley H. and Haviland G., 1950
"Bending Vibrations of a Pipeline Containing Flowing Fluid"
Journal of Applied Mechanics, 17, 229-232

3. Housner, G.W., 1952
"Bending Vibrations of a Pipe Line Containing Flowing Fluid"
Journal of Applied Mechanics, 19, 205-208

4. Lighthill M.J., 1952
"On Sound Generated Aerodynamically"
Proceedings of Royal Society (London), A, 211, 564 -

5. Taylor G.I., 1952
"Analysis of Swimming of Long and Narrow Animals"
Proceedings of Royal Society (London), A, 214, 158-183.

6. Miordson F.I., 1953
"Vibrations of a Cylindrical Tube Containing Flowing Fluid"
Kungliga Tekniska Hogskolans Handlingar, No. 73

7. Handelman, G.H., 1955
"A note on the Transverse Vibration of a Tube Containing Flowing Fluid"
Quarterly of Applied Mathematics, 13, 326-330

8. Long, R.H. Jr., 1955
"Experimental and Theoretical Study of Transverse Vibration of a Tube Containing Flowing Fluid"
Journal of Applied Mechanics, 22, 65-68

9. Burgree, D., Eyrness J.J., Benforado, D.M., 1958
"Vibration of Rods Induced by Water in Parallel Flow"
Transactions of A.S.M.E., 80, 991-1003

10. Lighthill, M.J., 1960
"Note on the Swimming of Slender Fish"
Journal of Fluid Mechanics, 9, 305-317

11. Benjamin, T.B., 1961 a
"Dynamics of a System of Articulated Pipes Conveying Fluid. I. Theory"
Proceedings of the Royal Society (London) A, 261 457-486.

12. Benjamin, T.B., 1961 b
"Dynamics of a System of Articulated Pipes Conveying Fluid. II. Experiments"
Proceedings of the Royal Society (London) A, 261, 487-499.

13. Willmarth, W.W., Woolridge, C.E., 1962
"Measurement of the Fluctuating Pressure at the Wall Beneath a Thick Turbulent Boundary Layer."
Journal of Fluid Mechanics, 14, 187-210

14. Bakewell, H.P., Jr., 1963
"Longitudinal Space-time Correlations in Turbulent Air Flow"
Journal of Acoustic Society of America, 35, 936-937

15. Benjamin, T.B., 1963
"Threefold Classification of Unstable Disturbances in Flexible Surfaces Bounding Inviscid Flow"
Journal of Fluid Mechanics, 16, 436-450

16. Bakewell, H.P. Jr., 1964
"Wall Pressure Correlations in Turbulent Pipe Flow"
Journal of Acoustic Society of America, 36, 146-148

17. Corcos, G.M., 1964
"The Structure of the Turbulent Pressure Field in Boundary Layer Flows"
Journal of Fluid Mechanics, 18, 353-378.

18. Röstorm, K.G., Anderson, N., 1964
"Boiler Element for Marviken, Vibration Tests With one Rod"
Arbetstrapport RPL-724
Aktiebolaget atomenergie, Stockholm (Sweden)

19. Röstorm K.G., 1964
"Seven Rod Fuel Element, Vibration Test"
Arbetstrapport RPL-726
Aktiebolaget atomenergie, Stockholm (Sweden)

20. Röstorm, K.G., Anderson N., 1964
"Boiler Element for Marviken, Vibration Tests with One Rod"
Arbetstrapport RPL-726
Aktiebolaget atomenergie, Stockholm (Sweden)

21. Hoerner, S.F., 1965
Fluid Dynamics Drag
2nd Edition, Hoerner Fluid Dynamics, Brick Town, N.J.

22. Paidoussis, M.P., 1965
"The Amplitude of Fluid Induced Vibration of Cylinders in Axial Flow."
Report AECL-2225, Atomic Energy of Canada Ltd.
Chalk River, Ontario, Canada

23. Pavlica, R.T., Marshal R.C., 1965
"Vibration of Fuel Assemblies in Parallel Flows"
Transactions of American Nuclear Society, 8, 599-600

24. Quinn, E.P., 1965
Vibration of SEFOR Fuel Rods in Parallel Flow
United States Atomic Energy Commission
Report GEAP -4966, Sept. 1965

25. Nemat-Nasser S., Prasad, S.N., Hermann, G., 1966
"Destabilizing effects of Velocity Dependent Forces in non-conservative Continuous Systems"
American Institute of Astronautics and Aeronautics Journal, 4, 1276-1280

26. Gregory, R.W. and Paidoussis, M.P., 1966 a
"Unstable Oscillation of Tubular Cantilevers Conveying Fluid. I. Theory"
Proceedings of the Royal Society (London) A, 293

27. Gregory, R.W. and Paidoussis, M.P, 1966 b
"Unstable Oscillation of Tubular Cantilevers Conveying Fluid. II. Theory"
Proceedings of the Royal Society (London) A, 293, 528-542

28. Hermann, G., 1967
"Stability of Equilibrium of Elastic Systems Subjected to Nonconservative Forces"
Applied Mechanics Reviews, 20, 103-108

29. Paidoussis, M.P., 1966 a
"Dynamics of Flexible Slender Cylinders in Axial Flow
I. Theory"
Journal of Fluid Mechanics, 26, 717-736.

30. Paidoussis, M.P., 1966 b
"Dynamics of Flexible Slender Cylinders in Axial Flow
II. Experiments"
Journal of Fluid Mechanics, 26, 737-751

31. Paidoussis, M.P., 1966
"Vibration of Flexible Cylinders With Supported Ends Induced by Axial Flow"
Institute of Mechanical Engineers Proceedings, 180, Part 3-J

32. Pavlica, R.T., Marshall, R.C., 1966
"An Experimental Study of Fuel Assembly Vibrations Induced by Coolant Flow"
Nuclear Engineering Design, 4, 54-60

33. Hermann, G., Nemat-Nasser, S., 1967
"Instability Modes of Cantilevered Bars Induced by Fluid Flow Through Attached Pipes"
International Journal of Solids and Structures, 3, 39-52

34. Paidoussis, M.P., Sharp, F.L., 1967
An Experimental Study of the Vibrations of Flexible Cylinders, Induced by Nominally Axial Flow
Report CRNL-76, Chalk River National Lab.
Chalk River, Ontario, Canada

35. Naguleswaran, S., Williams, C.J.H., 1968
"Lateral Vibration of a Pipe Conveying Fluid"
The Journal of Mechanical Engineering Science, 10, 228-238

36. Thurman, A.L., Mote, C.D., Jr., 1969
"Nonlinear Oscillation of a Cylinder Containing Flowing Fluid".
Journal of Engineering for Industry, Transactions of A.S.M.E., 91, 1147-1155

37. Paidoussis, M.P., 1970
"Dynamics of Tubular Cantilevers Conveying Fluid"
Journal of Mechanical Engineering Science, 12, 85-103

38. Paidoussis, M.P., Deksnis, E.B., 1970
"Articulated Models of Cantilevers Conveying Fluid, The Study of a Paradox"
Journal of Mechanical Engineering Science, 12, 288-300

39. Stein, R.A., Torbiner, M.W., 1970
"Vibration of Pipes Containing Flowing Fluids"
Journal of Applied Mechanics, 92, 906-916

40. Chen, S.S., 1971
"Flow Induced Instabilities of an Elastic Tube"
American Society of Mechanical Engineers, Paper 71-Vibr.-39.

41. Chen, S.S., 1971
"Dynamic Stability of Tube Conveying Fluid"
Journal of Engineering Mechanics Division,
Proceedings of the American Society of Civil Engineers,
97, 1469-1485

42. Chen, S.S., 1971
"Vibration and Stability of a Uniformly Curved Tube
Conveying Fluid"
Journal of Acoustic Society of America, 48, 773-775

43. Paidoussis, M.P., Denise, J.P., 1971
"Flutter of Cylindrical Shells Conveying Fluid"
Journal of Sound and Vibration, 16, 459-461

44. Chen, S.S., 1972
"Flow Induced In-plane Instabilities of a Curved Pipe"
Nuclear Engineering and Design, 23, 29-38

45. Chen, S.S., 1972
"Out-of-plane Vibration and Stability of Curved Tubes
Conveying Fluid"
American Society of Mechanical Engineers, Paper No.
WA/APM-36

46. Paidoussis, M.P., Denise, J.P., 1972
"Flutter of Thin Cylindrical Shells Conveying Fluid"
Journal of Sound and Vibration, 20, 9-26

47. Bohn, M.P., Hermann, G., 1973
"The Dynamic Behaviour of Articulated Pipes Conveying
Fluid with Periodic Rate"
American Society of Mechanical Engineers
Paper No. 73-APMW-32

48. Paidoussis, M.P. 1973
"Dynamics of Cylindrical Structures Subjected to
Axial Flow."
Journal of Sound and Vibration, 29, 365-385

49. Weaver, D.S., Unny, T.E., 1973
"On the Dynamic Stability of Fluid Conveying Pipes"
Journal of Applied Mechanics, 40, Trans. ASME, 95,
48-52

50. Weaver, D.S., Myklatun, B., 1973
"On the Stability of Thin Pipes with an Internal Flow"
Journal of Sound and Vibration, 31, 399-410

51. Chen, S.S., Rosenberg, G.S., 1974
"Free Vibrations of Fluid Conveying Cylindrical Shells"
Journal of Engineering for Industry, Trans. ASME, 96, 420-426

52. Bohn, M.P., Hermann G., 1974
"Instabilities of a Spatial System of Articulated Pipes Conveying Fluid"
Transactions of ASME, 96, I, 289-296

53. Chen, S.S., 1974
"Dynamics of a Rod Shell System Conveying Fluid"
Nuclear Engineering Design, 30, 223-233.

54. David, T.S., Srinivasan, A.V., 1974
"Flutter of Co-axial cylindrical Shells in an Incompressible Axysymmetric Flow"
AIAA Journal, 12, 1631.

55. Paidoussis, M.P., Issid N.T., 1974
"Dynamic Stability of Pipes Conveying Fluids"
Journal of Sound and Vibration, 33, 3, 267-294

56. Paidoussis, M.P., 1974
"Vibration of Cylindrical Structures Induced by Axial Flow."
Journal of Engineering for Industry, Trans. ASME, 96,B, 547-552.

57. Paidoussis, M.P., 1974
"The Dynamic Behaviour of Cylindrical Structures in Parallel Flow"
Annals of Nuclear Science and Engineering, 1, 83-106

58. Reynolds, A.J., 1974
Turbulent Flows in Engineering
John Wiley, London, 1974

59. Sundararajan, C., 1974
"Influence of End Support on the Stability of Non Conservative Elastic Systems"
Journal of Applied Mechanics, 40, Trans. ASME, 95, 313-315

60. Chen, S.S., 1975
"Vibrations of a Group of Circular Cylinders in a Liquid Flow"
Paper No. D 2/7
3rd Int. Conf. on SMRT, London, U.K., 1-5 Sept. 1975

61. Paidoussis, M.P., 1975
"Stability of Flexible Slender Cylinders in Pulsatile Axial Flow"
Journal of Sound and Vibration, 42, 1-11

62. Schumann U., 1975
"Numerical Investigation of the Wall Pressure, Fluctuations in Channel Flows"
Nuclear Engineering Design, 32, 37-46

63. Paidoussis, M.P., 1975
"Mathematical Model for the Dynamics of an Articulatd String of Fuel Bundles in Axial Flow"
Paper No. D 2/5
3rd Int. Conf. on SMRT, London (U.K.), 1-5 Sept. 1975

64. Shieh, R.C., 1971
"Energy and Variational Principles for Generalized (Gyroscopic) Conservative Problems."
International Journal of Non-linear Mechanics, 5, 495-509

65. Bolotin, V.V., 1964
The Dynamic Stability of Elastic Systems
Holden-Day, Inc., San Francisco, 1964, 209-248

66. Hsu, C.S., 1963
"On the Parametric Excitation of a Dynamic System Having Multiple Degrees of Freedom"
Journal of Applied Mechanics, 30, 367-372

67. Chen, S.S., Wambsganss, M.W., Jr., 1972
"Parallel Flow Induced Vibration of Fuel Rods"
Nuclear Engineering Design, 18, 253-278

68. Chen, S.S., 1975
"Vibrations of a Group of Circular Cylinders in a Liquid Flow"
Paper No. D 2/7
3rd International Conference on SMRT, London, 1-5 Sept., 1975

69. McCormic, M.E., Ripley, T.C., 1967
"An Experimental Study of Velocity Dependent Damping of A Turbulence Induced Vibration System"
Presented at the 74th Meeting of the Acoustical Society of America, Miami, Nov. 1967.

70. Lawn, C.J., Elliott, C.J., 1971
"Fully Developed Turbulent Flow Through Concentric Annuli."
Report No. 2D/B/N 1878, Central Electricity Generating Board, Research Department, Berkeley Nuclear Laboratories

71. Rehme, K., 1975
"Turbulence Measurements in Smooth Concentric Annuli with Small Radius Ratios."
Journal of Fluid Mechanics, 72, 189-206

72. Ralston, A., 1965
A First Course in Numerical Analysis
McGraw Hill Book Company, New York., 1965, 464-520

73. Meirovitch, L., 1967
Analytical Methods in Vibrations
Macmillon, N.Y., 1967

74. Grad, J. and M.A. Brebner, 1968
Eigenvalues and Eigenvectors of a Real General Matrix
Communications to the Association of Computing Machinery Journal, 11, 820.

75. Hydman, R.W., et. al., 1965
"EBR-II Self Excited Oscillations"
Transactions of American Nuclear Society, 8, 590-590

76. Dalke, C.A., 1965
"Elimination of Hydraulically Induced Core Vibrations in the General Electric Test Reactor."
Transcations of American Nuclear Society, 8, 2-2

77. Skaardal, R.C., 1965
"Flow Induced Vibrations"
Power Reactor Technology, 8, 273-275

78. Riesland, J.I. and Gustafson, E.A., 1965
"Work Performed on Fuel Channels and the Core Support Plate at Big Rock Point Nuclear Power Plant."
Transactions of American Nuclear Society, 8, 5-9

79. "Action on Reactor Projects Undergoing Regulatory Review"
Nuclear Safety, 6, 222-223

80. "Thermal Shield Vibration at Big Rock Point"
Nucleonics, 24, 64-65

81. Martens, F.H., 1966
"Design Foresight can simplify Reactor Modification"
Power Reactor Technology, 9, 74-79

82. Reed, G.A., 1965
"Major Operating and Refuelling Problems at the Yankee Atomic Electric Company Rowe Power Plant"
Transactions of American Nuclear Society, 8, 28-28

83. Reed, G.A., Tarnuzzer, E., 1966
"Examining Yankee Plant Performance in 1965
Nucleanics, 24, 42-47

84. Bierman, G.F., Miller, W.J., 1966
"Nuclear Plant Performance-good and getting Better"
Power Reactor Technology, 9, 110-122

85. Heffner, R.E., 1965
"Six Years Operating Experience with PWR Plant Components"
Transaction of American Nuclear Society, 8, 29-30

86. Oak Ridge National Laboratory, 1964
Molten-Salt Reactor Program Semiannual Progress Report for Period ending January 31, 1964
USAEC Report ORNL-3626, July 1964

87. Oak Ridge National Laboratory, 1965
Molten Salt Reactor Program Semiannual Progress Report for Period Ending July 31, 1964
USAEC Report ORNL-3708, November 1965